Effect Of Network Structure On Mechanical Behavior Of Epoxies.

INFORMATION TO USERS

This material was produced from a microfilm copy of the original document. While the most advanced technological means to photograph and reproduce this document have been used, the quality is heavily dependent upon the quality of the original submitted.

The following explanation of techniques is provided to help you understand markings or patterns which may appear on this reproduction.

1. The sign or "target" for pages apparently lacking from the document photographed is "Missing Page(s)". If it was possible to obtain the missing page(s) or section, they are spliced into the film along with adjacent pages. This may have necessitated cutting thru an image and duplicating adjacent pages to insure you complete continuity.

2. When an image on the film is obliterated with a large round black mark, it is an indication that the photographer suspected that the copy may have moved during exposure and thus cause a blurred image. You will find a good image of the page in the adjacent frame.

3. When a map, drawing or chart, etc., was part of the material being photographed the photographer followed a definite method in "sectioning" the material. It is customary to begin photoing at the upper left hand corner of a large sheet and to continue photoing from left to right in equal sections with a small overlap. If necessary, sectioning is continued again — beginning below the first row and continuing on until complete.

4. The majority of users indicate that the textual content is of greatest value, however, a somewhat higher quality reproduction could be made from "photographs" if essential to the understanding of the dissertation. Silver prints of "photographs" may be ordered at additional charge by writing the Order Department, giving the catalog number, title, author and specific pages you wish reproduced.

5. PLEASE NOTE: Some pages may have indistinct print. Filmed as received.

University Microfilms International
300 North Zeeb Road
Ann Arbor, Michigan 48106 USA
St. John's Road, Tyler's Green
High Wycombe, Bucks, England HP10 8HR

EFFECT OF NETWORK STRUCTURE ON MECHANICAL BEHAVIOR OF EPOXIES

by

SUBODH C. MISRA

A Dissertation Presented to the Graduate Faculty of
Lehigh University
in Candidacy for the Degree of
Doctor of Philosophy

in

Chemical Engineering
Lehigh University

1978

Approved and recommended for acceptance as a dissertation in partial fulfillment of the requirements for the degree of Doctor of Philosophy

May 11, 1978
(date)

John A. Manson
Professor in Charge

Accepted May 12, 1978
(date)

Special committee directing the doctoral work of Mr. Subodh C. Misra

J. A. Manson Chairman

A. J. McHugh

C. N. Robinson

L. H. Sperling

J. W. Vanderhoff

ACKNOWLEDGMENTS

The author wishes to express his sincere gratitude and appreciation to :

Dr. John A. Manson, under whose guidance and encouragement this work was undertaken, and who has at all times given the most generous assistance, patience, and understanding during the period of this study.

Drs. J. W. Vanderhoff, A. J. McHugh, L. H. Sperling, and C. R. Robinson for their discussions and interest, and for serving on the Dissertation Committee.

Dr. M. S. El-Aasser for his interest, encouragement, and readiness for help and discussion.

Mr. R. Korinstinsky and Mr. D. Bush for their assistance on the electron microscopic studies.

Mr. C. Worman, Air Products & Chemicals Inc., for performing the GPC characterizations.

The financial support from the Materials Research Center, Lehigh University; Air Force Materials Laboratory (Contract No. F33615-75-C-5167); Ford Motor Fund; and the Department of Chemical Engineering, Lehigh University.

Finally, Mr. Justice T. S. Misra and Mrs. S. Misra, the authors parents, for their love and encouragement which made possible the successful completion of this work.

TABLE OF CONTENTS

LIST OF TABLES

LIST OF FIGURES

ABSTRACT

Although crosslinked polymers are commonly used in applications such as coatings, adhesives and composite matrices, the relationship between network structure, morphology, and mechanical behavior is not very well understood.

The purpose of this study was to elucidate the effects of prepolymer state (bulk, solution, and emulsion) and composition on the network structure, viscoelastic behavior, and ultimate mechanical properties of bisphenol-A-type epoxies. A major question throughout was the distribution of crosslink density at molecular, supermolecular, and microscopic levels.

By using scanning and transmission electron microscopy it was shown that a multi-phase morphology, reflecting variations in crosslink density, is usually developed in curing in bulk, solution or emulsion. In the case of the latter a theory for emulsion curing, which involves both chemical curing and physical coalescence, was proposed after consideration of morphology in conjunction with differential scanning calorimetry. It was shown that emulsion curing is a diffusion controlled process.

By isolating microgel particles prior to gelation it was confirmed that, at least in typical systems, curing takes place by the process of microgel formation. Based on the morphological observations a theory of network formation was proposed in which primary microgel particles reactively sinter together first to give larger particles (secondary microgels). Later these secondary

microgels combine together (less coherently than the primary microgels) to give the final network (macrogel). The mechanical properties of the network, to a certain extent, depend on the size and coherence of the secondary microgels.

It was found that the DGEBA-type epoxy networks have a very restricted motion of the main chains even in the rubbery state. The β-transition temperature, glass transition temperature (T_g), rubbery modulus, charateristic creep time, impact strength, and the bulk density, increase with crosslink density. On the other hand, swelling, soluble content, height of the loss tangent peak near T_g, slope of the modulus temperature curve at T_g, decrease with crosslink density, whereas room temperature tensile properties, and apparent energies of activation for creep, both above and below T_g are independent of crosslink density. Furthermore, it was shown that impact strength is directly related to both the crosslink density and the loss tangent value at the temperature and frequency of impact.

Minor changes in the distribution of M_c do not affect any of the mechanical properties except for charateistic creep time; the latter increasės with an increase in the number of small chains in the network. However, properties such as T_g and the transition slope also became sensitive in networks having a major difference in distribution at the same average crosslink density. The network structure in highly crosslinked systems is not affected by the presence of small amounts of solvent during the curing process.

CHAPTER I

GENERAL INTRODUCTION

A. INTRODUCTION

Crosslinked polymer networks, because of their good dimensional stability and resistance to flow at elevated temperatures, fill many common engineering needs. High crosslink density networks based on such materials as epoxies, phenolics, and polyesters find many applications, for example as components for mechanical and electrical uses, as composite matrices, and as protective coatings. For many ordinary service demands, such crosslinked networks can be made easily with relatively little technical expertise and without any sophisticated technical knowledge. However, for more demanding technical specifications, as in the case of aerospace materials, much more must be learned about these networks. From the simplest point of view, an ideal polymeric network may be conceived as a three-dimensional system of connected chains forming a single macroscopic molecule (Fig.1a). Clearly, the behavior must depend on the tightness of the network or the crosslink density. A network having a high crosslink density (Fig.1b) would exhibit less swelling and a higher glass transition temperature (T_g) than the network having a low crosslink density (Fig.1c). However, for many real cases loops and dangling chain ends may also exist without direct chemical connection to the network (Fig.1d). Furthermore, the lengths of chains between crosslinks may vary depending on the structure of the monomers or prepolymers, or on the vagaries of the

reaction kinetics. Such a distribution will occur in a homogeneous system, whereas several such distribution will occur in a hetrogeneous system along with variations in crosslink density itself in the various phases (see Figures 1-e, and 1-f).

In the case of vulcanized rubbers, which exhibit high values of molecular weight between crosslinks (M_c) (say, 5000), much understanding has already been achieved. At room temperature, all such elastomers, of course, are above their T_g. If the crosslinked polymer is below its T_g, its molecular chains are incapable of long range coordinated motion, and the material becomes stiff and glassy. Unfortunately, with materials of this type which exhibit high degrees of crosslinking and great chemical complexity (M_c less than 5000; for some common epoxies, $M_c \approx 400$) equations useful for elastomers tend to fail and require empirical modification(1). Besides a few exceptions, for example recent studies of epoxies, to be discussed later, there is surprisingly little fundamental study of mechanical behavior using materials characterized to the limits of the state-of-the-art. Furthermore, the effect of distribution of M_c has yet to be established.

The principal objective of this study was to determine the influence of crosslinking and network structure on the engineering behavior of highly crosslinked networks. In particular, epoxies, which are one of the most useful and important resins and fall under this category, were selected for this study. Curing of these resins is commonly practiced both in bulk and solution, and,

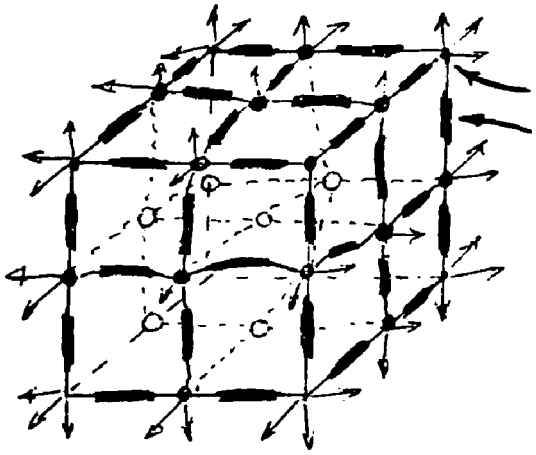

A) 3-D, Crosslinked Network with a functionality of 6.

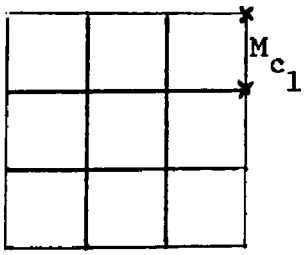

B) Ideal Network ($M_c = M_{c_1}$)

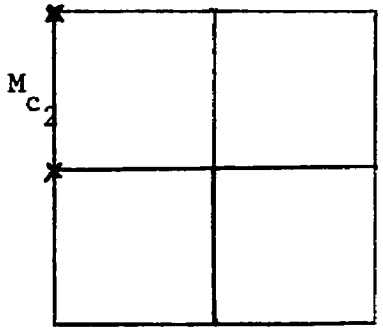

C) Ideal Network ($M_c = M_{c_2}$)

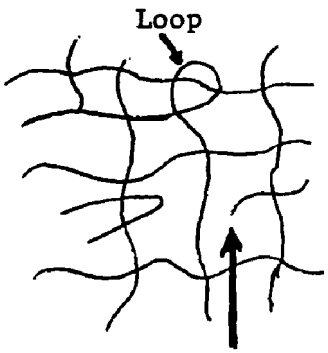

D) Network having loops and dangling chains.

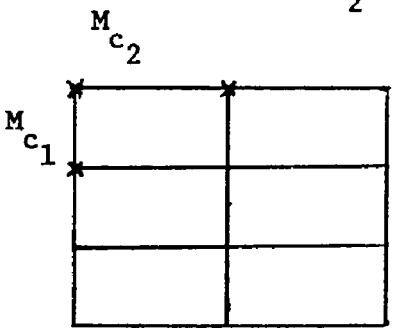

E) Network having a bimodal distribution of M_c.

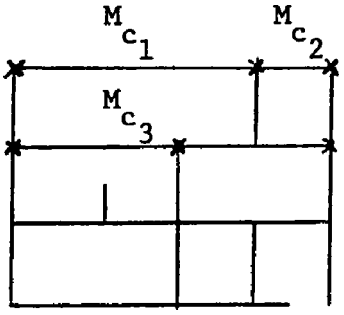

F) Network having a multiple distribution of M_c.

Figure 1. Scheme showing typical variations in crosslinked Networks.

more recently, from emulsion precursors as well. Bulk-curing is preferred for applications such as adhesives, castings, and laminates, whereas solution curing is primarily employed in applications such as primers, varnishes, coatings, linings , and product finishes. Epoxy emulsions, on the other hand, have not achieved widespread industrial acceptance except for some trial usage in fabric treatment(2). This has been primarily due to the inferior properties of the emulsion-cured films, attributed to the large particle size and poor stability of the emulsions. Recent developments(3,4) of stable epoxy emulsions having small particle size may lead to their widespread use as substitutes for solvent-based systems in coatings applications. Though curing is done in bulk, solution, and sometimes in emulsion, very little is known about how these different methods affect the properties of the final network. Since their first commercialization and particularly in the last decade, epoxy resins have been the subject of an enormous number of patents and technical publications dealing with different aspects such as: stoichiometry(5-9), prepolymer structure(10-12), diluents(8,13-16), fillers(17-26), heat treatment(7,26), and cure conditions(27-29). Though some studies covered tensile and impact behavior, the majority of the papers on mechanical properties dealt only with dynamic mechanical behavior. Some quantitative studies do exist which relate at least average or relative network properties such as M_c to stoichiometry(5-9), curing conditions(27-29), stress-strain behavior(8,9,30,31), fracture(32-37), and impact

strength(9,30,36). However, detailed studies of epoxy resins cured at equal stoichiometry are relatively few. Now the commercial epoxy resins usually exhibit a distribution of molecular weights which should result in a distribution of crosslink density in the final network. The broadening of the transition region has been qualitatively attributed to this distribution effect(1). Unfortunatly existing studies were of insufficient scope to permit a correlation between the engineering behavior of epoxy networks and distribution of crosslink density or M_c. From the standpoint of relevence to engineering applications, such a study should be of considerable interest. It seemed reasonable to conclude that a thorough characterization of viscoelastic behavior in blends of two epoxy resins, having quite different molecular weights, should enable correlations of distributions of M_c and other network variables with the engineering behavior.

B. OBJECTIVES

The overall objective of this study was to determine the influence of M_c and network structure on the engineering behavior of typical epoxies. In particular the effects of variations in distribution of crosslink density and average crosslink density were of interest, with emphasis on curing in bulk and emulsion.

C. SCOPE

The scope of this study includes epoxy networks formed by both emulsion and bulk curing, as follows:

a. Preparation of stable emulsions of different epoxies

and curing agents and characterization of the particle sizes.

b. Study of the mechanism of emulsion curing (which includes film formation) using dynamic mechanical spectroscopy(DMS), transmission electron microscopy(TEM), differential scanning calorimetry (DSC), and swelling and extraction tests.

c. Study of the effect of average M_c and distribution of M_c on the engineering properties of bulk-cured epoxy resins, in particular through DMS, TEM, DSC, tensile, creep, swelling and extraction tests.

d. Study of the morphological changes during crosslinking and the effect of network morphology on its mechanical properties.

The different aspects of network structure studied have been discussed in separate chapters:

1. Chapter 3 deals with the effects of average M_c and distribution of M_c. For this study a homologous series of diglycidyl ether of bisphenol-A(DGEBA) type epoxy prepolymers was selected and cured with stoichiometric amounts of methyline dianiline(MDA).

2. Chapter 4 deals with the morphological aspects of epoxy resins. The effect of stoichiometry, prepolymer molecular weight, M_c, and distribution of M_c have been discussed. A mechanism of curing in bulk is proposed.

3. Chapter 5 deals with emulsion curing per se. Film formation and curing mechanisms for epoxy emulsions have been proposed. For this study emulsions of Epon 1001 and Versamid 115 were selected.

4. Chapter 6 deals with the evaluation of epoxy networks prepared by curing in bulk, emulsion, and solution at three different levels of M_c. For this the DGEBA-type epoxies were cured with stoichiometric amounts of MDA.

REFERENCES

1. L.E.Nielsen, J.Macromol.Sci., (C) 3, 69(1969).

2. Schroeder,"Polyepoxide emulsions and methods of treating textile therewith", U.S. patents 2872427, and 2872428, (1959).

3. H.G.Winton, Wyatt Wadi (Unisearch Ltd.), German Offen., 2213051 Oct (1972), Australian applied 4365, March(1971).

4. J.W.Vanderhoff, M.S.ElAasser, J.A.Manson, G.W.Poehlien, K.A.Earhart, and S.C.Misra, Unpublished research results, Lehigh University, 1972-1977.

5. T.Murayama, and J.P.Bell, J.Polym.Sci.,A-2, 8,437(1970).

6. T.Hirai and D.E.Kline, J.Appl.Polym.Sci., 16,3145,(1972).

7. T.Hirai and D.E.Kline, J.Appl.Polym.Sci., 17,31,(1973).

8. D.A.Whiting and D.E.Kline, J.Appl.Polym.Sci.,18,1043(1974).

9. K.Selby and L.E.Miller, J.Mat.Sci.,10,12(1975).

10. N.Hata and J.Kumanotani, J.Appl.Polym.Sci.,15,2371(1971).

11. R.E.Johnson and A.L.Fricke, Proc. Cont. Reinf. Plast./Compos. Div., Soc.Plast. Ind.,27, 19F, 1(1972).

12. M.Kitoh and K.Suzuki, Kobunshi Ronbunshu,33,1,19(1976).

13. A.S.Kenyon and L.E.Nielsen, J.Macromol.Sci.,Chem. A3,(2), 275(1969).

14. N.Hata and R.Yamuchi, J.Appl.Polym.Sci., 17,473(1973).

15. N.Hata and J.Kumanotani, J.Appl.Polym.Sci., 21,1257(1977).

16. A.E.Moehlenpah, O.Ishai, and A.T.Dibenedetto, J.Appl.Polym.Sci., 13,1231(1969).

17. J.A.Manson and E.H.Chiu, ACS Polymer Preprints, 14(1),469(1973).

18. J.A.Manson and E.H.Chiu, J.Polym.Sci.-Symp.No.41,95(1973).

19. A.C.Meeks, Polymer, 15,675(1974).

20. W.S.DeRosset, J.Composite Mat., 9,114(1975).

21. W.D.Bascom, R.L.Cottington,R.L.Jones, and P.Peyser, J.Appl.Polym.Sci., 19,2545(1975).

22. I.Galparin, J.Polym.Sci., 11,1475(1967).

23. T.B.Lewis and L.E.Nielsen, J.Appl.Polym.Sci., 14,1449(1970).

24. P.Michael,P.Ebdon, and O.Delatycki, J.Polym.Sci.,Polym.Phy. ed., 12,1555(1976).

25. P.Peyser and W.D.Bascom, Polym. preprints, 17(2),157(1976).

26. G.T.Merrall and A.C.Meeks, J.Appl.Polym.Sci.,16,3389(1972).

27. R.J.Morgan and J.E.O'Neil, in "Chemistry and properties of crosslinked polymers", ed. by S.S.Labana, Academic Press, N.Y.,(1977), p. 289.

28. K.Suzuki et al., Kobunshi Ronbunshu, 33(5), 271(1976).

29. C.L.Brett, J.Appl.Polym.Sci., 20, 1431(1976).

30. J.P.Bell, J.Appl.Polym.Sci., 14, 1301(1970).

31. S.S.Labana,S.Newman, and A.J.Chompff, in "Polymer Networks" ed. by A.J.Chompff and S.Newman, Plenum,(1971), p.453.

32. M.Schrager,J.Polym.Sci., A-2,8,1999(1970).

33. J.O.Outwater and M.C.Murphy, 26th Annual Tech.Conf.,1971, Reinforced Plast./Comp. Div.,The S.P.I. Inc.,Sect. 10 A, p.1 .

34. S.A.Sutton, Eng.Fract.Mech.,6,587(1974).

35. B.Tomkins and W.D.Biggs, J.Mat. Sci., 4, 544(1969).

36. S.L.Kim,M.Skibo,J.A.Manson,R.W.Hertzburg, and J.Janiszewski, Polym.Eng.Sci. (in press).

37. A.T.DiBenedetto and A.D.Wambach, Int.J.Polym.Mat. ,1,159(1972).

CHAPTER II

EXPERIMENTAL

A. IDENTIFICATION AND SAMPLE PREPARATION FOR THE STUDY OF BULK CURED EPOXY NETWORKS

Several series of epoxy networks were prepared using a homologous series of diglycidyl ether of bisphenol-A (DGEBA) prepolymers and a common curing agent, methylene dianiline (MDA). Systems include blends to achieve equal equivalent weights but different distributions of molecular weight (and M_c), and also homopolymers of varying molecular weight to provide additional standards for comparision. Characteristics of those and related resins are described below.

a. Structure of Epoxies and Curing agent

All the epoxy prepolymers used in this study have the following structure:

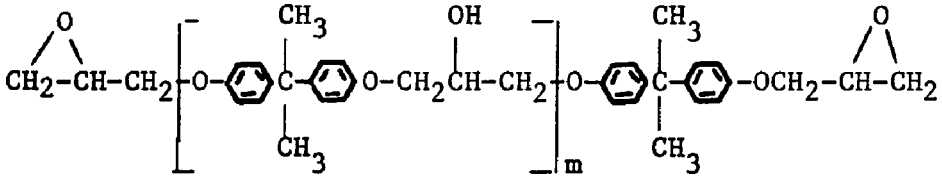

where m varies from 0 to 24 (1). As supplied commercially, a distribution of composition usually exists(2,3).

The curing agent is available in several forms and purities, the essential component being methylene dianiline (MDA), also called p,p'diaminophenyl methane (DDM). The structure is

given below.

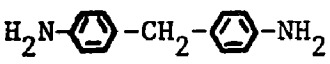

b. Stoichiometry and M_c

For estimation of M_c, the calculation of Bell(4) was employed. Bell developed equations for M_c based on the stoichiometry of the curing reaction and the amount of primary amine and epoxy groups remaining in the polymer at a given time. The calculated values were shown to agree with the values estimated from measurements of swelling and the polymer solvent-interaction term χ_1. With curing conditions used in Bell's study as well as in this study, several idealized structures may be expected, depending on the stoichiometry. In principle, the epoxy prepolymer is difunctional and the amine tetrafunctional so that under conditions of equivalence of functional groups, the following reaction will occur :

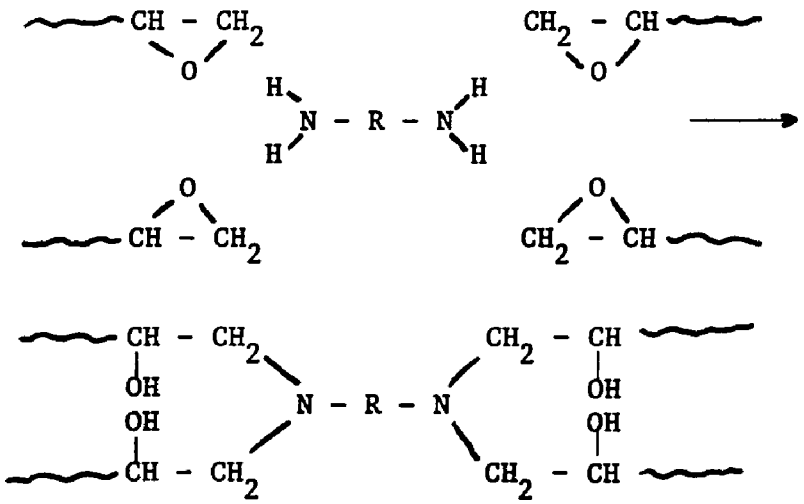

(1)

At other stoichiometries, structures can be readily visualized by reference to Bell's paper. For the case of equal stoichiometry M_c is given by the following equation (4):

$$M_c = (aM_A + bM_B)/3(b-a) \qquad (2)$$

where, a and b are the number of moles of amine and epoxy, respectively, (b=2a) ; M_A and M_B are the molecular weights of the amine and epoxy, respectively.

c. Identification

Series A (Varying Stoichiometry)

Epon 828 (epoxy resin) and Tonox (MDA, curing agent) of Shell Chemical Co. were used as received. The compositions of the different samples are given in Table I.

TABLE I. NETWORKS FROM VARYING STOICHIOMETRY.

Designation	Amine/Epoxy Ratio	M_c (theoretical)[a]
A-7	0.7 : 1	1523
A-8	0.8 : 1	526
A-9	0.9 : 1	383
A-10	1.0 : 1	326
A-11	1.1 : 1	370
A-14	1.4 : 1	592
A-16	1.6 : 1	924
A-18	1.8 : 1	1922
A-20	2.0 : 1	∞(linear)

[a] For reasons discussed by Bell(4) actual M_c values for specimens A-16 to A-20 may be in error. In any case, the error will not affect any trends observed in properties as a function of stoichiometry.

Series E (Unblended Resins, equal stoichiometry)

To provide a baseline for examining the effects of M_c at constant stoichiometry, resins based on the following prepolymers were synthesized using MDA as the curing agent: Epon 825, 828, 834,1001,1002, and 1004.

TABLE II. NETWORKS FROM VARYING PREPOLYMER M.W.

Designation	Epon Prepolymer	M.W.[a] of Prepolymer	m[a]	M_c(theo.)[b]	Avg. no. of C's in the epoxy Molecules
E-1	825	352	0.042	308	10
E-2	828	380	0.141	326	11
E-3	834	542	0.711	430	15
E-4[c]	834	542	0.711	493	15
E-5[d]	1001	1000	2.32	740	26
E-6[d]	1002	1360	3.38	980	36
E-7[d]	1004	2000	5.41	1400	47

[a]Calculated from epoxy equivalent (equivalent weight in terms of epoxy functionality) determined by the ASTM D 1652-67 method.

[b]M_c calculated from stoichiometry using equation 2

[c]Inadvertent deviation from precise stoichiometry.

[d]Solid prepolymers.

Series F (Bimodal-distribution Blends)

It was possible to vary the distribution of M_c by preparing blends of epoxies that had the same average M_c values as Epon 828, Epon 834, and Epon 1001. This was done by blending Epon 825 (narrow distribution of molecular weight) with Epon 1004. Distributions of M_c may be expected to be essentially bimodal, with a little overlap. Details are given in Table III.

TABLE III. NETWORKS FROM VARYING DISTRIBUTION OF M.W.

Designation	Epoxy Equivalent	M_c (theor.)	wt. % Epon 825 in blend[a]
F-1	190	326	90.96
F-2	225	413	61.86
F-3	260.5	419	60.01
F-4	271	430	56.85
F-5	500	740	20.24

[a]Blend with Epon 1004. F-1, F-4, and F-5 are equivalents of Epons 828, 834, and 1001, respectively.

Series G (Different curing agent)

Sample G-1 was prepared by curing Epon 828 with Versamid 140 (General Mills Chemical Co.) at stoichiometric ratio of unity.

d. Preparation and curing

Samples of series A,E, and F, were prepared as given below.

For systems using liquid epoxy prepolymers with MDA as the curing agent, the curing cycle was similar to that used by Bell(4). After heating to 80°C, the resin and curing agent were mixed together, evacuated for 5 to 15 mins. to remove air bubbles, cast and cured as follows: 45 mins. in a circulating air oven at 60°C, 30 mins. at 80°C, 2.5 hrs. at 150°C, and finally slow cooling to room temperature. The mold assemblies comprised clamped 13-cm by 13-cm Mylar sheets, separated by 0.5-mm, 1.5-mm, or 6-mm Teflon or etylene-propylene copolymer spacers backed by glass plates. This cure cycle was reported by Bell to give complete curing.

Solid epoxies were first melted and then evacuated to remove the entraped air bubbles. In order to avoid air entrapment the curing agent was mixed in using a magnetic stirrer, under vacuum. Thick and thin samples were prepared using the following curing cycle: 1.5 hr at 100°C, 2.5 hr at 150°C, followed by slow cooling to room temperature.

Sample G-1 was prepared using the cure cycle described by Manson and Chiu(5), which is: overnight curing at room temperature, 2 hr at 60°C, 2 hr at 100°C, and 4 hr at 140°C.

Using these techniques it was possible to prepare reproducible samples suitable for testing, albiet with considerable

difficulty in the case of solid epoxies.

B. IDENTIFICATION AND SAMPLE PREPARATION FOR THE STUDY OF EMULSION CURED EPOXY NETWORKS

a. Materials and preparation of latexes

Epon 1001 (Shell Chemical Co., epoxy equivalent[1] 500) and Versamid 115 (a room-temperature curing agent, General Mills Chemical Co., amine equivalent[1] 235) were used as co-reactants. A Versamid curing agent is especially useful in a study of this kind because its molecules have an unsaturated double bond that can be stained by osmium tetroxide.

All emulsions were prepared separately by a direct emulsification technique(6,7), using a mixed emulsifier system of hexadecyltrimethylammoniumbromide (HDTMAB) with cetyl alcohol or n-decane. The emulsification procedure used for the preparation of the latex system was based on the earlier development of the mixed emulsifier system(8), which gives stable styrene emulsion droplets of about 200-nm diameter. The preparation of aqueous cationic epoxy resin and curing agent latexes comprised dissolving the resin in a water immiscible solvent, adding the solution to an aqueous solution of the mixed emulsifier system to form a crude emulsion and homogenizing using the Manton-Gaulin Submicron Disperser. The emulsions produced were stable when subjected to steam

[1]The terms "epoxy equivalent" and "amine equivalent" signify the equivalent weight of each component in terms of the epoxy and amine functionalities, respectively.

stripping under vacuum to remove the solvents. The solids content of the latexes after stripping were adjusted to about 40% for the epoxy emulsions and 15% for Versamid emulsions.

b. Identification

The various combinations evaluated and variations in treatment are listed in Table IV. In all cases, epoxy and amine concentrations corresponded to stoichiometric equivalence.

TABLE IV. COMPOSITIONS AND PROCESSING OF EPOXY/POLYAMIDE SYSTEMS EVALUATED.

System	Composition	Sample Designation				
		Series B[a]	Series C[b]	Series D		
I	Epon 1001- V-115	B-1	C-1	D-1[c]	D-2[d]	D-4[b]
II	Epon 1001-V-115 (aged in mixture at 55°C for 15 min. prior to casting)	B-2	C-2			
III	(Epon 1001-bisphenol-A 96/4 wt ratio) and V-115	B-3	C-3			
IV	Epon 1001-(V-115 Dion DPM-3-800-LC , 2/1 wt ratio)	B-4	C-4			
V	Epon 1001- V-115 (Control, cast from 1:1 toluene: methyl-isobutyl ketone)	B-5	C-5	D-3[c]		

[a]Emulsion curing done at room temperature.

[b]Samples were later post cured at a curing cycle of 2hr. at 60°C 2hr. at 100°C, and 4hr. at 140°C.

[c]Cured at 50°C, 24 hr.

[d]Cured at 50°C, 48 hr.

It has been reported(9) that traces of bisphenol-A (2,2-bis(4'-hydroxyphenyl) propane) form hydrogen bonds between the epoxy and phenolic hydroxyl groups, thus facilitating the opening of the epoxy ring by amine. Dion DPM-3-800-LC, a mercaptan-terminated polymer of high viscosity (Diamond Shamrock Chemical Co.), is also reported to cure epoxy systems rapidly in combination with amines.

c. Preparation and curing

Film formation was studied by casting 0.05-mm thick films of samples B-1 to B-4, at 20°C and 50% R.H., on glass microscope slides then replicating their surfaces at different aging times.

For mechanical characterization the different combinations described in Table IV were allowed to stand for from 15 to 20 min. at room temperature so that the entrapped air bubbles could escape. Thin films (0.12-mm to 0.20-mm thick) were cast on glass plates treated with Mold Release 225 (Ram Chemical Co.). Emulsion curing was effected at room temperature, at several elevated temperatures, and with several curing cycles, as shown in Table IV.

C. SAMPLE PREPARATION FOR THE STUDY OF THE EFFECT OF PREPOLYMER STATE

Epoxy prepolymers (Epon 1001, Epon 1002, and Epon 828) were cured in bulk, solution, and emulsion with stoichiometric amounts of MDA. Emulsions of all the prepolymers were prepared by the direct emulsification technique discussed earlier in section B.

Laboratory-grade acetone (J.T. Baker Chemical Co.) was used as the solvent. Except for a few modifications for solvent-based systems, curing of the prepolymers in bulk, solution, and emulsion was done by the same general procedure described in section A. For solvent-based systems the high-temperature curing cycle was employed after the evaporation of most of the solvent at room temperature. This modification helped to avoid solvent bubbling and to achieve bubble free samples. Bell(4) has shown that crosslinking does not take place in the presence of acetone. Therefore, it can be assumed that negligible curing took place in the solvent- based samples during the process of solvent evaporation at room temperature.

D. GENERAL CHARACTERIZATION OF THE NETWORKS

a. Crosslink Density

Properties of crosslinked networks depend on the degree of crosslinking, which is conveniently specified through the M_c. The value of M_c can be determined theoretically on the basis of the chemical structure and stoichiometry of the prepolymers and experimentally by swelling or rubbery modulus measurements(4,10). For highly crosslinked networks, none of these methods give exact values; nevertheless, they are very useful in correlating structural differences of networks to their properties(11,12). Although the kinetic theory of rubber (see Equation 3) is not valid for highly crosslinked networks it was used as a relative comparison of the present epoxy networks.

$$G = nRT = \rho RT/M_c \qquad (3)$$

where G is the shear modulus, ρ the density, n the number of moles of network chains per unit volume, and M_c the average molecular weight between crosslinks.

M_c values were calculated from the swelling data using the Flory-Rehner equation(10).

$$\frac{V_1}{\overline{V} M_c} = \frac{\ln(1-V_{2m}) + V_{2m} + \chi_1 V_{2m}^2}{V_{2m}^{1/3} - 2V_{2m}/f} \qquad (4)$$

where V_1 = molar volume of the solvent,

$\overline{V}$ = specific volume of the polymer,

V_{2m} = volume fraction of the polymer in the swollen material at equilibrium,

χ_1 =polymer solvent interaction parameter,

f = functionality of the network (f=3, for the present case)

When experimental data are not available χ_1 can becalculated theoretically from the Huggins(13) equation:

$$\chi_1 = \beta + \frac{V_1(\delta_1 - \delta_2)^2}{RT} \qquad (5)$$

where δ_1 = solubility parameter of the polymer,

δ_2 = solubility parameter of the solvent ,

β = constant = (1-1/m)/Z ;Z=coordination no, m=chain length.

For Versamid-115 cured epoxies the value of β was taken as 0.3 because Scott and Magat(14) had shown that this value of β gave reasonable values of χ_1 for all solvents. For poor solvents the solubility parameter for Epon 1001 is given(15) to be in the

range of 21.67x 10^3 to 22.69 x 10^3 $(J/m^3)^{1/2}$ and for toluene it is 18.2 x10^3 $(J/m^3)^{1/2}$. Using these values χ_1 for toluene was calculated as 0.97.

b. Dynamic Mechanical Spectroscopy

Measurements of complex Young's moduli were made using a Rheovibron viscoelastometer, model DDV-11, (Toyo Measuring Instrument Co.). The instrument applies a sinusoidal tensile strain to one end of a sample, and measures the stress sensed at the other end. Transducers permit the reading of the absolute dynamic modulus, E^* (the ratio of maximum stress to maximum strain) and the phase angle δ between the strain and the stress. The storage modulus E', the loss modulus E", and the dissipation factor, $\tan\delta$, are given as follows:

$$E' = E^* \cos\delta$$
$$E'' = E^* \sin\delta \qquad (6)$$
$$\tan\delta = E''/E'$$

E" and $\tan\delta$ are measures of the energy dissipated irreversibly, and E' is a measure of the energy stored reversibly Measurements were made, depending on the curing agent, over a temperature range from -80°C or -45°C to about 40°C above T_g, at 110 Hz and a heating rate of 1°C/min. Icing of the specimens at low temperature was avoided by sweeping dry nitrogen through the chamber. The absolute value of $\tan\delta$ in the glassy region as determined by the Rheovibron was very sensitive to the cross-sectional area of the test specimens. The range of cross-sectional areas checked was 10^{-3} to 10^{-2}

cm^2. However, cross-sectional area did not affect the tanδ values in the transition region. Therefore, to avoid any discrepancy, measurement of tanδ in the glassy region was made at a constant cross-sectional area of 0.77×10^{-3} cm^2.

The β-transition has been observed in epoxies in the range of -60°C to -100°C, depending on the frequency of test(16-28). The general consensus(16-21,23,25)is that the β-transition is caused by the rotation of the hydroxy-ether linkage, $-CH_2CH(OH)CH_2O-$, which is the reaction product of the epoxy and the amine groups. Since β-transitions have also been observed in epoxy networks which do not have the hydroxy-ether linkage(18,21,24), some investigators(26) have proposed that the diether linkage of bisphenol-A is responsible for them, although this would require that the backbones of the epoxy components be in a stretched conformation. The actual mechanism is still a matter of controversy.

c. Tensile Study

Tensile studies were done on the Instron tester at room temperature, according to ASTM test D-638-68, type IV, with a crosshead spead of 1mm/sec (0.05"/sec). Young's modulus, E, ultimate tensile strength, σ_u, yield strength, σ_y, and ultimate elongation, ε_u, were determined. Three to four specimens per sample could be obtained, in all cases, that did not fail prematurely.

d. Impact Tests

Impact resistance of a material is the ability to dissipate the energy of an impact through non-destructive mechanical

loss processes and therefore is generally desired even at the cost of some loss in modulus. Since a mechanical loss process is related to impact resistance, it may appear that the dynamic mechanical loss property would be related to impact strength. Indeed, for many thermoplastics it has been shown(29-40) that various correlations do exist between toughness and secondary dynamic mechanical loss at or below room temperature. Several investigators have dealt with the integration of the dissipation factors between two arbitrary temperatures, or to the presence or the absence of low temperature loss peaks. Recent studies(36-40) have indicated that impact strength (toughness) does not arbitrarily depend on the secondary loss peak of the dynamic mechanical loss spectrum, but is correlated to the dynamic dissipation factor at the temperature and equivalent frequency of the impact. Higher values of the dynamic energy dissipation at the test conditions result in higher impact strength. Clearly the energy dissipation would be accomplished more by the main chain motion than that of the side chains.

Impact tests were conducted according to the ASTM test D-256-70, method B (Charpy type, notched). On the average 4 to 5 specimens were tested.

e. Creep Study

Studies of creep as a function of time and temperature were carried out using a Gehman Torsional Stiffness Tester(41). Creep experiments covered the entire range of viscoelastic behavior

from the glassy to the rubbery region. Modulus readings were taken at various intervals of time between 10 sec and 1000 sec. The inverse compliance, 1/J(t), was calculated from the angle of twist of the specimen induced by the torsion wire as indicated by the apparatus, and Young's modulus, E(t) was assumed to approximately equal 3/J(t).

Master curves were obtained by shifting data obtained at various temperatures with respect to a reference temperature. Each curve of reduced modulus was shifted with respect to the curve at 129°C (reference temperature) until all fit together to form a smooth curve. Master curves for various materials could then be easily compared. Temperatures corresponding to a value of 0.2 GPa for E(10 sec) were taken as T_g's.

f. Swelling, Extraction and Density Measurements

Swelling measurements were conducted at room temperature for MDA-cured samples, using acetone as the solvent. It has been shown(42) that solvent may act as a plasticizer, thus increasing the diffusivity of the reactants and helping in further reaction. Therefore, the swelling tests for Versamid-cured samples (expected to have incomplete curing) were conducted at -20°C to reduce the reactivity of the curing agent so that curing becomes reaction-controlled instead of diffusion-controlled. Toluene was used as the solvent for these samples. Equilibrium swelling was achieved within 15 days, and swell-ratios, q, were calculated from the formula:

$$q = \frac{\text{swollen volume of the network}}{\text{extracted, dry volume of the network}} \qquad (7)$$

Density measurements were made at room temperature, 20°C, using the density gradient method. Duplicate runs were made in all cases.

g. Degree of cure and unreacted functional group analysis

A differential scanning calorimeter (DSC 1-b, Perkin Elmer Corporation) was used to determine the extent of cure; 10-mg to 20-mg specimens were tested at a scanning rate of 10°C/min. Differential scanning calorimetry gives a measure of the difference in the rate of heat absorption or release by a sample with respect to an inert reference as the temperature is raised at a constant rate. An exothermic peak on the thermograph indicates the heat of reaction whereas an endothermic peak in the amorphous polymer indicates the presence of residual stresses or the occurrence of a transition such as T_g. The presence of an exothermic peak in the DSC-scan of a pre-cured sample is an indication of incomplete curing.

The unreacted epoxy and amine groups present in the samples (degree of cure) was determined by chemical titration, using the procedure outlined by Bell(4) with a slight modification. Cured epoxy samples were filed and about 1 gm of powder was placed into a round-bottomed flask with 50 ml of 0.2N pyridinium chloride, 50 ml of reagent isopropanol, and 25 ml of distilled water. The mixture was refluxed for 30 min and stirred continuously

with a magnetic stirrer. After cooling to room temperature this solution was poured into a 250-ml beaker. Using a potentiometer and a burete, standardised 0.505N NaOH was added in 5-ml increments until the pH increased to 7.0. From this point, 0.2-ml increments were added until a sharp increase in pH was noted (pH ca 10.5). Then 5 ml of CS_2 was added and stirring was continued for 1/2-hr (pH decreased to 8.0 to 8.5). The titration was continued further by adding 0.2 ml of 0.505N NaOH every 10 min until the amine end-point was reached (pH ca. 10.5). Since the response in the amine titration region was very slow and the pH did not stabilize until 8 to 10 min. after each addition of NaOH, the readings were made at 10-min intervals.

h. Electron Microscopy

Various techniques were tried to study the micro- or macro-structure of MDA-cured epoxy networks ("macro" implying a morphological feature on the scale of 1 μm or larger). After the examination of the etched samples under the SEM it was concluded that Cr_2O_3 etching was more effective than the following techniques: etching for 30 min with HF acid; etching for 15-days with acetone; etching for 10 hr with argon at high voltage under vacuum; ething for 7 hr with a 1 M aqueous solution of Cr_2O_3 at 80°C. The study of etching time indicated that atleast one hr was needed to produce adequate etching with Cr_2O_3. Chemical etching renders the lower molecular weight polymer constituents more soluble in water without appreciably affecting the solubility of the high molecular

weight material. If the high molecular weight material is connected by weak bonds to the matrix then these weak bonds would be attacked first thus etching out the unattached high molecular weight material first, before etching the low molecular weight matrix. To study the microstructure of the cured resins, etching times of four and seven hours were found convenient for samples having M_c's above and below- 500, respectively. The gross morphology was studied under the SEM, while the fine structure was studied under the transmission electron microscope (TEM), using two-stage carbon-platinum replicas of the etched surfaces. One must be very careful in interpreting statements about features seen in replicas. A bump on a two-stage replica arises from a dimple on the polymer surface.

The network structure of the Versamid-115 -cured samples was determined by examining stained microtomed sections (60-nm thick) under the TEM (Phillips 300). Staining was effected by exposure to osmium tetroxide vapors for one week.

The particle size distribution of the latexes was measured using cold-stage electron microscopy. The emulsion was diluted to 10 ppm, and a drop placed on a polymer coated grid which was in turn placed on the cold stage of the electron microscope. To prevent distortion of the particles, the specimens were freeze-dried in situ.

Morphological changes during stage-1 of film formation (see Chapter V for the discussion of the various stages) were

studied by measuring the particle dimensions of the Versamid-115-epoxy emulsion mixtures at different aging times, using cold-stage electron microscopy. Film formation during stages II and III was studied by making two-stage carbon-platinum replicas at various aging times up to 33 or 45 days.

REFERENCES

1. C.A.May and Y.Tanaka, ed., "Epoxy Resins, Chemistry and Technology", Marcel Dekker Inc., N.Y., 1973.

2. H.Batzer and S.A.Zahir, J.Appl.Polym.Sci.,19,585(1975).

3. W.A.Dark,E.C.Conrad,and L.W.Crossman, J.Chromat.,91,247(1974).

4. J.P.Bell, J.Poly.Sci.,A-2, 8, 417(1970).

5. J.A.Manson and E.H.Chiu, J.Polym.Sci.-Symp.No.41, 95(1973).

6. M.S.El-Aasser, J.W.Vanderhoff, S.C.Misra, and J.A.Manson, J. of Coatings Technology, 49(635), 71(1977).

7. M.S.ElAasser, J.W.Vanderhoff, and G.W.Poehlein, ASC Priprints, Vol. 37, No. 2, 92(1977).

8. J.Ugelstad,M.S.ElAasser, and J.W.Vanderhoff, Polym.Letters, 11,503,(1973).

9. B.Nagy, Adesive Age, 10,20(1967).

10. P.J.Flory,"Principles of Polymer Chemistry",Cornell Univ.Press, Ithaca,N.Y., (1950); (a)p 464, (b) p 575.

11. D.A.Whiting and D.E.Kline, J.Appl.Polym.Sci.,18,1043(1974).

12. T.Murayama and J.P.Bell, J.Polym.Sci.,A-2,8,437(1970).

13. M.L.Huggins, J.Chem.Phys.,9,440(1941).

14. R.L.Scott and M.Magat, J.Polym.Sci.,4,555(1940).

15. H.Burrell, in "Polymer Handbook, second edition, J.Brandrup and E.H.Immergat, John Wiley and Sons, Inc., 1975, p IV-337.

16. D.H.Kaelble, SPE J., 15,1071(1959).

17. D.E.Kline,J.Polym.Sci.,47,237(1960).

18. C.A.May and F.E.Weir, SPE Trans.,207(1962).

19. F.R.Dammont and T.K.Kwei, J.Polym.Sci.,A-2,6,457(1968).

20. N.Shito and M.Sato, J.Polym.Sci.,C-16,1069(1967).

21. H.Van Hoorn, J.Appl.Polym.Sci.,12,871(1968).

22. O.Delatycki,J.C.Shaw, and J.G.Williams, J.Polym.Sci.,(A2), 7, 752(1969).

23. J.C.Patterson-Jones and D.A.Smith, J.Appl.Polym.Sci., 12, 1601(1968).

24. G.A.Pogany, Polymer, 11,66(1970).

25. R.G.C.Arridge and J.H.Speake, Polymer, 13-9, 443(1972).

26. E.F.Cuddihy and J.Moacanin, J.Polym.Sci., A-2,8,1627(1970).

27. T.Hirai and D.E.Kline, J.Appl.Polym.Sci., 17,31(1973).

28. Y.Fukasawa and E.Wada, Kobunshi Ronbunshu, 32,9,518(1975).

29. H.Oberst, Kunststoffe, 53,1(1963).

30. J.Heijboer, J.Polym.Sci.,(c), 16,3755(1968).

31. J.Heijboer, Br.Polym.J., 1,3(1969).

32. R.F.Boyer, Polym. Eng. Sci.,8,161(1968).

33. P.I.Vincent, Polymer, 1,425(1960).

34. Y.Wada and T.Kasohara, J.Appl.Polym.Sci.,11,1661(1967).

35. W.Retting, European Polym.J.,6,853(1970).

36. J.C.Radon, Polym.Eng.Sci.,12,425(1972).

37. P.I.Vincent, Polymer,15,111(1974).

38. M.D.Skibo,R.W.Hertzberg, and J.A.Manson,"Fracture" Proceedings of the fourth International Conf. on Fracture ,Waterloo, Canada, ed., D.M.P.Taplin,Vol. 3,p 1127(1977).

39. E.Sacher, J.Macromol.Sci.,B-9,163(1974).

40. E.Sacher, J.Appl.Polym.Sci., 19,1421(1975).

41. ASTM D-1043, American Soc. of Testing Materials,Phila.,Pa(1974)

42. A.S.Kenyon and L.E.Nielsen,J.Macromol.Sci.-Chem., A3(2), 275(1969).

CHAPTER III

EFFECT OF M_c AND DISTRIBUTION OF M_c ON THE ENGINEERING BEHAVIOR

A. INTRODUCTION

A good fundamental knowledge of relationships between characteristics, synthesis or processing, structure and mechanical and other properties is required of crosslinked networks used for critical and demanding applications. Epoxy resins, which are widely used in such applications, have received great attention in the past decade. In spite of the numerous papers that have covered many aspects of epoxies (see Chapter I) there is very little mention of the effect of M_c on the engineering behavior of networks prepared at equal stoichiometry. The few studies that exist(1,2) are of limited scope (cover a very narrow range of M_c and only deal with dynamic mechanical properties). Furthermore the existing studies do not deal with the question of the distribution of M_c in networks.

This chapter deals with the effects of M_c and the distribution of M_c on the engineering behavior of epoxy resins cured with stoichiometric amounts of curing agent. The crosslink density was varied by curing a homologous series of DGEBA prepolymers with a common curing agent, MDA, which gave networks (Series-E) having similar chemical structures but different M_c's. Similarly different distributions of M_c at the same average value of M_c were obtained by mixing the lowest and highest molecular weight resins of this homologous series such that the blends had the same molecular weight as

the commercial intermediates.

The following properties were characterized: M_c by swelling and measurements of rubbery modulus; the state of cure by DSC, chemical analysis, and DMS; viscoelastic response per se by DMS; and long term and short term loading characteristics by creep, stress-strain and impact tests.

B. RESULTS AND DISCUSSION

a. Distribution of molecular weights in the commercial Epon resins

The gel permeation chromatography(GPC) indicated that the liquid and semi-solid prepolymers (Epon 825, 828, and 834) were composed of m=0 (M.W.,340) and m=1 (M.W.,620) components. The percentage of m=0 and m=1 species was dependent on the average molecular weight of the prepolymer, as given in Table I. The solid prepolymers were composed as follows: Epon 1001, m=7 (M.W.,2328) m=3 (M.W.,1192) and m=1; and Epon 1002 and 1004, m=12 (M.W.,3748), m=3, and m=1 (the major component being m=12). The exact composition of each component in the solid prepolymers could not be determined because the peak of the m=3 component could not be completely resolved from the peaks of m=7 or m=12 components.

TABLE I. COMPOSITION OF THE COMMERCIAL EPOXY RESINS.

Sample	Epon Resin	M.W.	Components present in the prepolymer
E-1	825	352	m=0 (96%) and m=1 (4%)
E-2	828	380	m=0 (86%) and m=1 (14%)
E-3	834	592	m=0 (29%) and m=1 (71%)
E-5	1001	1000	m=1, m=3, and m=7 (major component)
E-6	1002	1360	m=1, m=3, and m=12 (major component)
E-7	1004	1996	m=1, m=3, and m=12 (major component)

The bimodal blends (Series-F) of Epon 825 and Epon 1004, therefore, had the following components: m=0, m=1, m=3, and m=12. The amount of m=0 component would be at a maximum in sample F-1 but at a minimum in sample F-5. On the other hand, samples F-2, F-3, and F-4 would have both m=0 and m=12 species in appreciable quantities.

b. Degree of cure

The degree of cure was determined by functional group analysis and differential scanning calorimetry. The unreacted amine and epoxy functional groups in the samples were determined by pH-titration following the method described by Bell(3). The results given in Table II indicate almost complete reaction in all samples. DSC also did not show the presence of exothermic peaks, nor did DMS indicate signs of further reaction. These results imply that the reaction of functional groups in all the samples went to completion.

TABLE II. UNREACTED EPOXY AND AMINE CONCENTRATION IN THE CURED SAMPLES.

Designation	Epoxy Content meq/g sample	Amine Content meq/g sample
E-1	0.00	0.00
E-2	0.06	-0.02
E-3	0.00	0.00
E-4	0.09	-0.04
E-5	0.04	0.00
E-6	0.03	0.00
F-1	0.00	0.00
F-2	0.00	-0.09
F-3	0.03	0.03
F-4	0.04	0.04
F-5	0.09	0.06

c. Dynamic mechanical properties

The different parameters characterizing the dynamic mechanical behavior of Series E and Series F are summarized in Table III and shown in Figure 1 (for Series E, only).

To a good approximation, the viscoelastic behavior of the epoxy networks of Series E is governed by M_c and hence the average crosslink density. Several of the viscoelastic parameters will now be discussed in more detail.

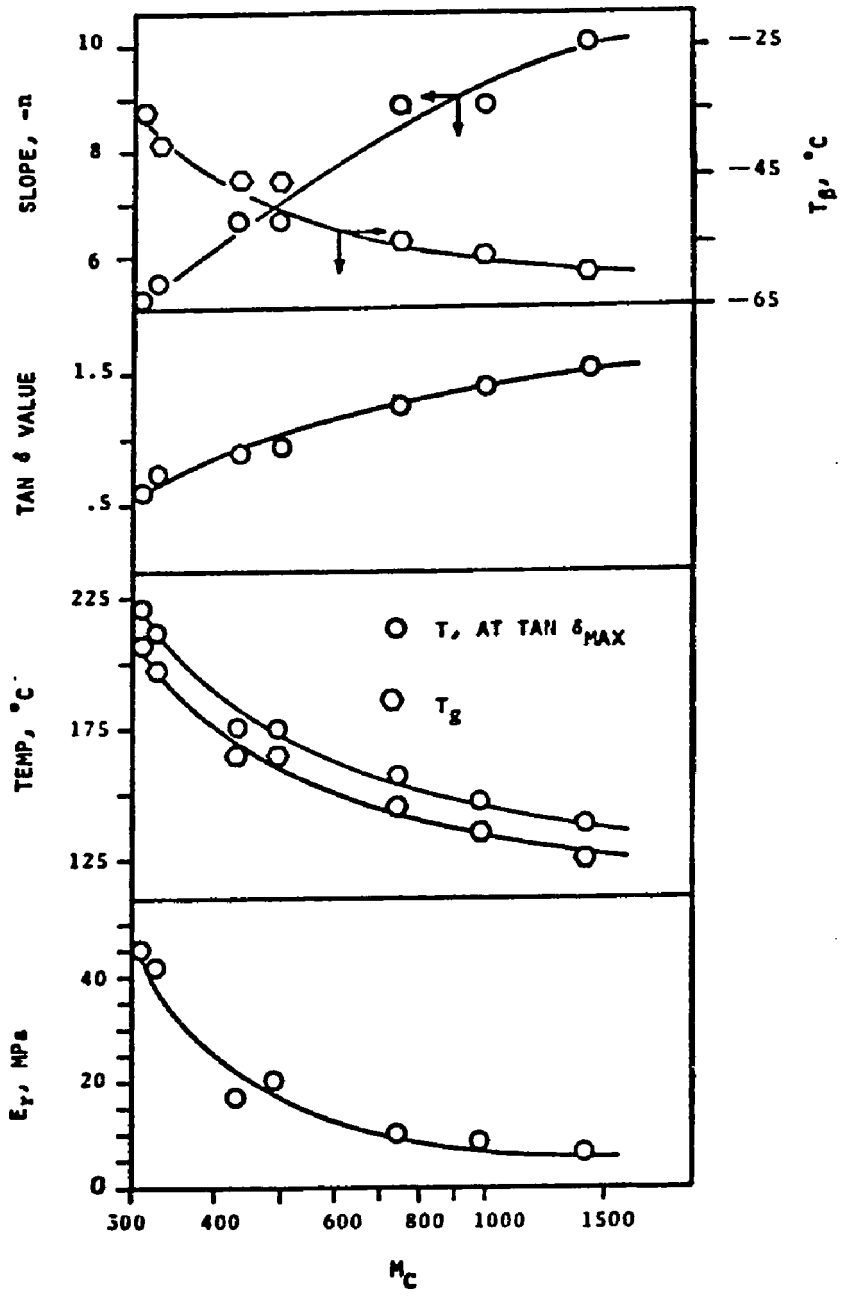

Figure 1. Dynamic mechanical behavior of Series E networks.

TABLE III. DYNAMIC MECHANICAL PROPERTIES OF SERIES E AND SERIES F EPOXY NETWORKS.

Specimen	M_c (theor.)	T_β[a],	Tan δ_{max} (at T_α)		T_g,	E', GPa[c] x 10		$-n$[d]
			Value	T, °C	°C	E'_r	E'_g[b]	x10^2
E-1	308	-35	0.62	221	207	0.45	22	5.2
E-2	326	-40	0.75	211	197	0.42	21	5.6
E-3	430	-46	0.90	175	165	0.17	20	6.7
E-4	493	-46	0.95	175	165	0.21	20	6.7
E-5	740	-55	1.25	157	145	0.10	19	9.1
E-6	980	-57	1.40	147	135	0.085	18	9.1
E-7	1400	-60	1.52	138	125	0.065	18	10.0
F-1	326	-40	0.75	211	197	0.42	21	5.6
F-2	413	-45	0.75	185	174	0.21	21	5.6
F-3	419	-45	0.80	175	166	0.17	21	5.9
F-4	430	-46	0.75	168	150	0.17	20	5.6
F-5	740	-55	1.25	157	145	0.10	19	9.1

[a] From maximum in tan δ

[b] E'_g refers to the glassy state

[c] 1 GPa = 10^{10} dynes/cm^2

[d] $n = d(\log E')/dT$, at $T_g \pm 4$°C

Glass transition temperature: Values of T_g obtained from DMS were checked independently using DSC and the Gehman creep tester. As shown in Figure 2 , excellent agreement was obtained after allowance for the differences in the effective frequency. The dynamic tests were run at 110 Hz, and the creep tests had an effective frequency of 0.1 Hz (≡ 10-sec-measuring time). T_g's from the dynamic and creep tests differed by an average of 24°C, which is in good agreement with the prediction that T_g should increase by up to about 13°C per decade increase in frequency. Also, values of the temperature at which tanδ was a maximum were consistently about 8°C higher than T_g (obtained from peak in E"), as expected.

Dimarzio(4), using a thermodynamic criteria that the configurational entropy is zero at T_g, derived a correlation, given below, between T_g and degree of crosslinking(X).

$$T_g - T_o = (T_o K X)/(1-K X) = T_o K/(M_c - K) \qquad (1)$$

where, T_o is the T_g of the uncrosslinked network, M_c is the molecular weight between crosslinks, and K is a constant independent of the material.

However, several investigators(5-8) have experimentally shown that a similar but simple empirical equation, given below, can be used to correlate T_g to M_c for different polymeric networks.

$$T_g - T_o = K'/ M_c \qquad (2)$$

where, K' is a constant and is found to vary from 3.0×10^4 to 2.1×10^5, depending on the polymer.

The present epoxy networks prepared from commercial resins

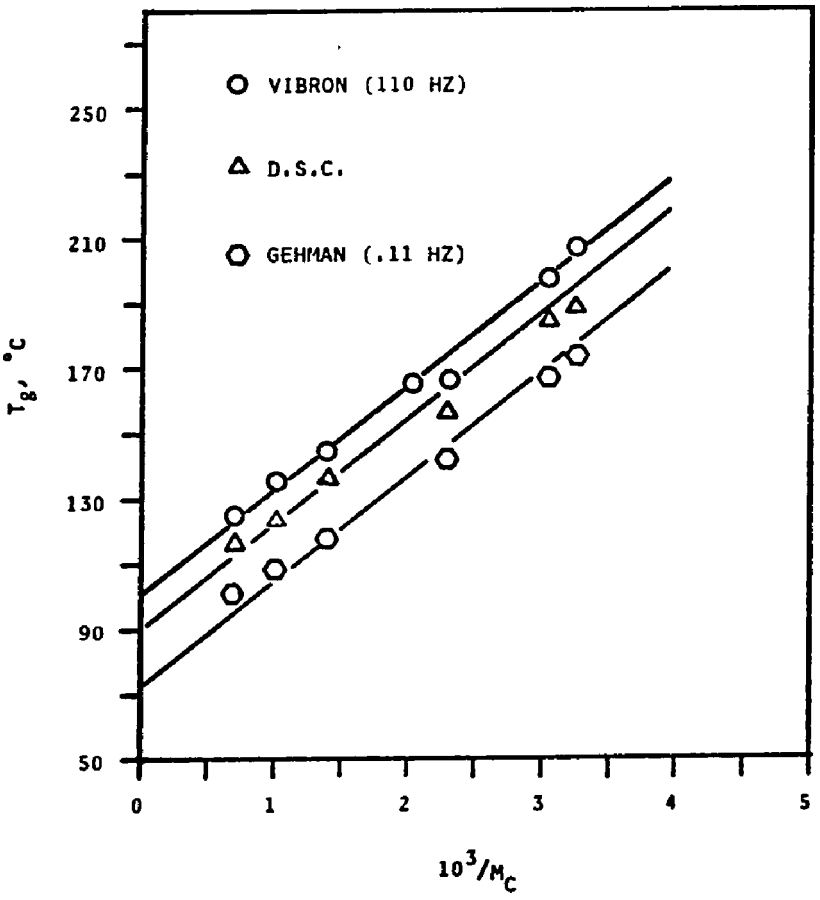

Figure 2. Glass transition temperature of Series E networks determined through different methods.

(series E) also followed the simple inverse relationship given in equation 2. For this case, T_o was 110°C (110 Hz) which was determined by extrapolating T_g at M_c=infinity; K' was found to equal 3.07×10^4.

Once established for a given epoxy system, equation 2 could be used as the basis for a simple test to determine M_c for any resin of the same type (of course, T_g is of interest in its own right). A major advantage is that T_g can be measured quickly and precisely by a variety of techniques, for example, DSC, which is more convenient and less time consuming than creep tests or DMS.

The effect of the distribution of M_c on T_g is shown in Figure 3. At M_c 430, the T_g of the blend sample F-4 was 13°C lower than that of its commercial counterpart sample E-3. This indicates that the longer chains, though present in the same amount as the shorter chains (see Section A-a), dominate the final network and thus control the T_g of the blend sample F-4. Due to the higher reactivity, the longer molecules react first (also see Chapter IV) to give microgels swollen with the unreacted smaller molecules which react later to form an interpenetrating network. Thus the secondary microgels result in a shell and core type structure (see Chapter IV). On the other hand, at M_c=326 and M_c=740, the blend samples F-1 and F-5 did not have a T_g different from their commercial counterparts, E-2 and E-5, respectively. At these M_c's big differences in distribution between blends and commercial resins could not be obtained because the possible permutations of distribution

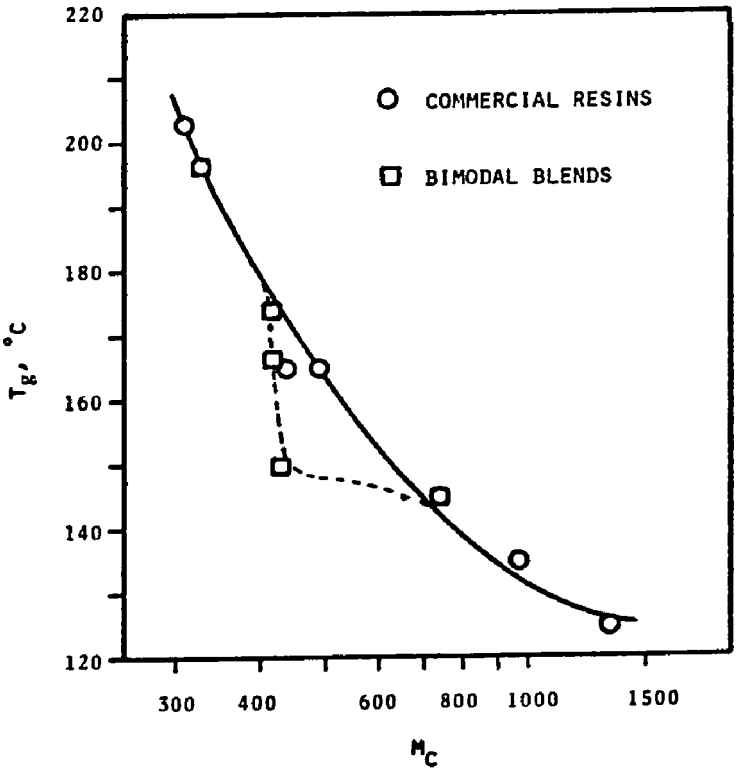

Figure 3. Glass transition temperature as a function of M_c for Series E and Series F networks.

at these M_c's was very restricted; at low M_c (326) Epon 825 was the major component (90%) whereas at high M_c (740) Epon 1004 was the major component (80%).

Young's Modulus: As expected, Young's modulus at room temperature, E'_g, was found to be nearly independent of M_c or the distribution of M_c (Table 3). All values fall within the range of 2 ± 0.2 GPa compared to an average of 1.3 GPa obtained from tensile stress-strain curves (to be discussed later).

Rubbery Modulus: The rubbery modulus, E'_r, was found to be related to the modulus in the glassy state, E'_g, and to $E'_{r\infty}$, the rubbery modulus of the network having $M_c = \infty$, by the following expression:

$$\frac{E'_g - E'_r}{E'_r - E'_{r\infty}} = K_1 (M_c - M_o) \qquad (3)$$

where, K_1 is a constant = 0.68, M_o is the value of M_c corresponding to E'_g (that is a value which corresponds to the case of no glass transition ; M_o = 262), and $E'_{r\infty}$ = 4 MPa (obtained by extrapolation.

It should be noted that Equation 3 is an empirical relationship which correlates M_c to E'_r and E'_g, and therefore should be quite useful. However, the simple theory of rubber elasticity, (see equation 3, Chapter II) which correlates M_c to E_r, and absolute temperature (T), also showed reasonable agreement with the experimental data

in many cases (discussed later). Figure 4 shows that the rubbery modulus of the present networks is unaffected by the distribution of M_c. Graessley(9) calculated the free energy of deformation and the equilibrium dimensions of network chains for networks of Gaussian random coils and showed that the elastic properties of such networks depend upon the total number of elastically active chains (average M_c) and elastically active junctions, but are independent of the chain length distribution (M_c distribution), junction functionality distribution, and the detailed pattern of connectivity. Thus, the present experimental results are in agreement with the theoretical predictions of Graessley.

Height of the tan δ peak: The value of the $\tan\delta_{max}$ increased asymptotically with M_c. The experimental data indicate that the value of the asymptote (i.e. at $M_c=\infty$) would be 1.9 . As expected, the bimodal blend samples F-2, F-3, and F-4, which showed broader transition regions than their counterparts of the commercial resin samples of Series E, also showed broader and flatter tan δ peaks, (Figure 5). This broadening is attributed to the broadening of the distribution of M_c.

Slope of the transition region: The slope (n) of the E' vs. Temperature curve also varied with M_c. The following expression was found to correlate the experimental data well:

$$\log_{10}(n/n_\infty) = -K_3/M_c \qquad (4)$$

where n_∞ = 0.119, (slope, n, for $M_c=\infty$), and K_3=110 for this case.

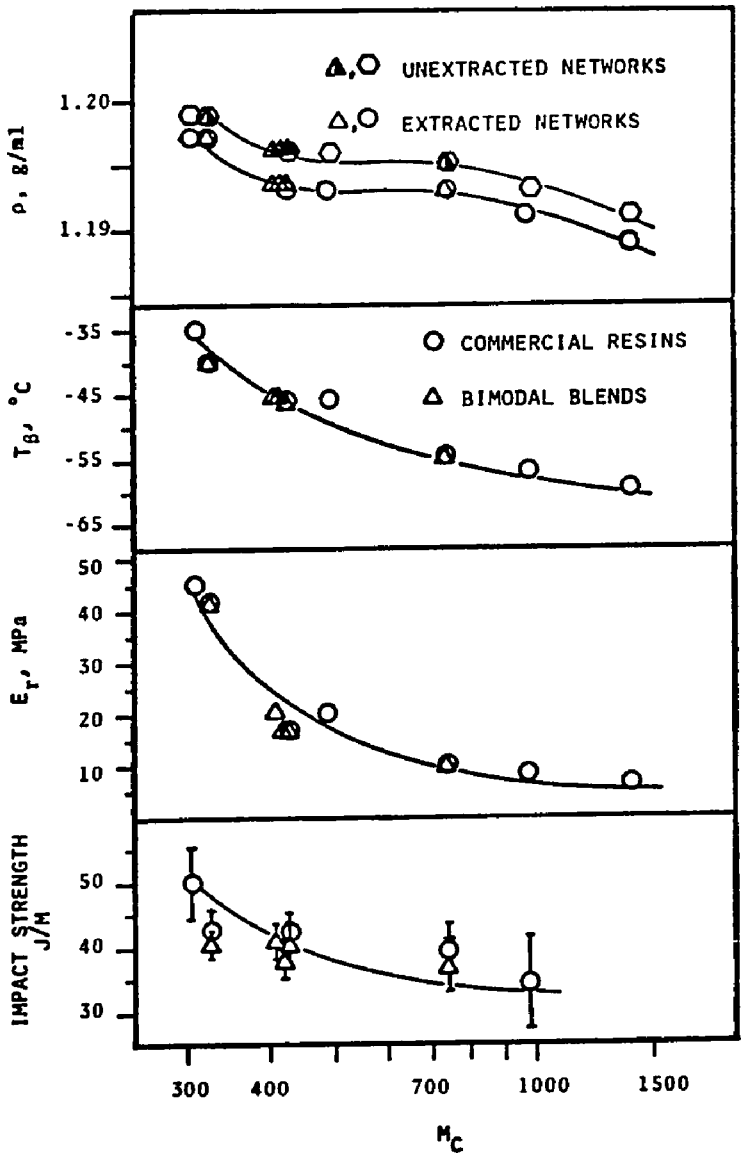

Figure 4. Impact strength, E_r, T_β, and density as a function of M_c for Series E and Series F networks.

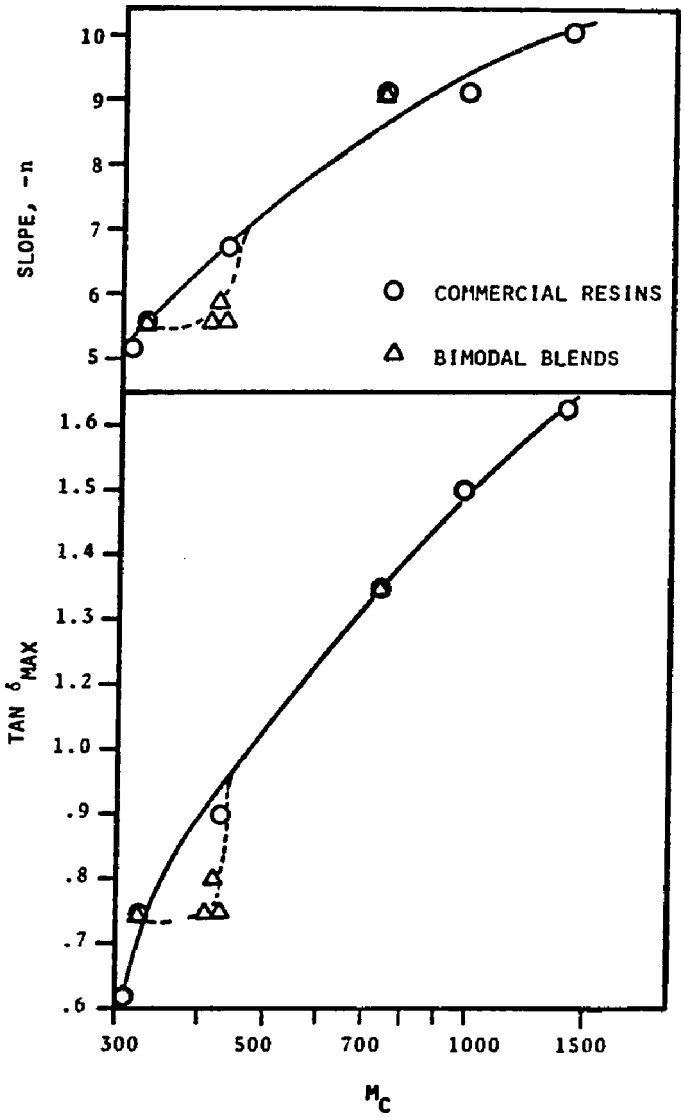

Figure 5. Tanδ_{max} and slope of the transition region as a function of M_c

In all the cases a correlation coefficient greater than 0.99 was obtained.

In accordance to the creep results (discussed later) the slope of the glass transition region, obtained from the dynamic mechanical data (see Figure 5), of the blend samples F-1, F-2, F-3, and F-4 was close to that of the commercial-resin-sample E-1 whereas, the slope of the blend sample F-5 was steeper than that of its commercial counterpart, sample E-5. The broadening of the transition region of the blend samples F-1 to F-4 is attributed to the presence of broad distributions of M_c in them.

Kwei(4) and Delatycki et al.(2) have studied a DGEBA system cured with a homologous series of diamine. Both of these studies were of limited scope, and covered a very narrow range of M_c's (245 to 295) as compared to the present range of M_c's (308 to 1400). Therefore, data points of those studies fell very close to each other, making it difficult to compare them with the present correlations.

β-Transition Temperature: The β-transition temperature increased with M_c but was unaffected by the changes in the distribution of M_c. This is so because T_β is a result of the motion of small segments of the main chain and not the entire main chain itself. T_β therefore depends on the average M_c than on the distribution of M_c, as can be seen in Figure 4.

Pogany(11), and Arridge and Speake(12), observed a similar behavior when they changed M_c by changing the degree of cure or stoichiometry (in the case of epoxy excess only). On the other hand, Delatycki et.al.(2) did not find any appreciable changes in T_β when they changed the M_c by changing the length of the amine molecule. The following is proposed to explain the above discrepancies: The crosslink junctions cause steric hindrances to the motion of the flexible chains which are generally formed as a result of epoxy-amine reaction. In the case where the crosslink density is varied by changing the length of the amine molecule the T_β is unaffected because the steric hindrance caused by the network junctions does not change. In the case where the crosslink density is increased by an increase in the degree of cure or by moving towards stoichiometry, the steric hindrance caused by the network junctions increases because of the increase in the number of the crosslink points and results in a higher T_β. In the present study the crosslink density was varied by changing the length of the epoxy molecule. A change in its length causes a change in the number of flexible chain segments present in the central portion of the molecule (see the structure shown in Chapter II). These chain segments, being located in the center of the molecule are not affected by the crosslink junctions. Thus, when the crosslink density is decreased by increasing the length of the epoxy molecule, the nuber of flexible chain segments that are free from steric hindrances of the crosslink junctions is increased, resulting in a lower

T_β. The three different ways of varying M_c are illustrated in Figure 6. The β-transition temperature was also found to be linearly related to the bulk density of the networks (Figure 7). The steepness of the slope was dependent on the network structure. T_β was more sensitive to density for networks prepared with stoichiometric amounts of reactants than for networks prepared from non-stoichiometric amounts. Although Heijboer(14) has shown that T_β is independent of free volume for some thermoplastics, it appears that a reduction in free volume in crosslinked networks, caused by an increase in density, results in a higher T_β. Thus it is concluded that T_β, besides being affected by the resistance caused by the crosslink junctures, also depends on free volume -- atleast in the present epoxy networks.

Value of the tanδ peak at T_β: The loss tangent spectra of all the samples in the glassy region are shown in Figure 8. An increase in crosslink density results in the broadening as well as an apparent decrease in the height of the β-transition peak. It has been demonstrated by several investigators(2, 10-13) that the β-transition peak depends on the concentration of the flexible chain segments produced after the crosslinking reaction of the DGEBA epoxy resin and the curing agent. When the reactants are used at stoichiometric amounts then the peak height is directly proportional to the DGEBA resin concentration in the network(13). Since the functional group analysis had shown nearly complete reaction in all the samples (see p 36, Table II) the β-trans-

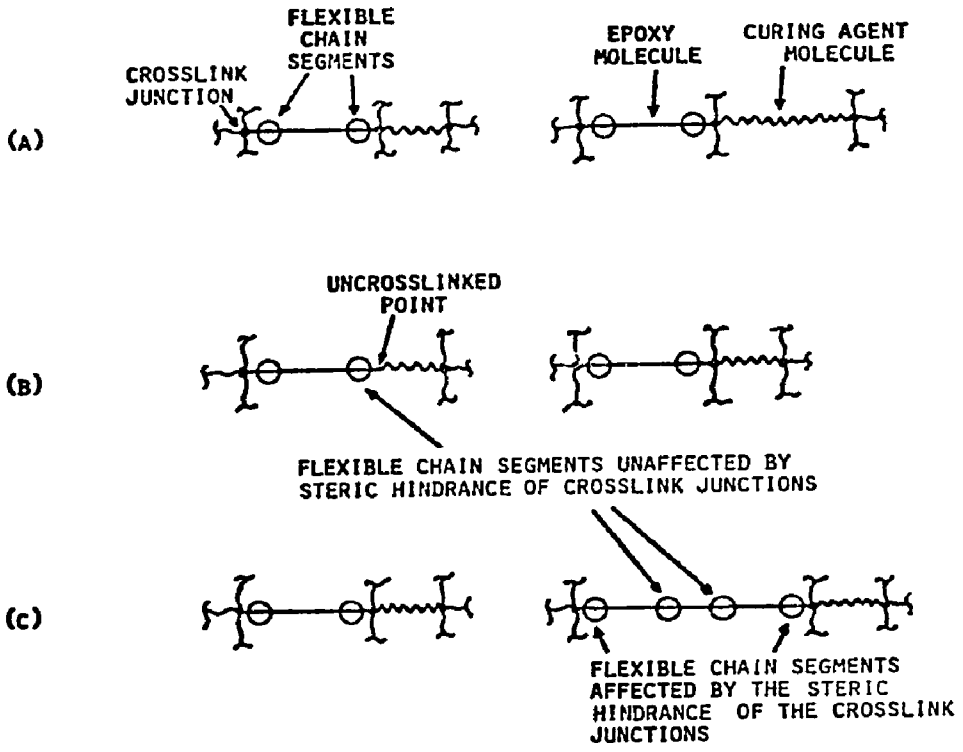

Figure 6. Different ways of changing the crosslink density.
(A)- By changing the length of the amine molecule.
(B)- By changing the degree of cure or by moving towards stoichiometry.
(C)- By changing the length of the epoxy molecule.

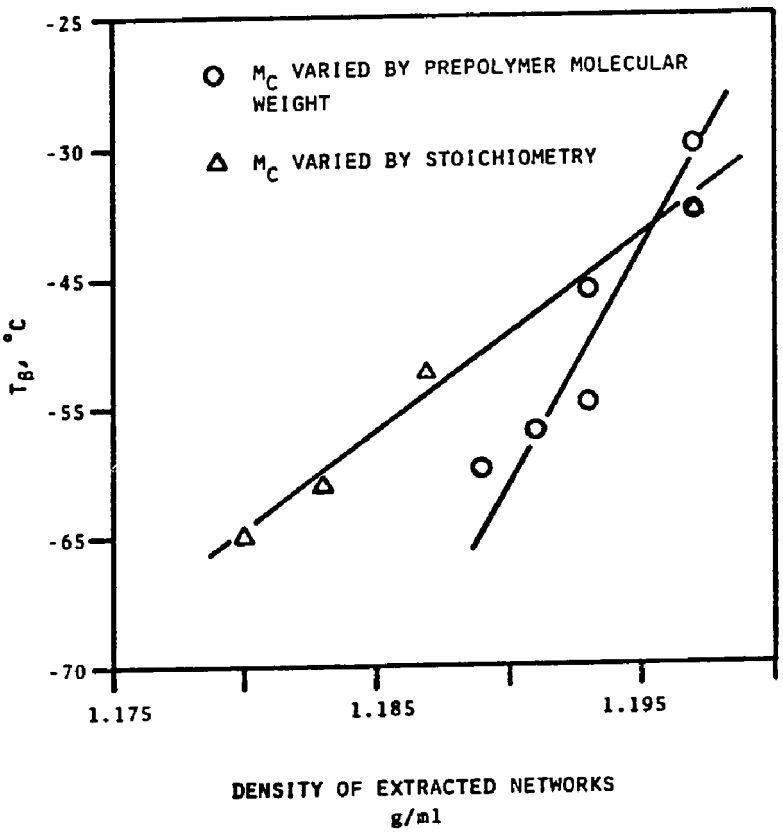

Figure 7. Relationship between T_β and density of the networks.

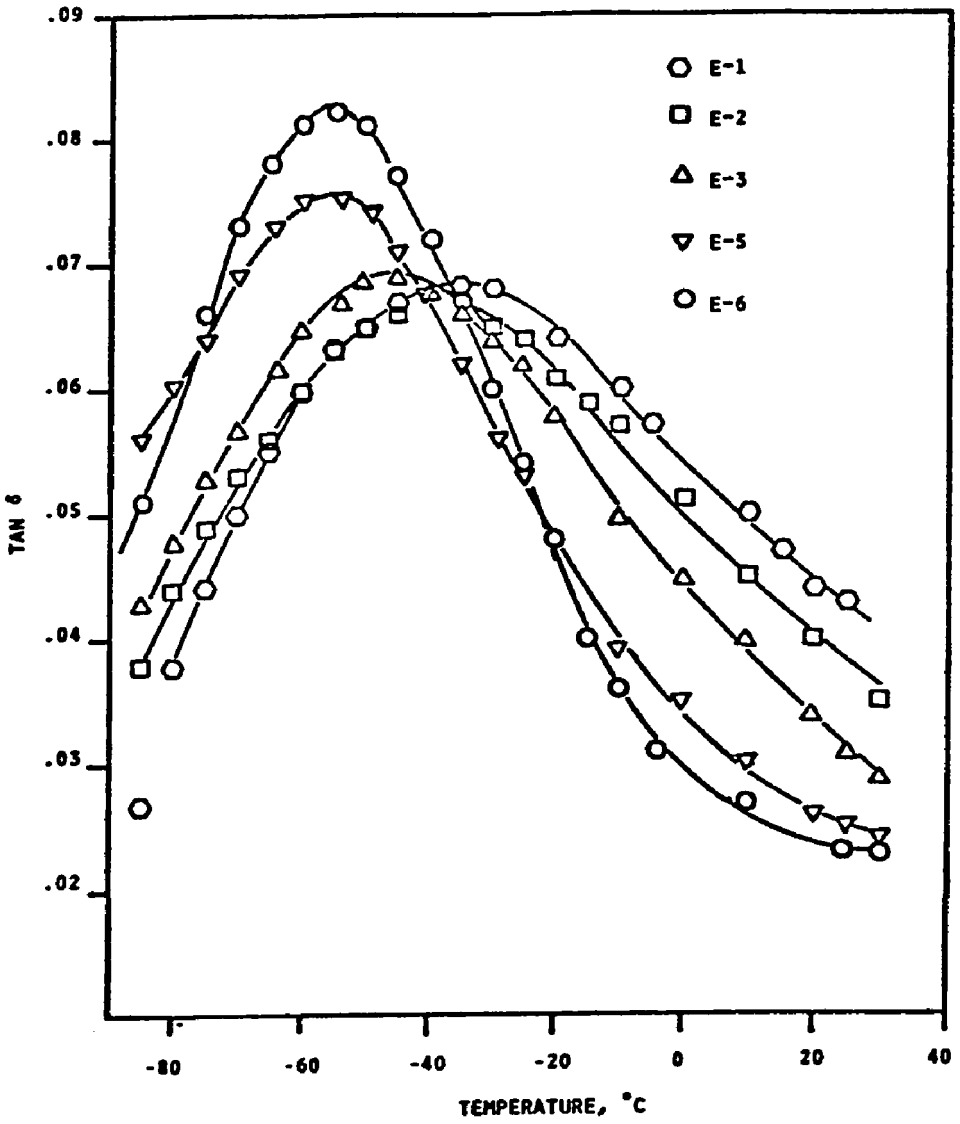

Figure 8. Tanδ spectrum for Series E networks in the glassy state.

ition peak values were normalized with respect to the concentration of the epoxy prepolymer in the network, hydroxy-ether linkage, and the diether linkage, respectively. Results are shown in Table IV.

TABLE IV. TANδ PEAK VALUES NORMALIZED WITH RESPECT TO DIFFERENT VARIABLES.

Specimen	Density g/ml	Tanδ value (T) at T_β	a	b $\times 10^3$	c $\times 10^3$	T/a	T/b $\times 10^3$	T/c $\times 10^3$
E-1	1.197	0.068	0.638	3.774	3.696	0.107	18.017	18.388
E-2	1.197	0.068	0.649	3.898	3.657	0.105	17.450	18.595
E-3	1.196	0.069	0.696	4.394	3.481	0.099	15.704	19.822
E-5	1.195	0.076	0.754	5.013	3.260	0.101	15.162	23.289
E-6	1.193	0.082	0.773	5.212	3.201	0.106	15.773	25.616
				Average value		0.104	16.421	21.142
				Std. Deviation		0.003	1.238	3.180
				% Variation		2.9%	7.5%	15.1%

[a]concentration of the epoxy molecules in the network in g/ml

[b]concentration of the diether linkage in no./ml

[c]concentration of the hydroxy-ether linkage in no./ml

Normalization with respect to the concentration of the epoxy prepolymer gave a constant value of tanδ at T_β with 2.9% variation, which is within experimental error. This is in agreement with the observations of other investigators(2,10-13). No conclusions could be drawn on whether the hydroxy-ether linkage or the diether linkage causes the β-transition. Indeed, it appears

that the β-transition in DGEBA epoxy networks is caused by the motion of more than one linkage, as pointed out by Patterson-Jones and Smith(10). Thus, it is possible that both the hydroxy-ether and the diether linkages of the bisphenol-A participate in the β-transition, the former having a predominant effect.

d. Impact Strength and its correlation to tanδ and M_c

Very little information is available on the toughness-dissipation factor correlation for crosslinked polymers, especially epoxies. Some investigators have proposed that impact strength increases with the height of the β-transition peak(13), and the ratio of the areas of the tanδ peak(15). Such relationships, as pointed out by Sacher(16,17), could be a matter of coincidence and may not apply in general to all systems. It has been established that impact strength for amorphous polymers is related to the tanδ value obtained at the temperature and equivalent frequency of impact(16-17).

The Charpy impact strength, determined at room temperature, is given in Table V. It was found that the impact strength increases with a decrease in M_c but is unaffected by the distribution of M_c (see Figure 5). Intutively, an opposite behavior would be expected (i.e. an increase in impact strength with M_c). Table 5 also indicates that impact strength increases with a decrease in tanδ peak value, which is the opposite of what Cuddihy and Moacanin(13) had suggested. This indicates that in general, impact strength is not related to the tanδ peak value at the β-

transition but, as for amorphous polymers, could be related to the temperature and equivalent frequency of impact, which for the present case would correspond to 20°C and 1000 Hz, respectively.

TABLE V. IMPACT STRENGTH OF SERIES E NETWORKS.

Specimen	M_c (theo.)	Impact Strength J/M	Tanδ Value at 110 Hz, 10°C.	$Tan\delta_{max}$ Value	T_β °C
E-1	308	50.2 ± 5.9	0.050	0.068	-35
E-2	326	42.7 ± 3.2	0.045	0.068	-40
E-3	430	42.2 ± 3.7	0.039	0.069	-46
E-4	740	39.5 ± 4.3	0.031	0.076	-55
E-5	980	34.2 ± 7.2	0.027	0.082	-57

The tanδ values, in the present study, were obtained at 110 Hz. Fakusa and Wada(18) have shown that a ten fold increase in the test frequency, in a DGEBA epoxy network, does not affect the general shape of the tanδ curve but shifts the peak towards the higher temperature side by approximately, 10°C. Therefore, tanδ at 10°C would roughly correspond to the tanδ at 1100-Hz and 20°C. A least-squares fit showed that 88% of the variation in impact strength could be accounted for by tanδ at 10°C and 79% of the variation could be accounted for by $1/M_c$, suggesting that impact strength is a linear function of both the tanδ value and M_c. Finally the following relationship, which could account for 98% of the variation in impact strength, was obtained through multiple linear regression analysis :

$$\text{Impact Strength(J/m)} = A_0 + A_1 \tan\delta - A_2 (1/M_c) \qquad (5)$$

where $A_0 = -4.97$, $A_1 = 2.01 \times 10^3$, and $A_2 = 1.4 \times 10^4$.

For high molecular weight linear polymers ($M_c = \infty$) Equation 5 would reduce to the same form proposed by Sacher(17). Therefore, Equation 5 is of a general type which can be applied to crosslinked as well as linear polymers that have brittle failure. For polymers that do not have brittle failure, the effect of plastic flow will have to be accounted for separately. Furthermore, the constants A_0, A_1, and A_2 would be different at different temperatures.

e. Tensile Behavior

The tensile data are given in Table VI and shown as a function of M_c in Figure 9.

In general, the tensile properties of all the samples varied within twice the maximum standard deviation. E_g and σ_u were not affected by the changes in the distribution of M_c or changes in M_c per se. The percentage elongation to break, for bimodal blends, was slightly lower by 15% than for their counterparts prepared from commercial resins. Since the differences are small, it would be appropriate to conclude that the tensile properties at room temperature are independent of M_c or the distribution of M_c. This general relative insensitivity to changes in M_c and distribution of M_c is not surprising, because the glassy state properties are more closely related to the cohesive energy density than to network structure(19). Furthermore the shift

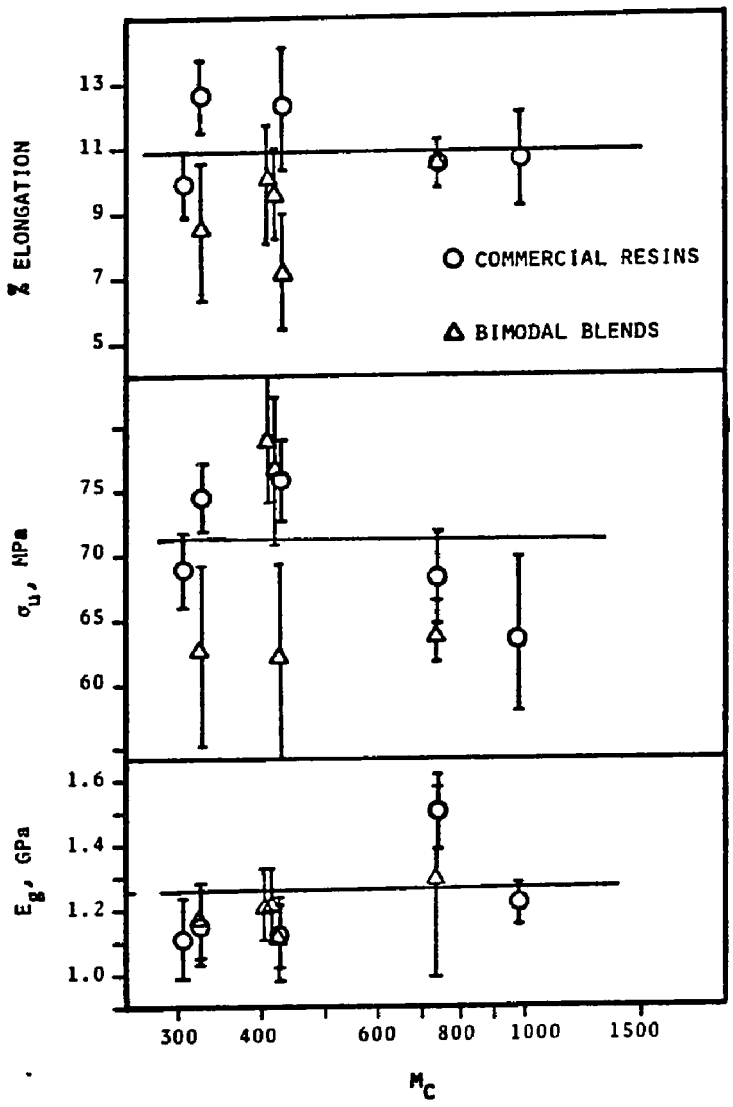

Figure 9. Tensile properties of Series E and Series F networks as a function of M_c.

factors (log a_T) obtained from creep experiments (see below) had indicated that the motion of the main chains of these networks is very restricted. Therefore, as observed experimentally, it can be expected that the room temperature tensile properties of these epoxy networks having bulky bisphenol-A groups would be independent of average M_c or distribution of M_c.

TABLE VI. TENSILE DATA FOR SERIES E AND SERIES F NETWORKS.

Sample	M_c (theor.)	% elong.	E_g[a], GPa	σ_u, MPa[b]	σ_y, MPa[c]
E-1	308	9.9±1.0	1.12±0.12	69±3	-
E-2	326	12.7±1.2	1.15±0.12	75±2	-
E-3	430	12.3±2.2	1.13±0.10	76±3	-
E-4	493	9.0±0.5	1.34±0.10	74±3	-
E-5	740	10.5±0.7	1.52±0.13	69±3	75±2
E-6	980	10.8±1.7	1.23±0.05	64±7	74±1
F-1	326	8.5±2.0	1.19±0.11	63±7	-
F-2	413	10.1±1.6	1.23±0.05	79±5	-
F-3	419	9.6±1.4	1.24±0.13	77±6	-
F-4	430	7.2±1.8	1.10±0.10	62±7	-
F-5	740	10.5±0.7	1.30±0.31	64±2	73±5

[a] Young's modulus, determined from initial slope

[b] Actual stress at fracture

[c] Yield strength (where observable)

f. Creep Behavior

The effect of M_c and distribution of M_c on the different viscoelastic parameters concerning creep behavior will be

discussed separately.

Glass transition temperature: The (10-sec) modulus-temperature curves are shown in Figure 10. The T_g values predicted from the creep test are in good agreement with those obtained from DMS. Both creep experiments and DMS indicate that the T_g is the same for the following pairs of samples: E-2 and F-1, E-5 and F-5, and E-3 and F-3.

Shift factor (a_T): Experimental shift factors were determined by plotting master curves with T_g as the reference temperature. The density corrections were assumed to be small and were neglected. Temperature corrections were made only above T_g. These corrections were small (5-10%) and within the range of experimental error. A composite curve of log a_T vs $(T-T_g)$ was obtained for all the samples. Figure 11 shows the composite curve of the shift factors and also indicates that the shift factors do not follow the WLF equation(20):

$$\log a_T = - (17.44[T-T_g])/(51.6 + [T-T_g]) \qquad (6)$$

Instead, they appeared to follow an equation of the Arrhenius type given below (also see Figure 12):

$$\log a_T = - H_a/2.303\ RT \qquad (7)$$

where R is the gas constant, T is the absolute temperature, and H_a is the apparent activation energy.

Activation energies of 230 kcal/g-mole above T_g and 75 kcal/g-mole below T_g, were obtained for all the samples irrespective of the differences in M_c (Figure 12). Interestingly, these values

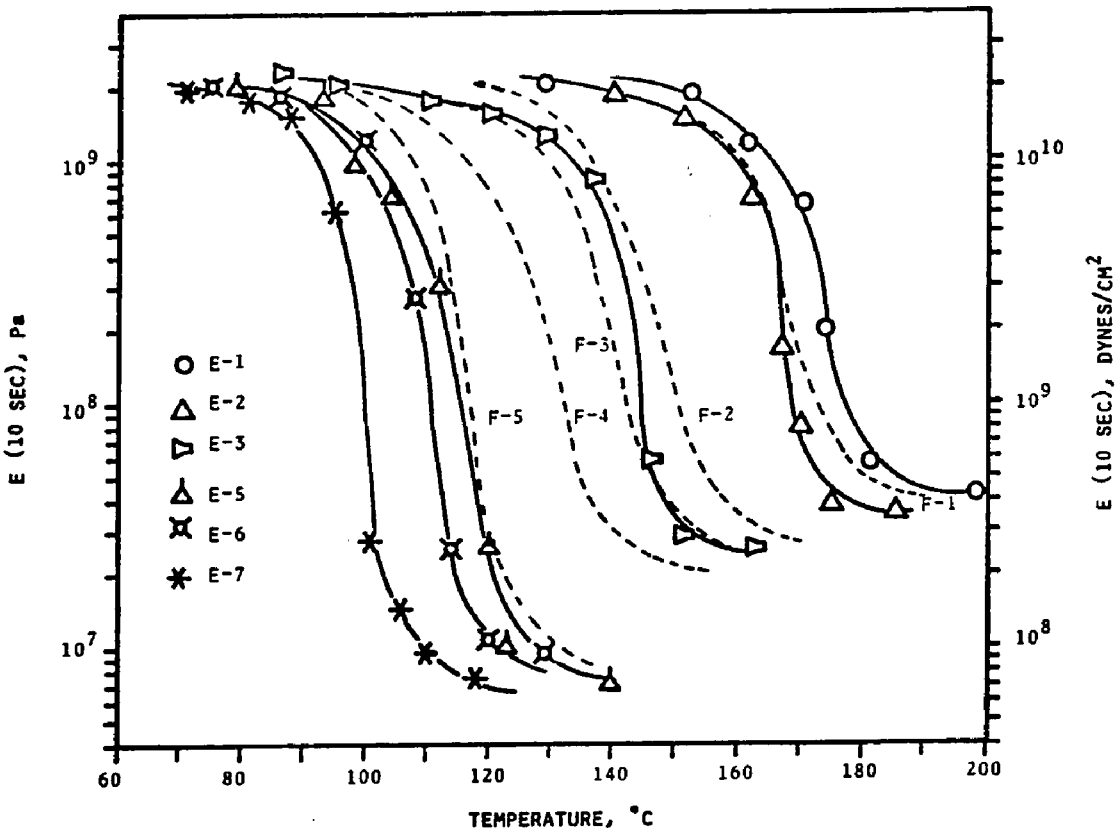

Figure 10. Modulus(10-sec) - temperature curves determined through Creep tests for Series E and Series F networks.

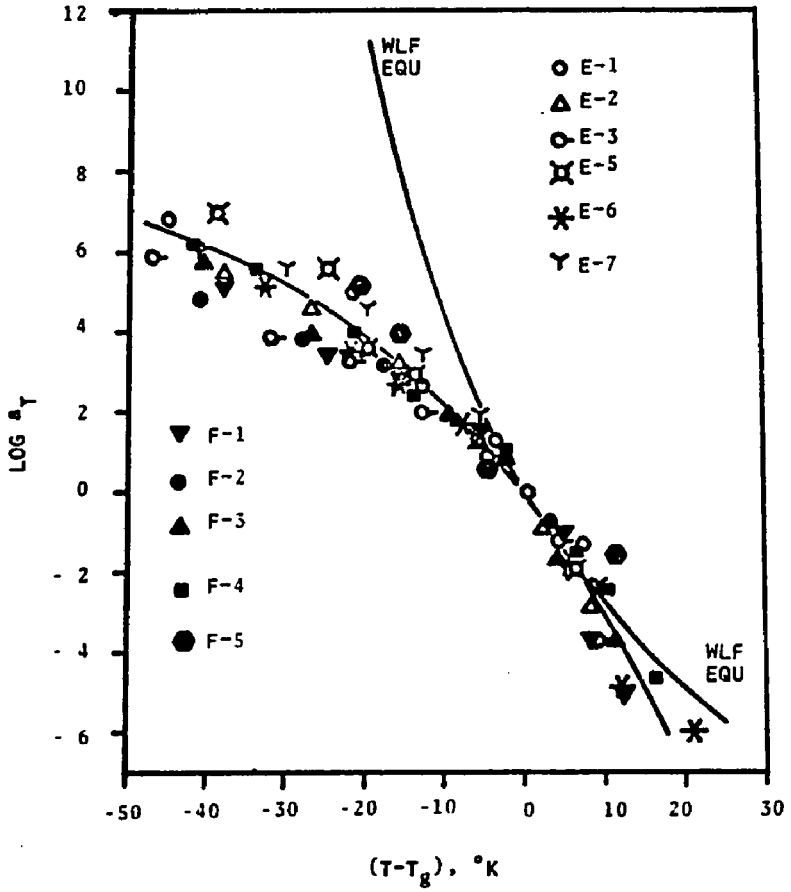

Figure 11. Shift factors as a function of $(T-T_g)$ for Series E and Series F networks.

are in good agreement with the results of Kitoh and Suzuki(21) who found a value of 230 kcal/g-mole above T_g and 91 kcal/g-mole below T_g, for a bisphenol-A epoxy cured with meta phenylene diamine. Their observed activation energy below T_g was slightly higher , probably because they had applied the temperature correction to the entire spectrum.

A composite curve (Figure 12) was also obtained by plotting log a_T vs $(1/T-1/T_g)$. Some epoxy resins which do not have the bisphenol-A group in the main chains have been reported to follow the WLF relationship(21-23). However, all the samples of the present study, including samples E-5, E-6, and E-7 which have relatively long chains (see Table II of Chapter II) and would be expected to be flexible, followed the Arrhenius type of relationship. Generally, polymers in the glassy state follow the Arrhenius type of relationship(24). Thus it appears that the motion of the main chains of the present epoxy networks is relatively restricted even beyond the glassy state. The chemical structure of the DGEBA epoxies indicates that an increase in the length of the molecule results in an increase in the number of the bisphenol-A groups in the main chains. It appears that the bulky bisphenol-A groups are responsible for the restricted motion of the main chains observed even beyond the glassy state. It is concluded that the activation energy is independent of M_c and the distribution of M_c in networks such as those studied here.

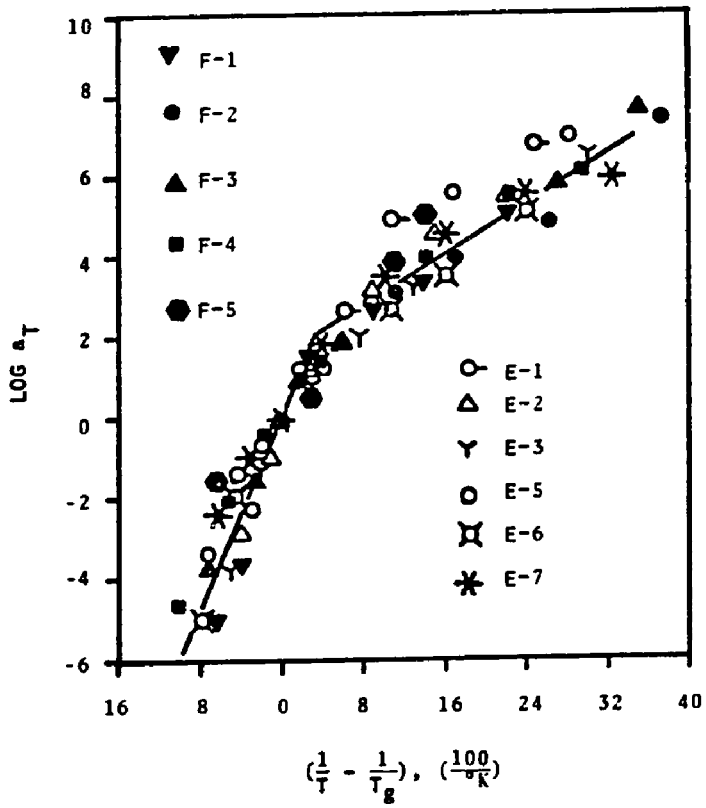

Figure 12. Shift factors as a function of $(1/T - 1/T_g)$ for Series E and Series F networks.

Master Curves: As an illustration, individual data points of creep studies for Sample E-3 are shown in Figure 13. On an average, about 10% deviation was observed in duplicate runs. To determine the effect of M_c on creep, master curves for all the samples were drawn at 129°C instead of selecting T_g as the reference temperature. The temperature corrections were not used to draw the master curves shown in Figure 14 because these corrections, as mentioned earlier, were small and the experimental data did not extend to long ranges in the rubbery region. The characteristic creep time (τ_c) was taken as the time required to relax to a value of $\log E(t) = (\log E_g + \log E_r)/2$, where E_g and E_r are the glassy and rubbery moduli , respectively. The slope (n) of the master curves was determined at the time τ_c. Results are shown in Table VII.

Except for the rubbery region the master curves at a fixed reference temperature, for linear polymers, are unaffected by a change in molecular weight(25,26). For lightly crosslinked rubbers, on the other hand, a change in crosslink density not only changes the rubbery modulus but also shifts the master curves on the time axis(27). It was found that the master curves of these highly crosslinked epoxy networks were similar to those for lightly crosslinked rubbers -- both the rubbery modulus and τ decreased with an increase in M_c.

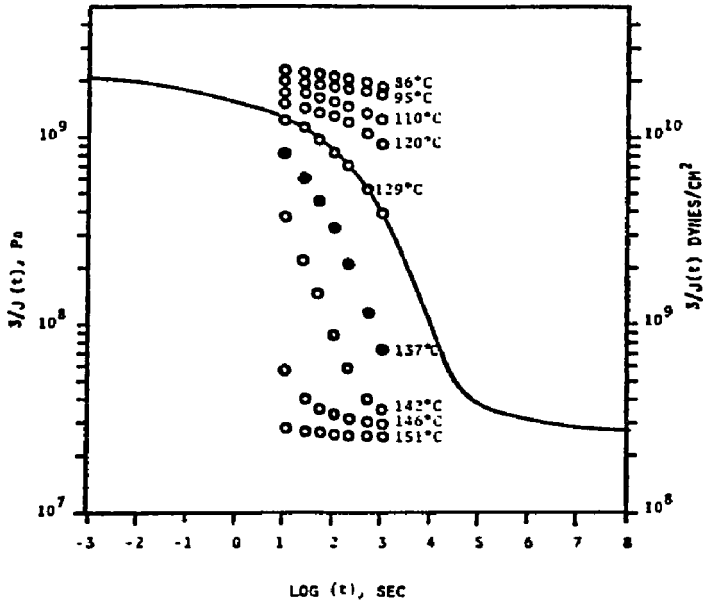

Figure 13. Creep data for Sample E-3.

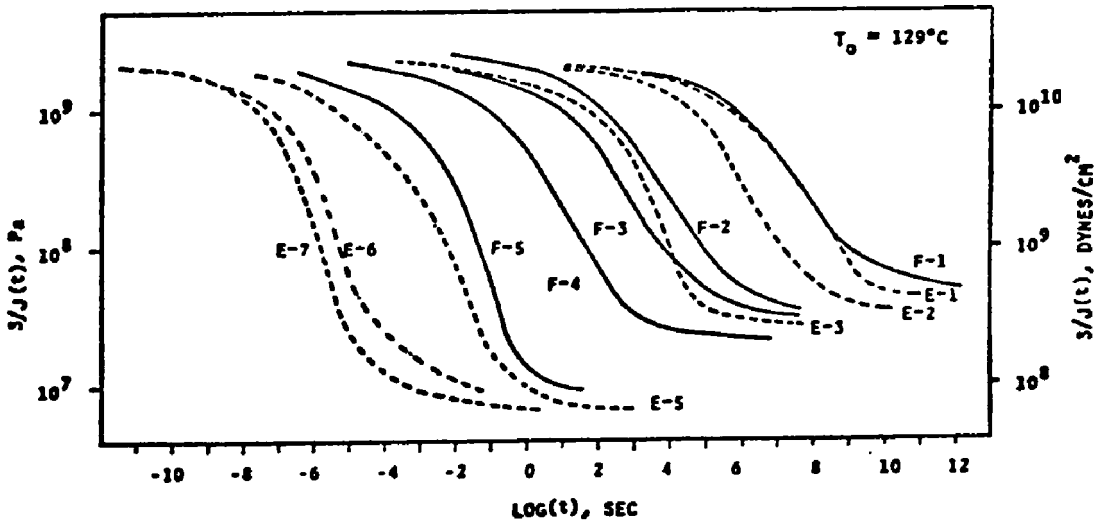

Figure 14. Master curves for Series E and Series F networks.

TABLE VII. CREEP DATA FOR SERIES E AND SERIES F NETWORKS (REDUCED TO 129°C).

Sample	T_g, °C	E_r^a, MPa	log τ_c	$-n^b$	M_c (thoer.)
E-1	174	45	7.6	0.38	308
E-2	167	45	6.0	0.46	326
E-3	142	30	3.4	0.63	430
E-5	118	8	-2.5	0.59	740
E-6	108	9	-5.4	0.71	980
E-7	101	7	-6.0	0.80	1400
F-1	167	45	7.6	0.38	326
F-2	147	30	3.6	0.40	413
F-3	139	30	2.4	0.39	419
F-4	129	30	0.8	0.44	430
F-5	118	8	-1.6	0.71	740

[a] At T_g + 35°C

[b] d [log E(t)]/ d[log t]

Characteristic creep time: The characteristic creep time (τ_c) was found to be inversely related to M_c by the following relationship:

$$\log (\tau_c/\tau_{co}) = K_1 / M_c \qquad (8)$$

where $\log \tau_{co} = -10.1 = (\tau_c \text{ at } M_c = \infty)$, obtained by extrapolation

$K_1 = 5.4 \times 10^3$ = constant

The statistical correlation coefficient was 0.99, showing excellent fit.

Figure 15 shows that the blend samples F-1 and F-5 have a higher τ_c than their counterparts E-2 and E-5 respectively, which were prepared from commercial resins. On the other hand, sample F-4 has a lower τ_c than its commercial counterpart E-3. These results indicate that the differences in distribution of M_c affect τ_c. Samples E-2 and E-3 have network chains composed of epoxy molecules having molecular weights (M.W.) of 340 and 620, respectively whereas the major portions of samples E-5, E-6, and E-7 are composed of epoxy molecules having a M.W. of 2328 or 3748. Furthermore, the blend samples F-1 and F-5 have a larger proportion of epoxy molecules having a molecular weight of 340 than their respective counterparts E-2 and E-5 (commercial resins); this results in a higher τ_c. On the other hand, the blend sample F-4 has two epoxy species having M.W.'s of 340 and 3748, respectivly, in equal amounts and its commercial counterpart sample E-3 has epoxy species having M.W.'s of 340 and 620. The appreciable amount of large molecules in F-4 results in a lower τ_c. Thus, it is concluded that τ_c, besides being sensitive to M_c, is also very sensitive to the distribution of M_c; τ_c would be larger or smaller depending upon whether the network has greater amounts of smaller or larger chains, respectively.

Slope of the transition region: The slope of the transition region was found to broaden with a decrease in M_c (Figure 15). These results indicate that an increase in crosslink density results in the broadening of the slope and that at a certain crosslink

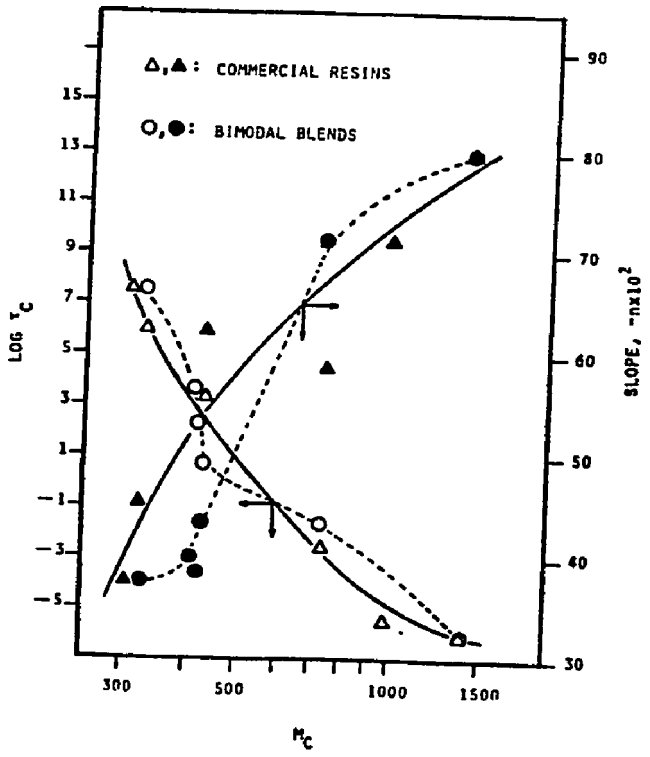

Figure 15. Characteristic creep time and slope of the transition region as a function of M_c for Series E and Series F networks.

density, no transition would be observed. From the dynamic mechanical studies of polyesters, Shibayama and Suzuki(28) had also shown that the dispersion broadens with an increase in crosslink density. The slope (n) for Series E networks was found to be inversely related to M_c by the relationship given below.

$$\log (n/n_o) = K_2/M_c \qquad (9)$$

where n_o = 0.90 = slope for a network having $M_c = \infty$, obtained by extrapolation, and K_2 = 100.62 = constant.

Furthermore, the bimodal blend samples F-1 to F-4 have slopes close to that of sample E-1, prepared from the commercial resin whereas sample F-5 (bimodal blend) has a slope close to that of sample E-7 (commercial resin). The lower values of slope observed in the blend samples F-1 to F-4 are a result of a broader distribution of relaxation times which is not present in the respective counterparts of Series E. Similarly, sample F-5 showed a higher slope than its counterpart E-5 because the former had a narrower distribution of molecular weights which resulted in a narrower distribution of relaxation times (see Table I).

It is concluded that the broadening of the transition region could take place either by an increase in the crosslink density or by the broadening of the distribution of crosslink density.

Distribution of the relaxation times and the relaxation time spectrum: The distribution of relaxation times, $H(\tau)$, can be determined as a first approximation as follows(29):

$$H(\tau) = -[\, d[E(t)]/d(\ln t)]_{t=\tau}$$

$$= -[E(t)[d(\log E(t))]/d(\log t)]_{t=\tau} \qquad (10)$$

where E(t) is the relaxation modulus at time t.

The relaxation time spectrum, log $H(\tau)$ vs. logτ was plotted for all the samples. All the curves exhibited the wedge shape described by Tobolsky(29), and had a slope that was independent of M_c. Using horizontal shifts of log a_x, these curves could be superimposed to a reference curve as shown in Figure 16. The shift factors are given in Table VIII, and could be correlated to M_c, for Series E, as follows:

$$\log a_x = K_3[1/M_{co} - 1/M_c] \qquad (11)$$

where M_{co} = reference M_c, and K_3 = 5.8 = an empirical constant.

TABLE VIII. HORIZONTAL SHIFT FACTORS FOR THE COMPOSITE RELAXATION SPECTRUM SHIFTED TO M_c=308.

Sample	M_c (theor.)	log a_x
E-1	308	0.0
E-2	326	1.4
E-3	430	4.6
E-5	740	10.6
E-6	980	13.8
E-7	1400	14.6
F-1	326	0.0
F-2	413	2.0
F-3	419	2.5
F-4	430	7.2
F-5	740	9.9

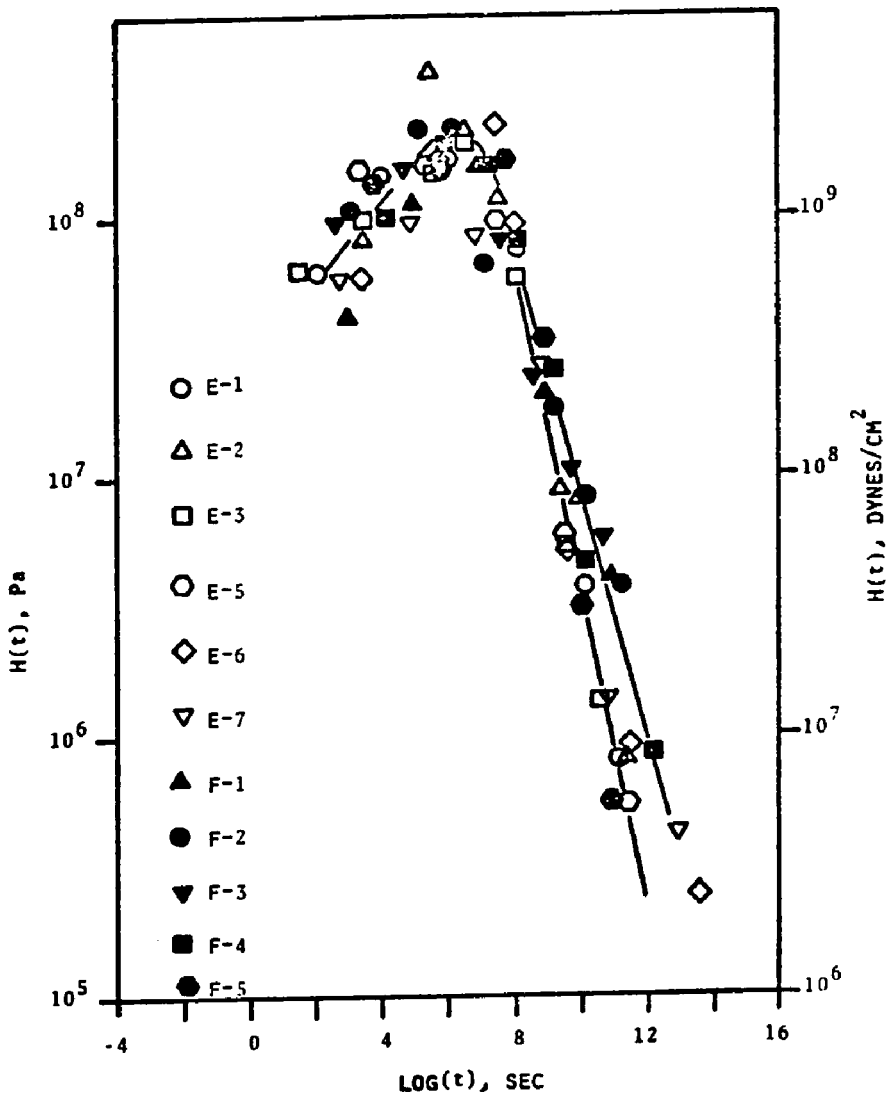

Figure 16. Relaxation time spectra for Series E and Series F networks.

These results indicate that the slope of the relaxation spectrum of highly crosslinked networks, having similar chemical structure, is independent of M_c. In a study of crosslinked rubbers Plazek(27) had also observed that the slope near the rubbery region is independent of crosslink density. Tobolsky(30) has theoretically shown that the relaxation spectrum for three- two- and-one-dimensional lattices should have slopes of -1.5, -1.0, and -0.5, respectively. The slope of the relaxation time spectrum of Series E networks, prepared from commercial resins, is -0.63, which is close to the average value of slopes predicted for two- and one-dimensional lattices. Furthermore, these slope values are close to those predicted by the Zimm(31) and Rouse(32) theories, which primarily were developed for very dilute polymer solutions. The Zimm theory predicts a slope of 0.67 whereas the Rouse theory predicts a slope of 0.5. The basic difference between the Zimm and Rouse theories is that the former considers hydrodynamic interaction as predominant whereas the latter considers it as negligible.

Thus it appears that even in highly crosslinked networks such as those of the present study, $H(\tau)$ is mainly controlled by the linear chains between the crosslinks and, to a lesser extent, by the crosslink junctions.

The blend samples of Series F had a broader slope (-0.5) than their counterparts of Series E (-0.63). Though the differences are not large, the broadening of the slope for the blend samples is attributed to the broadness in distribution of M_c.

Finally, from the relaxation time spectra it may also be concluded that the distribution of relaxation times for these epoxy networks consists of three components: components at short and long times, independent of M_c, and a medium-time portion that exhibits considerable scatter. The kinetics of approach to equilibrium stress in stress relaxation is solely a function of the distance from equilibrium and not of crosslink density. The length of the region where $H(\tau)$ is independent of crosslink density may vary, depending on the chemical structure of the network.

g. Swelling and Extraction

The swelling and extraction data are given in Table IX and shown in Figure 17.

The glass transition temperature of the blend sample F-4, which had 57% Epon 825 and 43% Epon 1004, had indicated that Epon-1004 forms the more continuous network. The swell ratio of this sample is the same as that of its commercial counterpart, sample E-3. Similarly the blend samples F-1 and F-5 also have swell ratios that are same as their respective commercial counterparts E-2 and E-5. This indicates that the swell ratio is not very sensitive to the distribution of M_c. On the other hand, samples F-2 and F-3 have swell ratios that are lower than expected (see Figure 17).

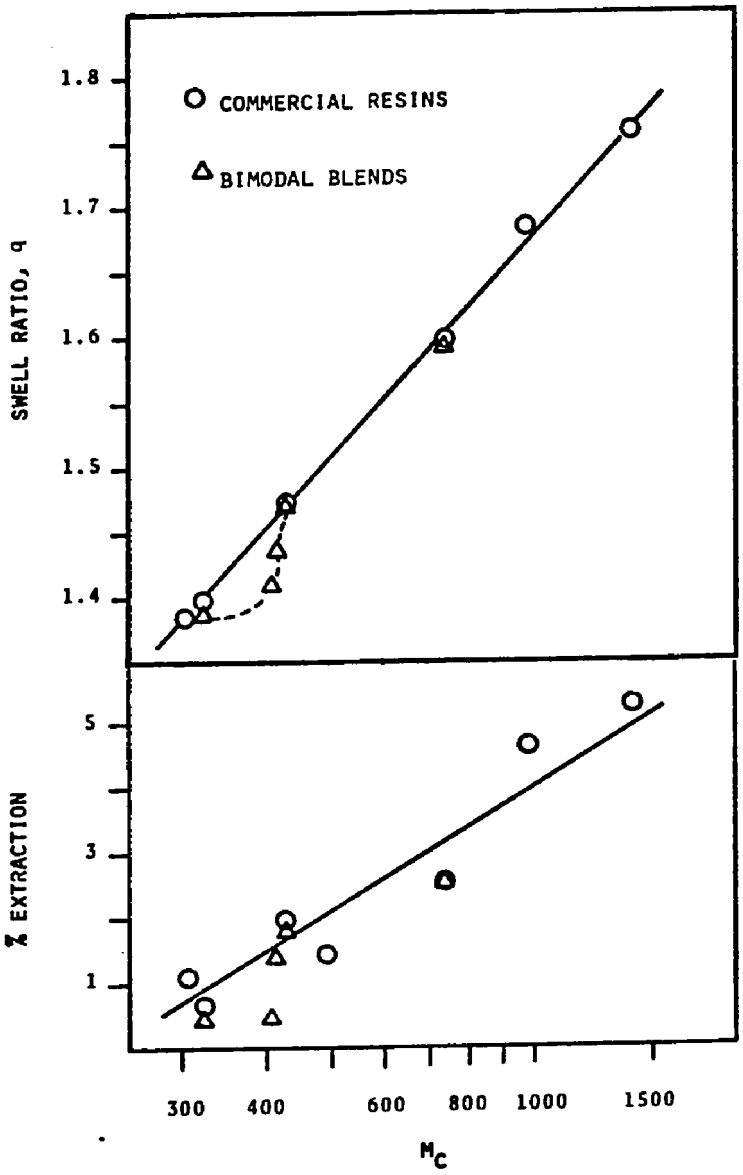

Figure 17. Swell ratio and % extraction as a function of M_c for Series E and Series F networks.

TABLE IX. SWELLING AND EXTRACTION DATA FOR SERIES E AND SERIES F NETWORKS.

Sample	M_c (theor.)	% extractables[a] (avg. values)	Swell ratio[b] (avg. values)	ρ_1[c]	ρ_2[d]
E-1	308	1.11	1.385	1.197	1.199
E-2	326	0.61	1.399	1.197	1.199
E-3	430	1.96	1.471	1.193	1.196
E-4	493	1.40	1.471	1.193	1.196
E-5	740	2.54	1.598	1.193	1.195
E-6	980	4.68	1.688	1.191	1.193
E-7	1400	5.28	1.759	1.189	1.191
F-1	326	0.42	1.388	1.197	1.199
F-2	413	1.43	1.411	1.194	1.197
F-3	419	0.49	1.439	1.194	1.197
F-4	430	1.93	1.472	1.194	1.197
F-5	740	2.56	1.592	1.193	1.195

[a] Max. Std. Dev. = ± 0.15

[b] Max. Std. Dev. = ± 0.005

[c] Density of the extracted-dry- networks, at room temperature, g/ml

[d] Density of the unextracted networks, at room temperature, g/ml.

These samples have a higher proportion of low M.W. pre-polymer (i.e. , 62 and 60% by weight, respectively). It is highly probable that the composition of these samples is in the critical range where a phase inversion exists, in other words, that some part of the network has Epon 1004 as the more continuous phase while another part of the network has Epon 825 as the more continuous phase. This sort of a phase inversion could result in an anomalous

swelling behavior, with slightly lower values of the swell ratio, than expected.

The soluble content in the networks increased steadily with M_c but was unaffected by changes in the distribution of M_c, as shown in Figure 17. The observed increase in the soluble content can be partly due to the decrease in coherence with M_c (observed in the present networks through electron microscopy -- see Chapter IV), and partly because an increase in M_c results in an increased diffusivity of the solvent into the network, and of the soluble material out of the network. These results, as expected, also indicate that the distribution of M_c does not affect the average diffusivity.

The density of the networks decreased with an increase in M_c but was insensitive to changes in the distribution of M_c. An increase in crosslink density of the network (decrease in M_c) results in a lower free volume and thus a higher density.

h. Crosslink Density Determination

The molecular weight between crosslinks M_{cr} and M_{cs} were determined from the rubbery modulus (obtained through DMS , using the theory of rubber elasticity(33)) and swelling data (using the Flory-Rehner Equation(33)), respectively. The front factors corresponding to M_{cr} and M_{cs} were determined by the following relationships:

$$\phi_r = M_c/M_{cr} \qquad \text{and} \qquad \phi_s = M_c/M_{cs} \qquad (13)$$

The results are shown in Table X.

TABLE X . M_c VALUES DETERMINED BY DIFFERENT METHODS.

Sample	M_c (theor.)	M_{cr}	M_{cs}	ϕ_r	ϕ_s
E-1	308	344	144	0.90	2.14
E-2	326	362	148	0.90	2.20
E-3	430	837	187	0.51	2.30
E-4	493	678	187	0.73	2.64
E-5	740	1363	239	0.54	3.10
E-6	980	1565	303	0.63	3.23
E-7	1400	1995	311	0.70	4.50
F-1	326	362	145	0.90	2.25
F-2	413	691	155	0.60	2.67
F-3	419	840	168	0.50	2.49
F-4	430	920	189	0.47	2.28
F-5	740	1361	236	0.54	3.14

The M_{cr} values determined from the rubbery modulus for these highly crosslinked epoxies are in good agreement with those predicted from stoichiometry. The front factors ϕ_r are close to but consistently less than unity. This indicates the presence of imperfections in the networks, which was also confirmed from electron microscopy (see Chapter IV). The M_{cs} values calculated from swelling data, using the Flory-Rehner equation, do not look reasonable. It appears that the Flory-Rehner equation does not hold well for highly crosslinked networks.

C. CONCLUSIONS

The effect of M_c and distribution of M_c may be summarized as follows:

1. Properties that are affected by the distribution of M_c

a. The glass transition temperature , as is well known, increases with a decrease in M_c. Slight changes in the distribution of M_c do not affect T_g. However, when significant changes in the distribution of M_c exist, T_g is governed by the dominant component in the final network.

b. The slope of the transition region at T_g increases with M_c but decreases (ie. broadens) with an increase in the breadth of the distribution of M_c.

c. The height of the tanδ peak increases with M_c. Furthermore, as expected, an increase in the breadth of the distribution of M_c results in a broadening of the tanδ peak along with a decrease in the height of the peak.

d. The characteristic creep time (τ_c) is the most sensitive variable to the distribution of M_c. Its value is higher or lower depending on whether the network is composed of higher fractions of short or long chains, respectively.

2. Properties that are not affected by the distribution of M_c

a. The rubbery modulus (E_r) decreases with an increase in M_c, but as predicted theoretically(15), is not affected by the distribution of M_c.

b. The room-temperature tensile properties for the present epoxy networks are independent of M_c or the distribution of M_c. This independence is ascribed to the restricted motion of the main chains, even above T_g, as deduced from the creep experiments.

c. The soluble content increases steadily with M_c but is not affected by changes in the distribution of M_c.

d. The density increases with a decrease in M_c but is not affected by changes in the distribution of M_c.

e. The swell ratio increases with M_c but is unaffected by the distribution of M_c, except in some unusual networks having a phase inversion.

f. The room-temperature impact strength increases with a decrease in M_c but is unaffected by the distribution of M_c.The impact strength is a linear function of the dynamic dissipation factor ($\tan\delta$) determined at the temperature and frequency of impact, and M_c.

g. The β-transition temperature increases with a decrease in M_c but is not affected by the distribution of M_c. T_β depends on the steric hindrance caused by the network junctions, and is linearly related to the density of the networks.

h. The experimental shift factors, for DGEBA-epoxy networks, are independent of M_c or the distribution of M_c. Instead of following the WLF equation, values of the shift factor follow an Arrhenius-type relationship with temperature, indicating that the chain

segment mobility is restricted even in the rubbery state.

i. At long times the slope of the relaxation time spectrum is unaffected by M_c but decreases slightly with an increase in the breadth of the distribution of M_c.

REFERENCES

1. T.K.Kwei, J.Polym.Sci., A-2, 4, 943(1966).
2. O.Delatycki et. al., J.Polym.Sci., A-2, 7, 752(1969).
3. J.P.Bell, J.Polym.Sci., A-2, 8,417(1970).
4. E.A·Dimarzio, J·Res.Nat.Bur.Stand.,(A),68,611(1964).
5. L.E.Neilsen,J.Macromol.Sci.,(C) 3, 69(1969).
6. K.Ueberreiter and G.K.Kanig,J.Chem.Phys., 18,399(1950).
7. T.G.Fox and S.Loshak, J.Polym.Sci., 15, 371(1955).
8. F.Rietsch et.al., Polymer, 17(10), 859(1976).
9. W.W.Graessley, Macromolecules, 8(6), 865(1975).
10. J.C.Patterson-Jones and D.A.Smith, J.Appl.Polym.Sci.,12.1601 (1969).
11. G.A.Pogany, Polymer, 11, 66(1970).
12. R.G.C.Arridge and J.H.Speake,Polymer, 13(9),443(1972).
13. E.F.Cuddihy and J.Moacanin,J.Polym.Sci.,A-2, 8, 1627(1970).
14. J.H.Heijboer,Annals of the N.Y. Acad.of Sci.,Vol.279,104(1976).
15. T.Miyamoto and T.Sugano,Polymer J.,6, 5, 45(1974).
16. E.Sacher, J.Macromol.Sci.,B-9, 163(1974).
17. E.Sacher, J.Appl.Polym.Sci., 19, 1421(1975).
18. Y.Fukasawa and·E.Wada, Kobunshi Ronbunshu,32,9, 518(1975).
19. D.A.Kaelble, in "Epoxy Resin Chemistry & Technology", ed. C.A.May and Y.Tanaka,Marcel Dekker Inc.,N.Y.(1973),Chapt. 5.
20. J.D.Ferry, "Viscoelastic properties of polymers", second ed. John Wiley & Sons Inc.,N.Y. 1970, Chapter 11.
21. M.Kitoh and K.Suzuki, Kobunshi Ronbunshu, 33,1, 19(1976).
22. D.H.Kaelble, J.Polym.Sci., 9, 1213(1965).

23. N.Shito, J.Polym.Sci., (C),23, 569(1968).

24. N.G.McCrum and E.L.Morris, Proc.Roy.Soc., A-281,258(1964).

25. N.Ninomiya and H.Fujita, J.Colloid Sci., 12, 204(1957).

26. T.Fujimoto et.al., J.Polym.Sci.,A-2, 6, 129(1968).

27. D.J.Plazek, J.Polym.Sci., A-2, 4, 745(1966).

28. K.Shibayama and Y.Suzuki, J.Polym.Sci., A-3, 2637(1965).

29. A.V.Tobolsky,"Properties and structure of Polymers",John Wiley and Sons Inc.,N.Y.1960, Chapter 3.

30. A.V.Tobolsky, J.Chem.Phys., 37, 1575(1962).

31. B.H.Zimm, J.Chem.Phys., 24, 269(1956).

32. P.E.Rouse Jr., J.Chem.Phys., 21, 1272(1953).

33. P.J.Flory, 'Principles of Polymer Chemistry', Cornell Univ. Press, Ithaca , N.Y., (1953), (a) p 464, (b) p 579.

CHAPTER IV

NETWORK MORPHOLOGY AND ITS RELATIONSHIP TO MECHANICAL BEHAVIOR

A. INTRODUCTION

Since the properties of thermosetting polymers depend on their network structures, the morphology of such polymers has long been a subject of considerable theoretical and practical interest. Thus, it is well known that the tensile strength of thermoset resins is less than predicted theoretically on the basis of the breakage of primary van der Waal's bonds(1,2), and it was proposed long ago(3) that this discrepancy was due to the rupture of weak regions created during network formation. Indeed, it has been shown(4) that high internal stresses can be developed during curing, especially when the curing rate is low. This view of the role of structural defects is also given credence by modern theories of fracture mechanics(5), which emphasize the concept of the concentration of stress at a flaw.

Other investigators(4,6-32,44) have emphasized a view of the network as essentially a composite, with a high-crosslink-density (essentially spherical) phase (often considered as a microgel) embedded in a less crosslinked matrix. In fact, it is probably generally accepted that, regardless of specific details, the curing of thermosets results in an inhomogeneous, two-phase network. Inhomogeneity has been attributed to compatibility problems or non-optimum curing conditions(8), but has also been proposed to be inherently characteristic of gelling systems(14). It has also been

postulated(7) that these microgels are colloidal in nature, atleast for some epoxy systems.

The existence of inhomogeneities has been inferred from results of diverse investigations using many techniques including electron and optical microscopy(13-26,29-32), thermo-mechanical measurements(33), differential swelling(12,34), and differential scanning calorimetry(35). Dispersed phases have been referred to by such terms as "micelles","globules", "floccules", "nodules", and "microgels". In this study, the term "microgel" will be used.

It has been suggested by Bobalek et al(27), Solomon et al(28), and Labana et al(14), that the two-phase system is produced by microgelation prior to the formation of the macrogel. Some investigators(4,14,16) have postulated that these microgels are loosely connected to the surrounding matrix and also suggested(12) that these loose connections are developed during the latter stages of the curing process.

In general, two levels of sizes have been reported in the literature -- one (type A) ranging from 6-nm to 40-nm, and the other (type B) ranging from 20-μm to 200-μm. It has also been shown(4) that slow curing rates result in larger microgels (type B) which result in a network having higher T_g, density, and resistance to etching. The surface properties of the network depend on the surface energy of the mold material and on the atmospheric environment(7,30). The size and density of these microgels have also been related to the presence of plasticizer(23),

radiation damage(26), prolonged exposure to heat(17) and aging of the resin(24).

Studies of interfaces(30,31) have also shown that certain substrates such as Teflon and silocone mold-release agent give featureless surfaces, but subsequent etching of the surface show a two-phase structure. It was further shown that the microgel size decreases with increasing amounts of catalyst. Microtomed thin sections and small-angle X-ray scattering fail to indicate two-phase structures(36).

Both low tensile strengths and nodular morphology in thermosets have been related to differences in crosslink density (7,10,14,27,28,32). At the same time, the fact that yield strength of some epoxies is fairly independent of stoichiometry has been atributed to the role of microgels as primary flow particles(29). Thus, morphology plays an important role in determining network properties. However, suface morphology should not affect the mechanical behavior of the network to the extent bulk morphology would do. Diffusion and permeation phenomenon, on the other hand, would depend on the morphology of both the outer surface and of the bulk.

As discussed earlier, though there have been several postulates of morphological changes during the crosslinking process and of the morphology of the final network, experimental evidence has been scarce. With this in mind, the present study was conducted on an epoxy system as a function of stoichiometry,

molecular weight, and the distribution of molecular weight.

B. RESULTS

Figure 1 shows the macrostructure with feature sizes of 10-μm to 40-μm, revealed by progressive etching by the aqueous solution of chromium trioxide. Etching for 4 hr to 7 hr was found to be the best. The effects of different variables on morphology are discussed below.

a. Effect of Stoichiometry

Examination of the etched surfaces under the SEM (Figures 2 and 3) revealed a two-phase structure. Dimples were observed on the surface, the dimple size increasing with the amount of MDA in the amine excess region. Samples having epoxy excess appeared to be smoother than samples having a similar M_c but excess amine. The sizes of these phases varied from 10-μm to 70-μm, depending on the percent excess of reactants, in agreement with sizes reported by Cuthrell(7) and Selby and Miller(36). It was also observed that above an amine/epoxy ratio of 1.6/1 the morphological differences were negligible.

The two-stage replicas examined with the TEM also revealed the existence of two phases on a much finer scale (Fig. 4). The replicas showed nodules on the surfaces, corresponding to dimples on the polymer surfaces. The phase sizes were in the range of 25-nm to 50-nm except for the case of 100% excess amine where a large distribution of sizes, ranging from 20-nm to 200-nm, was observed. The phase size was found to increase with the amount of

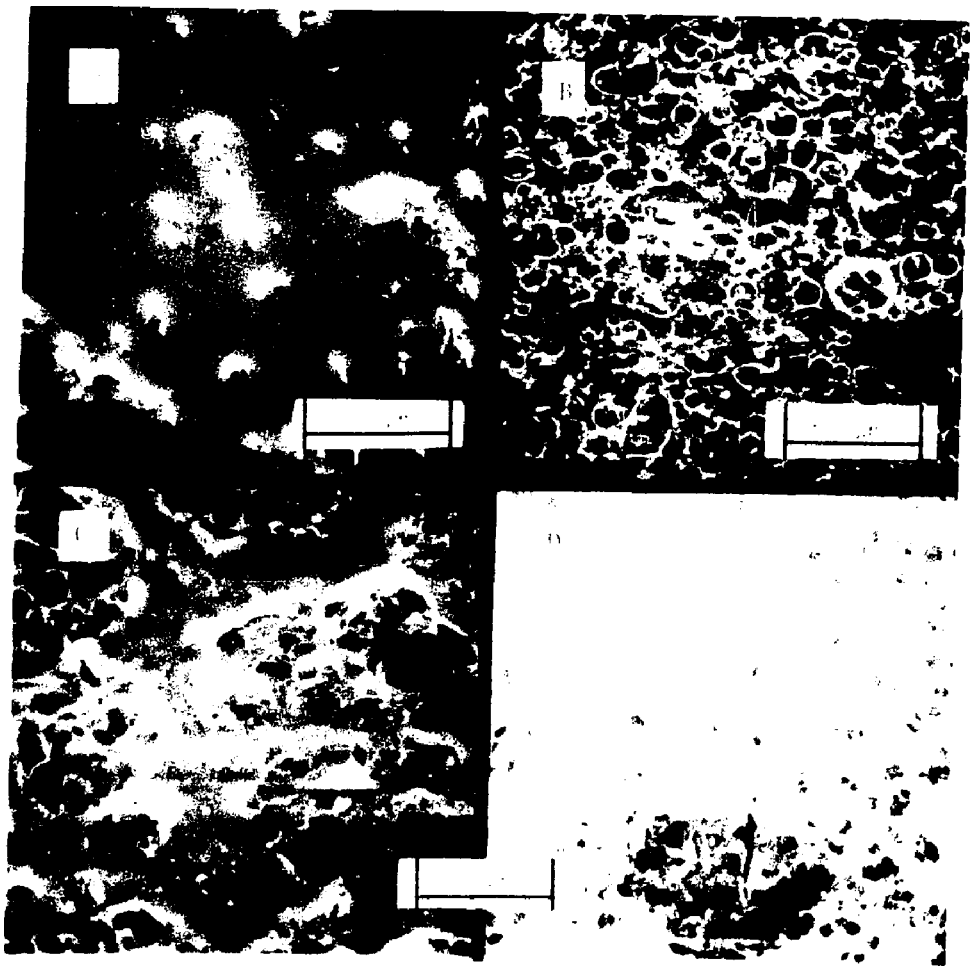

Figure 1. Micrographs of Cr_2O_3 etched surfaces of Specimen E-7.
A) 2 hr etching, B) 4 hr etching,
C) 7 hr etching, D) 11 hr etching.

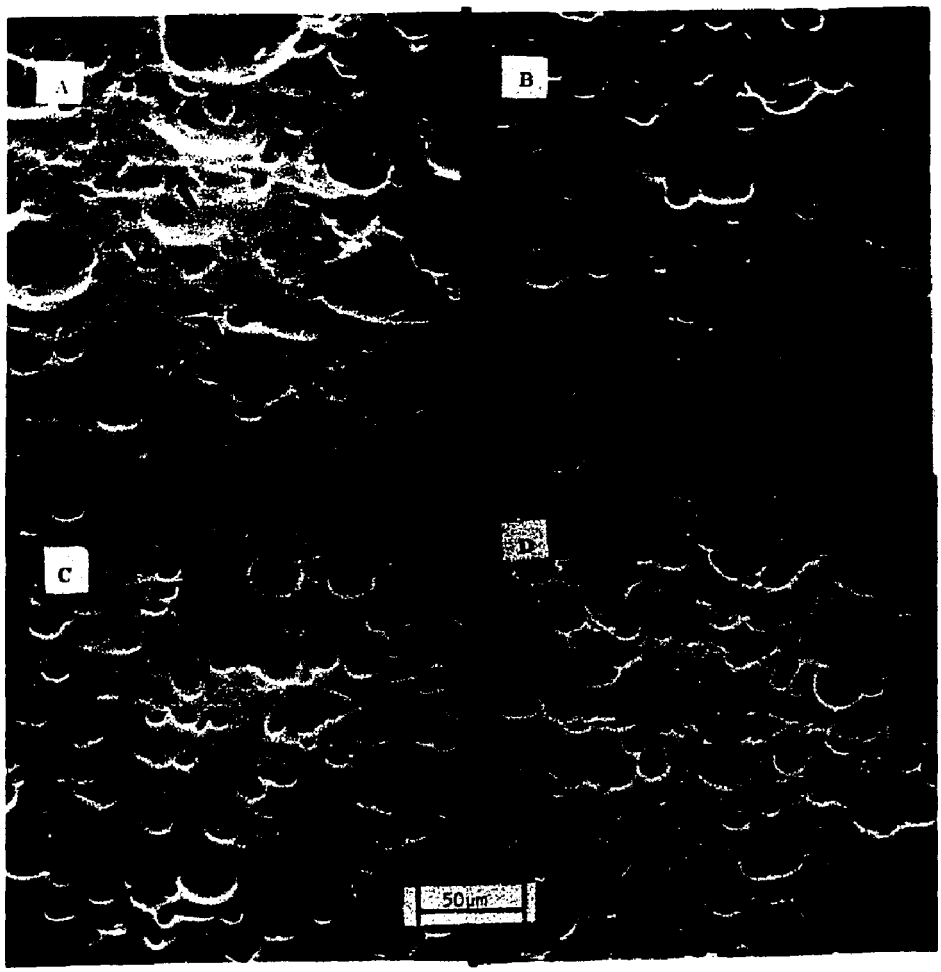

Figure 2. Scanning electron micrographs of 7 hr etched samples of Series A networks. A) A-7, B) A-8, C) A-10, D) A-11.

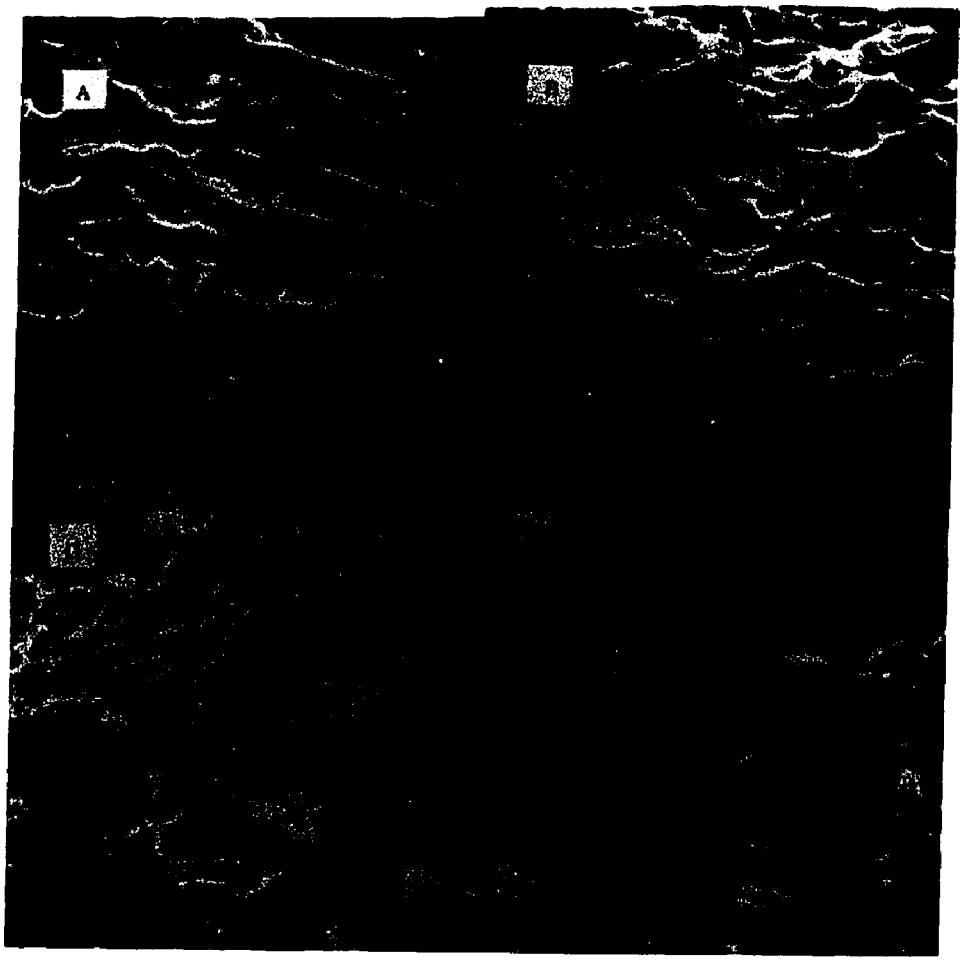

Figure 3. Scanning electron micrographs of 7 hr etched samples of Series A networks. A) A-14, B) A-16, C) A-18, D) A-20.

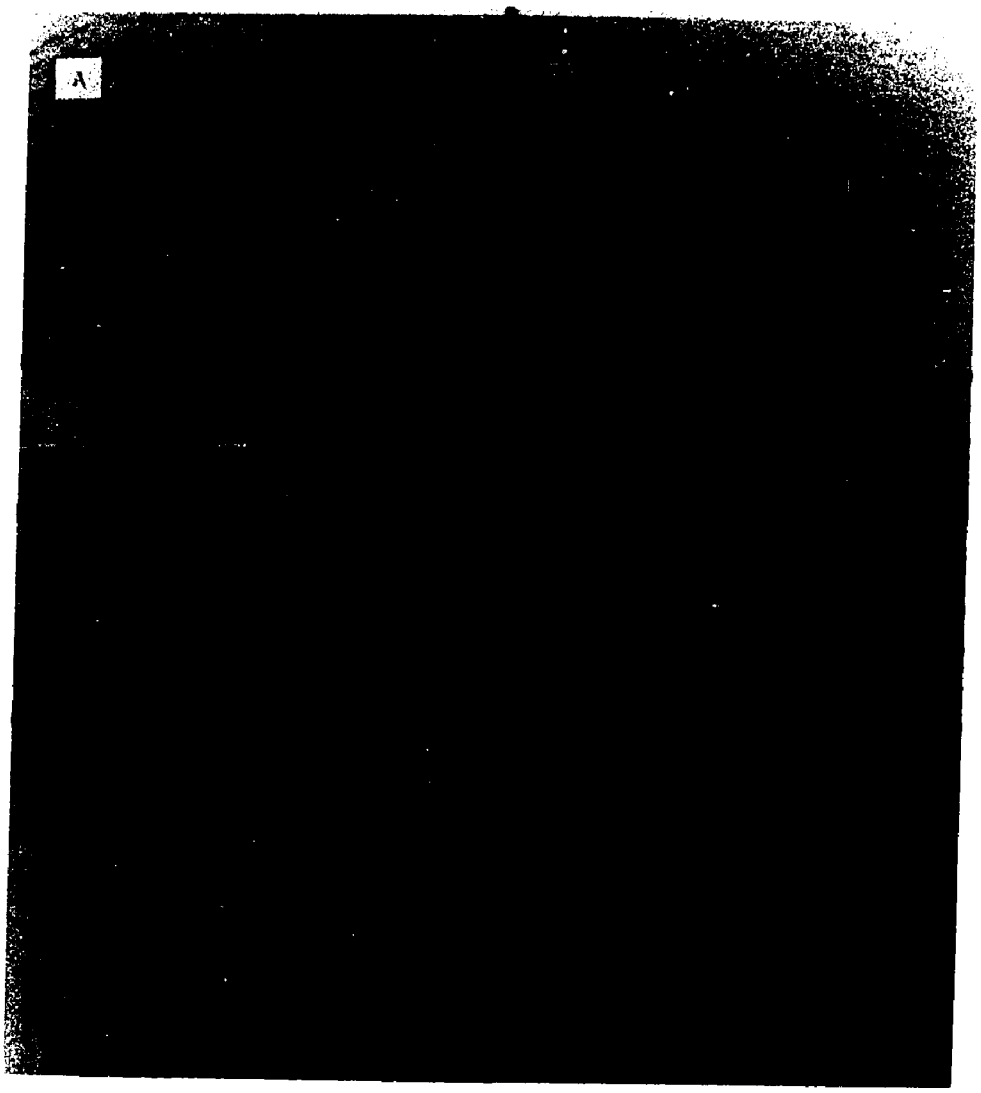

Figure 4. Transmission electron micrographs of replicas of Series A networks etched for 4 hr. A) A-7, B) A-8, C) A-11, D) A-14, E) A-16, F) A-20.

excess amine (from 25-nm at equal stoichiometry to 50-nm, Fig. 4, at amine/epoxy ratio of 1.6/1). On the other hand, an increase in the amount of excess epoxy did not show significant changes from the morphology observed at equal stoichiometry. These observations differ from those of Racich and Koutsky(31), who found that the domain size decreased with increasing amounts of catalyst or the presence of saturated vapor of the curing agent. They argued that the crosslink density increases with increasing amounts of catalyst resulting in smaller domain sizes. The present results indicate that the domain size increases with a decrease in crosslink density in the excess-amine case but is not significantly affected with changes in crosslink density for the excess-epoxy case.

b. Effect of molecular weight of the prepolymer

When the crosslink density was changed by changing the molecular weight of the epoxy prepolymers a two-phase structure, similar to the case of variable stoichiometry, was found even at the macro level (Figures 5 and 6). A marked difference in morphology was observed in networks prepared from liquid resins as compared to those from solid or semi-solid resins. The liquid-resin samples E-1 and E-2, had dimples which had a distribution of size ranging from 5-μm to 25-μm. In addition to dimples small ridges were also seen in both agglomerated and isolated forms. In samples from semi-solid and solid resins (E-3 to E-7, inclusive) highly crosslinked shells were observed throughout the cross-

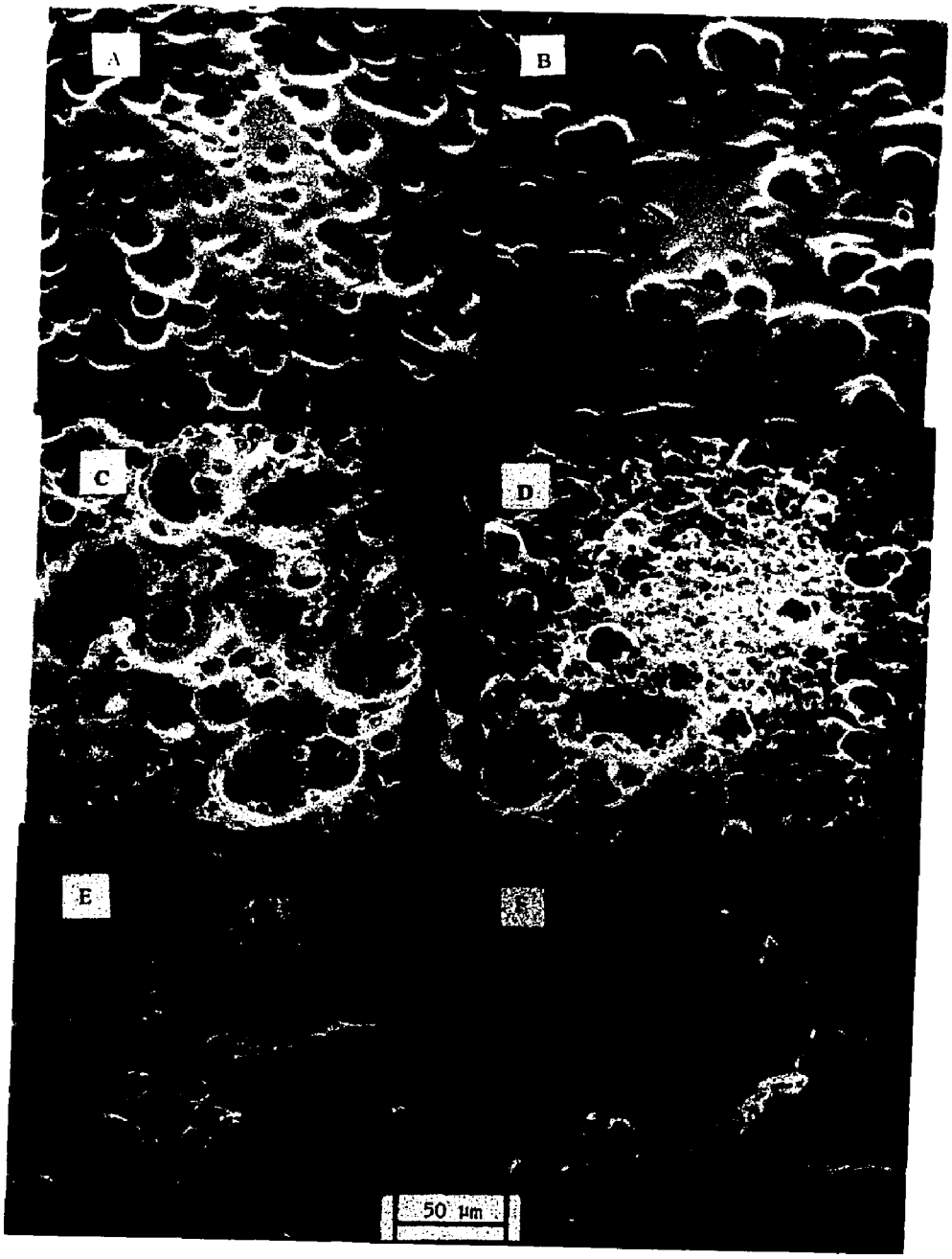

Figure 5. Scanning electron micrographs of Series E epoxy networks etched for 7 hr.
A) E-1, B) E-2, C) E-3, D) E-5,
E) E-6, F) E-7.

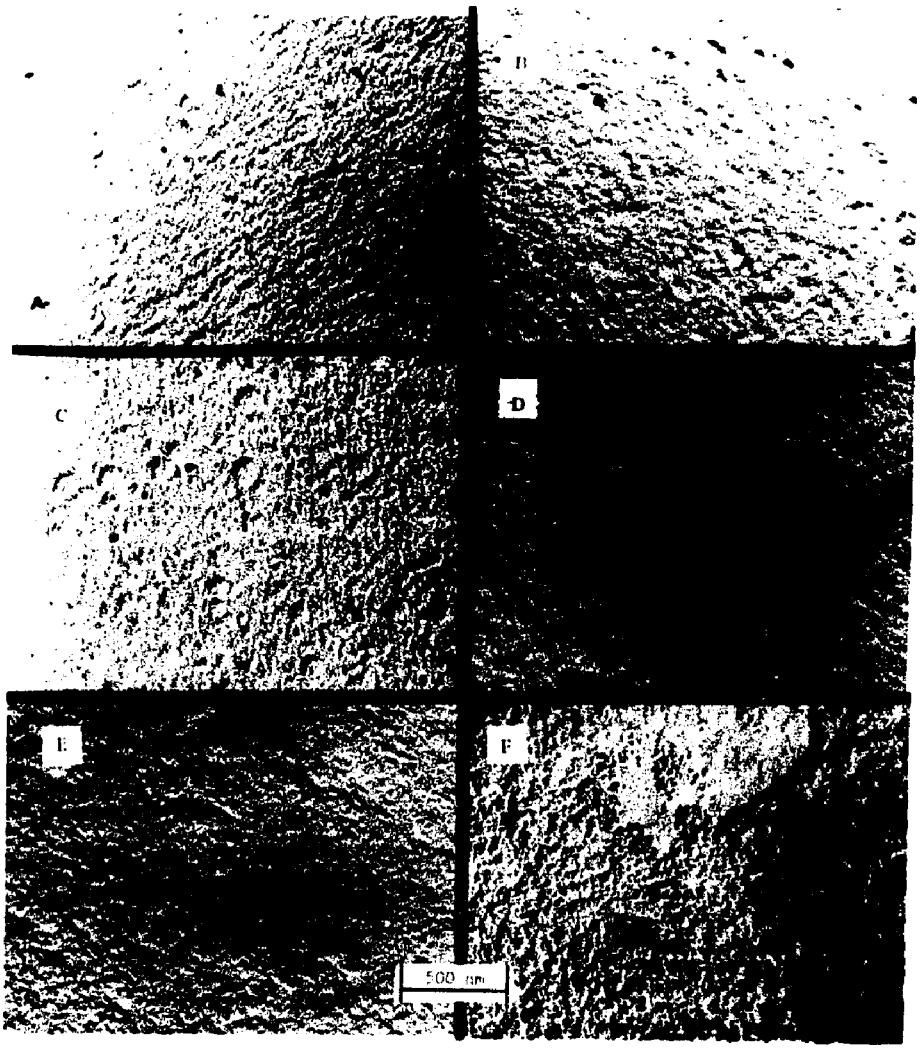

Figure 6. Transmission electron micrographs of replicas of Series E networks etched for 4 hr. A) E-1, B) E-2, C) E-3, D) E-5, E) E-6, F) E-7.

section (Figures 6 and 7), encapsulating the less crosslinked material. These shell-and-core-type structures were present in a range of sizes from 2.5-μm to 25-μm. It was found that the range narrowed but the size increased with an increase in the molecular weight of the prepolymer. This typical morphology was also observed in samples that were solvent-cast from acetone solutions and cured after most of the acetone evaporated. Since it has been shown that curing does not take place in the presence of acetone in the Epon-MDA system(37), it can be assumed that the acetone-cast samples were similar to the bulk-cured samples. Indeed no differences in mechanical properties in bulk and acetone-cast samples was observed (see discussion in Chapter VI). Etched under similar conditions, solvent-cast samples showed the same shell-and-core-type morphology (Figure 7d), indicating that this typical morphology was not due to inadequate mixing.

All the samples made from solid or semi-solid prepolymers had the same fine structure, with the size of the discontinuous phase in the range of 15-nm to 25-nm, whereas the samples made from liquid prepolymers had the discontinuous phase slightly bigger and in the range of 25-nm to 50-nm.

c. Effect of the distribution of molecular weight in the prepolymer

The gross morphology both at macro and micro levels, in the bimodal blend samples (Series F), appeared approximately

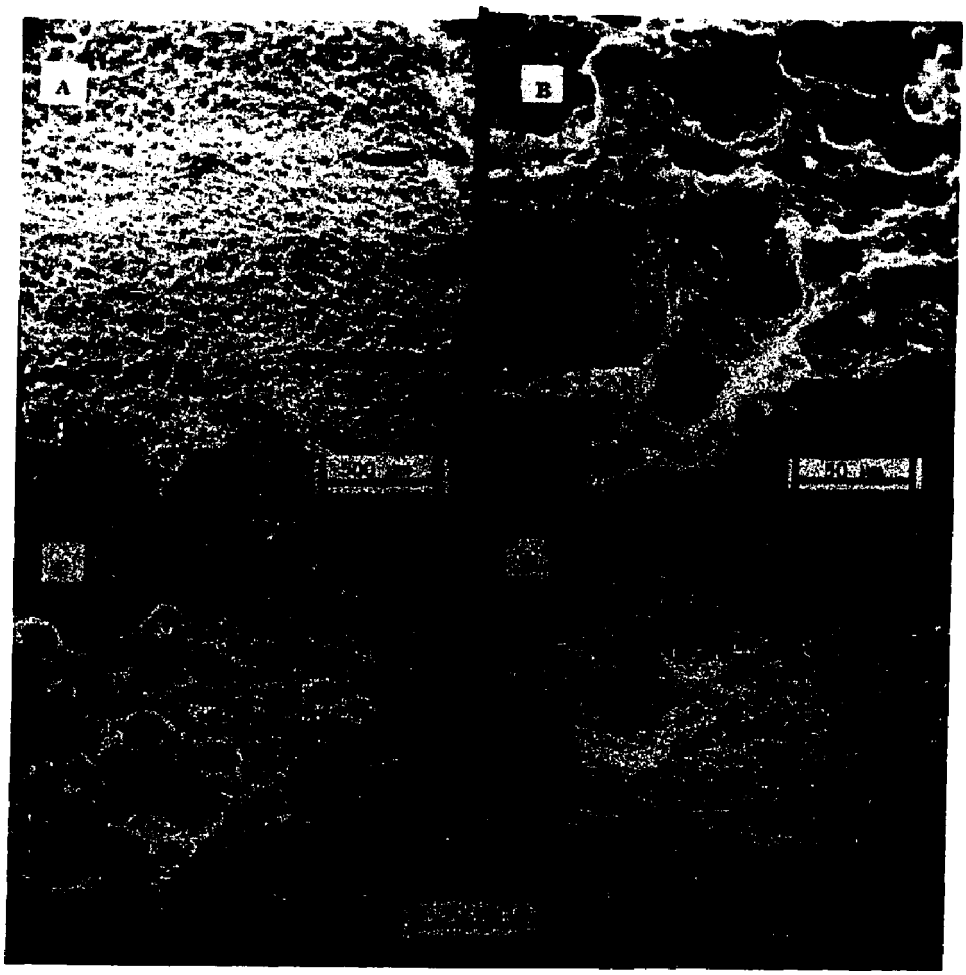

Figure 7. Scanning electron micrographs of Sample E-5 etched for 7 hr.
A) and B) Sample cross-section,
C) Sample surface,
D) Surface of solvent-cast sample.

similar to their equivalent counterparts prepared from commercial resins (Series E), as shown in Figures 8,9, and 10.

d. High molecular weight curing agent

Sample G-1, (cured with Versamid 140, a high-molecular-weight curing agent) also showed the shell-and-core-type morphology (Figure 11). The size of the shell-and-core structure (range 2.5-μm to 25-μm) and the discontinuous phase was larger than those cured with MDA, probably because this sample had a higher M_c. Figure 11 shows a shell (encircled in black) which was not etched open by the chromic acid at the time the sample was removed. A semi-open shell can also be seen which looks similar to a dimpled nodule (though of a much larger size) shown by Racich and Koutsky(31).

To check if the shell-and-core-type structure observed in semi-solid and solid prepolymers was due to fast curing, Epon 828 (liquid prepolymer) and MDA (at stoichiometric amounts) were cured at 150°C for 4 hr. This sample, after being etched as described earlier, did not show any difference in morphology from the sample cured through the regular curing cycle. It therefore appears that this peculiar morphology depends on the molecular weight of the prepolymer, and not on the rate of curing, or inhomogeneous mixing.

e. Isolation of the microgel

To determine whether the dimples observed in SEM and TEM were due to the extraction of high molecular weight material (i.e.,

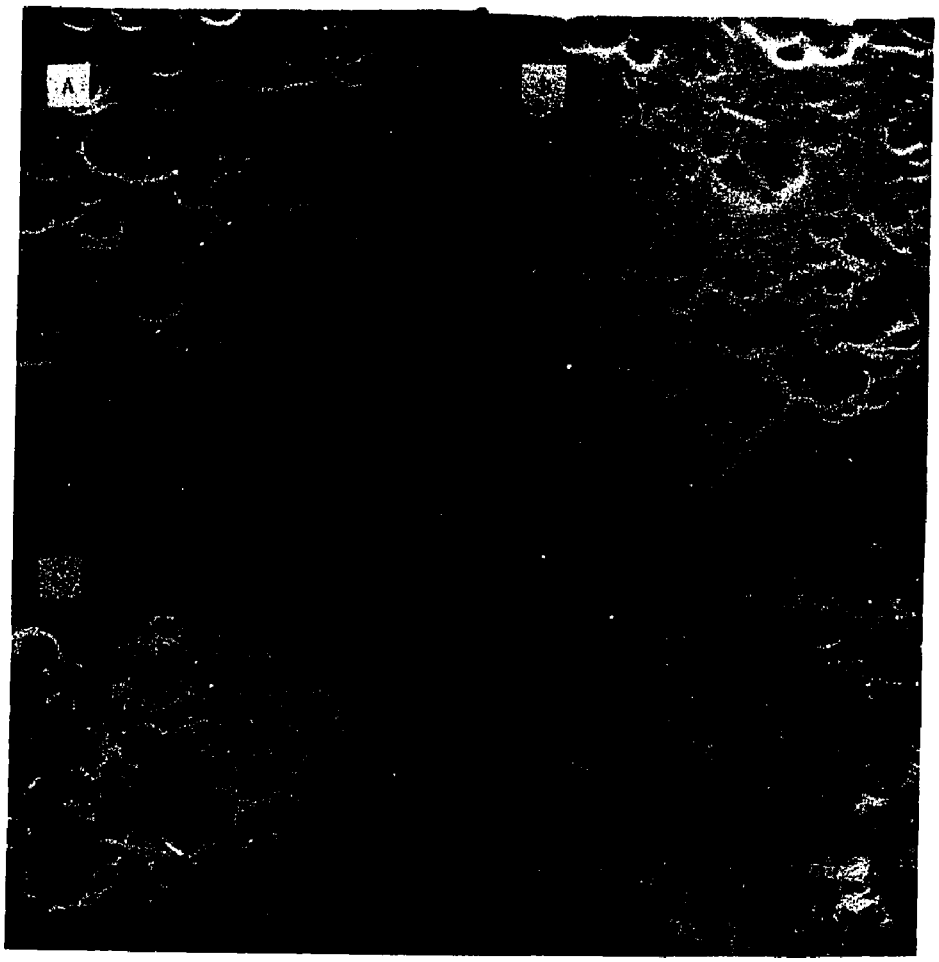

Figure 8. Scanning electron micrographs of Series F networks along with their Series E counterparts etched for 7 hr.
A) E-2, B) F-1, C) E-5, D) F-5.

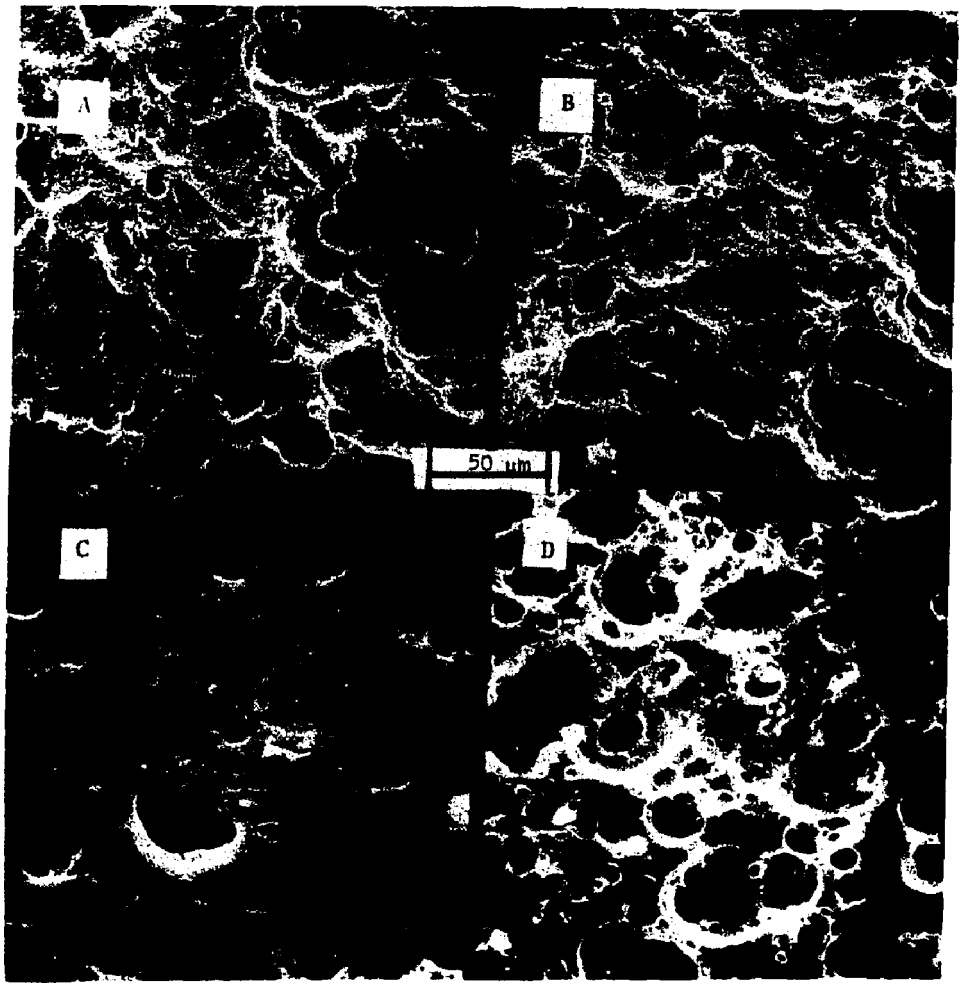

Figure 9. Scanning electron micrographs of Series F networks along with their Series E counterparts etched for 7 hr.
A) F-2, B) F-3, C) F-4, D) E-3.

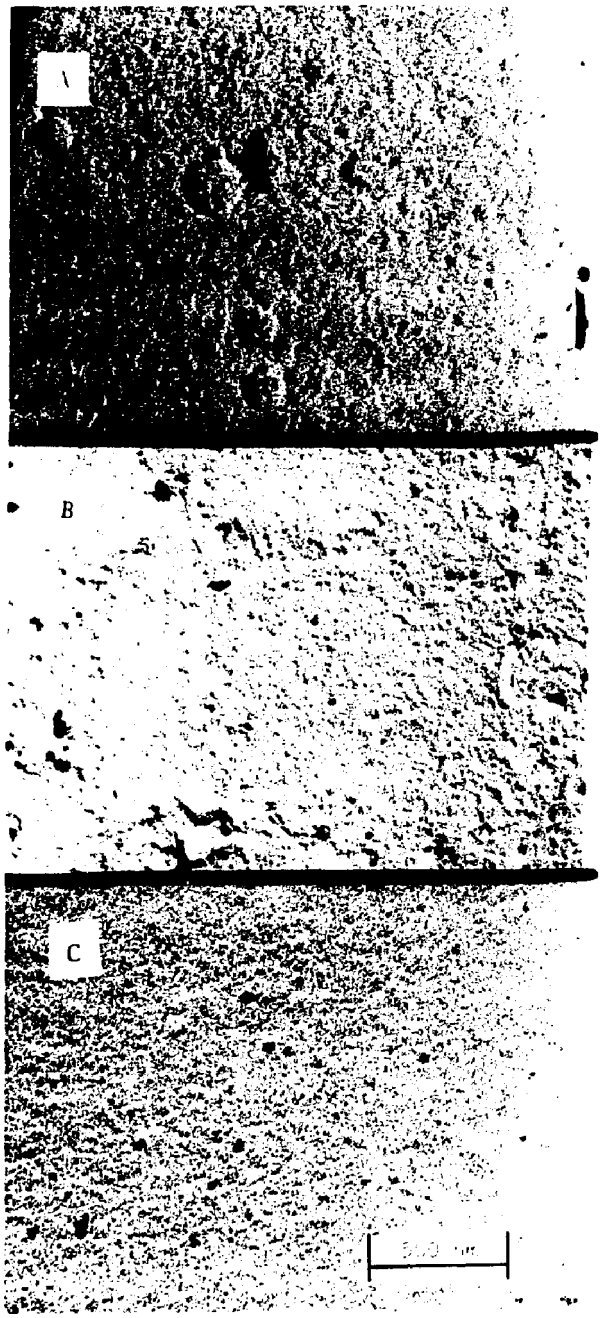

Figure 10. Transmission electron micrographs of replicas of Series F networks etched for 4 hr. A) F-1, B) F-4, C) F-5.

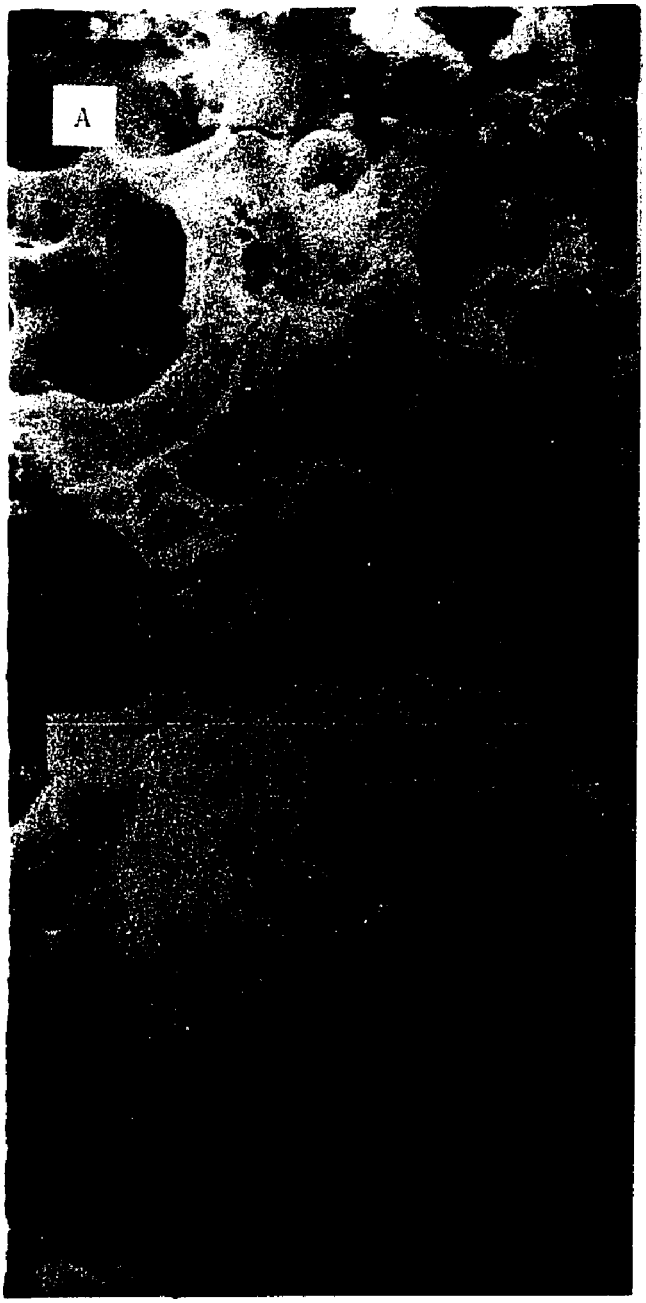

Figure 11. Scanning electron micrographs of Epon 828 resin cured with Versamid 40, network having 25% glass beads; etched for 7 hr.

clumps of microgels) or of the low molecular weight material, the following experiments were done.

1. Etched samples were removed, the etching solution was diluted with deionized water to a very low concentration, and electron microscope grids were prepared by platinum shadowing. Similarly,a less dilute solution (from the etching of sample E-5) was placed on a clean microscope slide, allowed to dry, and examined under the SEM. The electron micrographs (Figures 12 and 13a and 13b) clearly show the individual microgels (ranging in size from 20 -nm to 200-nm), and clusters of microgels that were etched out from the network surface. The appearance of these microgels is in good agreement with the observations made on replicas, and indicates that sample E-2 (prepared from liquid prepolymers) had larger microgels (sizes from 50-nm to 150-nm) as compared to sample E-5 (prepared from solid prepolymer, sizes from 25-nm to 60-nm). These experiments proved that the dimples observed through replicas, on the surfaces of the epoxy networks were due to the etching of the weak connections of the microgels or clusters of microgels and not the low crosslink density material. The platinum shadows in Figures 13a and 13b indicate that the microgels are solid and spherical in shape (a configuration having minimum surface energy) and can pack in a hexagonal array.

2. The formation of microgels during the curing process was verified experimentally on samples E-2 and E-5 by dissolving them in acetone, before gelation. Sample E-2, which has a longer gel-

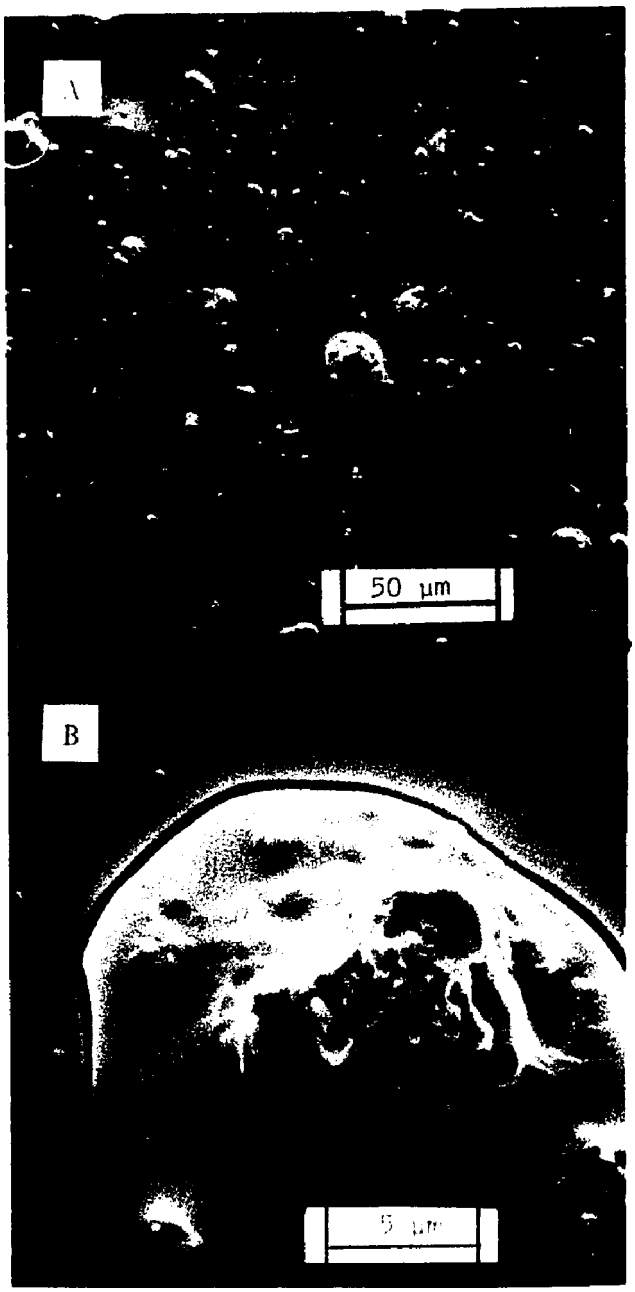

Figure 12. Scanning electron micrographs of isolated secondary microgels.

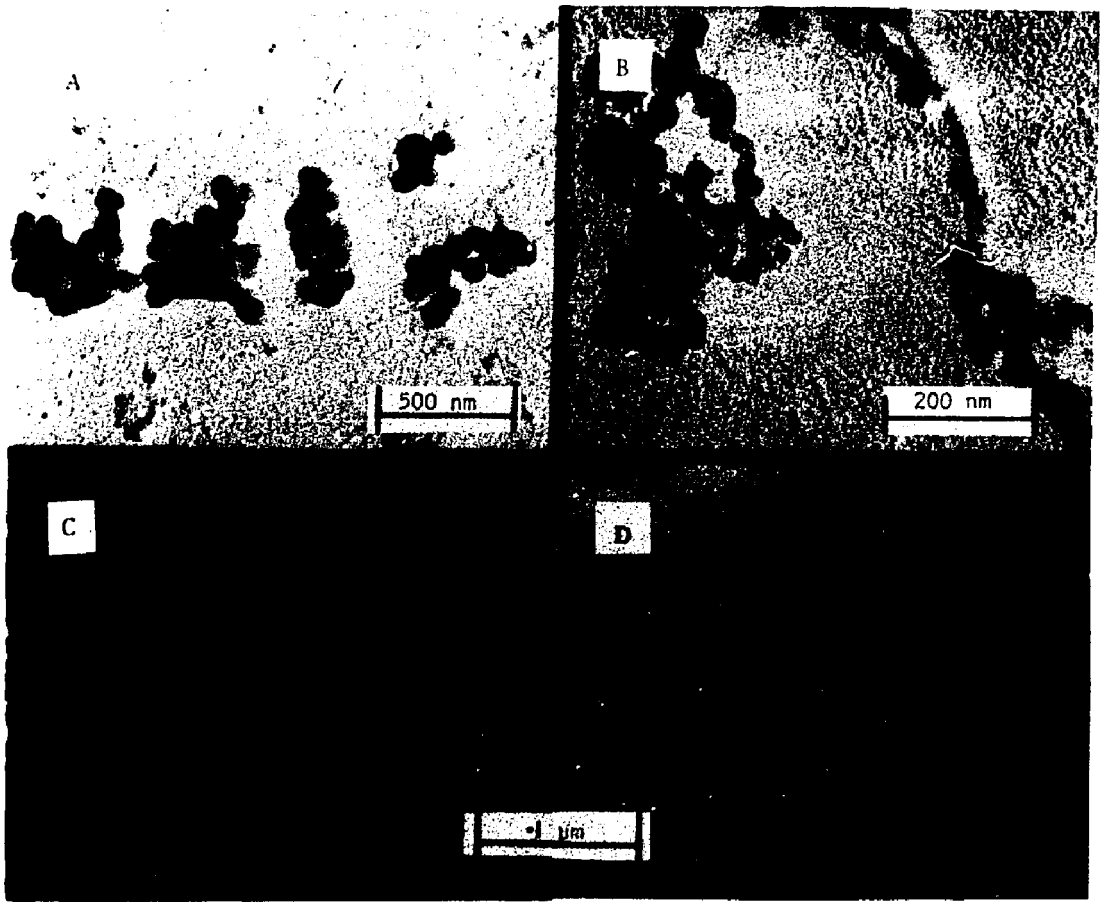

Figure 13. Transmission electron micrographs of isolated-primary microgels.
A) & B) Gel particles etched out by Cr_2O_3 solutions at 70°C after 4 hr.
C) & D) Microgels formed before gelation of the epoxy resins.
[A & C , Epon 828; B & D , Epon 1001.]

ation time than E-5 was dissolved after curing at 60°C for 30 minutes and at 80°C for another 15 minutes whereas sample E-5 was dissolved after curing for only 10 minutes at 100°C. The solution was diluted to a concentration of 100 ppm and electron microscope grids were made and examined under the TEM. The electron micrographs (Figures 13c and 13d) show the existence of microgels (darker phase) in the size range of 30-nm to 100-nm.

Thus in both cases microgels were observed, indicating that microgel formation takes place before gelation and that the microgels are dispersed and loosely connected to a weaker continuous phase. This experiment also showed that the discontinuous phase (though etched out first as clumps) is composed of microgels which are stronger than the continuous phase. It is the connections between the aggregates that are weak. The size and number of these gels continues to increase until the viscosity becomes high enough for physical gelation to take place.

C. DISCUSSION

Proposed model for network formation

As mentioned earlier electron microscopic evidence shows that microgel particles form prior to gelation (Figures 12,13), both with low and high molecular weight epoxies, and with epoxy and amine-rich systems. This observation is in accord with the suggestions of other investigators(14,27,28). Some investigators have observed these microgels in sizes smaller than 0.5-μm while others have reported larger than 5-μm. The present results indi-

cate the presence of microgels at both levels; a lower level of 10-nm to 50-nm size, and a higher level of 2-μm to 50-μm size. It is therefore highly probable that the systems studied by other investigators also had microgels at both levels. In order to differentiate between the two size levels the term primary microgels, in the present discussion, would refer to microgels in the size range of 10-nm to 50-nm, whereas secondary microgels will refer to sizes larger than 1-μm.

In view of the morphological and property data at hand a model for network formation is proposed. The principal points to consider include the following questions: the basic morphological units, the phase continuity, and the crosslink density and other properties of the various entities. The proposed mechanism, which is a modification of the mechanisms proposed by Bobalek et al.(27), Solomon(42) and Labana et al(14), considers that the formation of the macrogel takes place in three sequential steps (Figure 14) : formation of the primary microgels, formation of the secondary microgels, and formation of the macrogel. It is also proposed that the secondary microgels and the macrogel are not completely coherent (that is, they have some unconnected dangling chains).

1. Formation of the primary microgels : The reactivities of the primary and secondary amine groups in MDA are approximately in the ratio of 1.4/1(37). The primary amine groups should therefore react first to give a linear structure. Due to a combination of

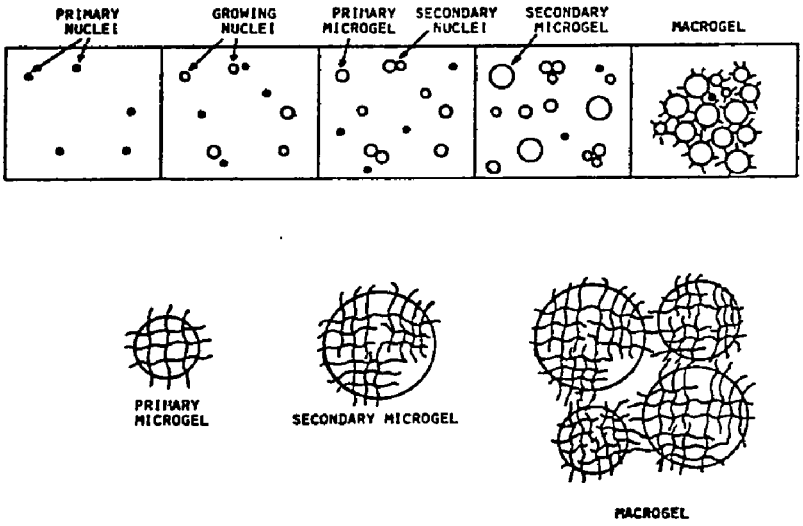

Figure 14. Proposed model for network formation.

an exothermic heat of reaction with poor heat transfer the temperature should rise in the vicinity of these molecules resulting in the reaction of the secondary amine groups. Indeed, it has been shown that the primary and secondary amine groups react almost simultaneously even when their reactivities differ by a factor of two(39). The growth of the nuclei continues till the reactive polymer molecules can diffuse to the reactive sites of the nuclei. During this process several new nuclei are also developed. Therefore, a distribution of size of the primary microgels would be expected at all times during the curing process. this phenomenon has been predicted statistically by Labana et al.(14), who termed it a nucleation process resembling the one that occurs in crystallization.

2. Formation of the secondary microgels : After a certain concentration has been reached, the primary microgels and the growing nuclei begin to interact with each other and give rise to new nuclei for what may be called "secondary microgels". These nuclei grow in size in part due to capillary forces which will encourage physical sintering, and in part due the reaction of unreacted functional groups in the primary microgels. Thus the secondary microgels are not as coherent as the primary microgels. The size of a particular secondary microgel would depend on the concentration of the primary microgels near the secondary nucleus. A size distribution in the secondary microgels should also be expected.

3. Formation of the macrogel (final network) : At a critical solids concentration (~74% for monodispersed spheres arranged in a hexagonal packing) the secondary microgels pack together and the experimental gel point is observed. At this stage phase inversion takes place in which the secondary microgels become the matrix and the unreacted or partially reacted prepolymers become the dispersed phase. By the time of complete reaction the secondary microgels become loosely connected to each other with the help of the interstitial prepolymer or due to self-diffusion of reactive dangling groups. Thus, the interconnections between the secondary microgels would be weaker than those between the primary microgels. The properties of the final network should be affected by the coherence of the network. In networks prepared by non-stoichiometric compositions the secondary microgels would be embedded in a matrix of lower crosslink density but still connected to each other through chemical bonds.

Based on the above model, the morphological differences and mechanical behavior observed in the samples of different series are interpreted below .

Morphological differences

In epoxy prepolymers the reactivity increases with the number of hydroxy groups present during the reaction(41). Thus an increase in the molecular weight of the epoxy prepolymer would not only reduce its diffusivity but would also increase its reactivity resulting in a reduced time of microgel formation. This combined

effect would result in a smaller size of the primary microgels, as observed experimentally.

In the case of non-stoichiometric compositions the size of the primary microgels should be governed by the distance between crosslinks and its structure because the diffusivity and the reactivities of the prepolymers would be almost same at all stoichiometries. In the Epon 828 and MDA system (Series A), an excess in amine concentration would initially yield many linear molecules whose length would depend on the amount of excess amine. The premature reaction of the secondary amines of these long molecules would result in larger microgels. Thus, in the case of amine excess the size of primary microgels, as observed experimentally, should increase with increasing amounts of excess amine. In the case of excess epoxy a branched structure having four epoxy molecules attached to one amine molecule is formed(37). Thus the size of the microgels formed at 100% epoxy-excess would be much smaller than those formed at 100% amine-excess. The experimental results showed a similar trend.

For systems having a slower rate of reaction (such as samples of Series A, sample E-1, sample E-2, and sample F-2, which were made from liquid prepolymers)there is more time to enhance continuity of the secondary microgels. This results in primary microgels that are more resistant to etching. However, the loose conections of the adjacent secondary microgels can get attacked resulting in the etching of the secondary microgels causing dimp-

les on the surface, as was observed experimentally. The semi-solid and solid resins are composed of high and low M.W. components; the amount of low M.W. component decreases with M.W. of the prepolymer (see Chapter III, Table I). The more reactive high M.W. components form the microgels which get dispersed in the low M.W. component, which reacts later to give a high crosslink density shell. A decrease in the low M.W. component should increase the size but decrease the number of the shell-and-core-type of structure, as was found experimentally.

Dynamic Mechanical Spectroscopy

As pointed out earlier the heterogeneous morphology, observed in the present study, is due to network flaws (weak connections between the primary and secondary microgels). The low cyclic strains applied in dynamic mechanical tests detect only the effect of the network structure and not the network flaws. Therefore, as observed experimentally (Chapter III), dynamic mechanical spectroscopy should not indicate heterogeniety in the samples.

Soluble Content of the Networks

The morphological studies had indicated an increase in the dimple size with M_c. A dimple actually represents a bit of material extracted from the network. This observation is in good agreement with the extraction results (see Chapter III) that showed an increase in soluble content with M_c.

Mechanical Behavior

At present, it is not possible to reconcile all the div-

erse dependences on stoichiometry. However, clearly there is no a-priori reason for trends in all properties to be related. By the Griffith equation

$$\sigma_u = (2 ES/ \underline{a})^{1/2} \qquad (1)$$

where σ_u = ultimate tensile strength

E = Young's modulus

S = fracture energy

$\underline{a}$ = characteristic flaw size

Thus σ_u at constant E depends on how S varies with $\underline{a}$; S may change while σ_u does not, if changes in $\underline{a}$ compensate for changes in S. For the Epon 828-MDA system several investigators(40,41) have shown that σ_u is almost independent of stoichiometry. Furthermore, it has also been shown that impact toughness is at a maximum not at 100% stoichiometry but at a 1/1.4 epoxy/amine ratio(36,40,41). The impact strength for excess epoxy was also reported to be higher than that at equal stoichiometry. Under these circumstances it has been shown that the critical flaw size $\underline{a}$ is a linear function of amine/epoxy ratio, changing from 32-μm to 141-μm(41).

Whether the critical flaw size corresponds to the aggregates first formed prior to phase inversion or whether it corresponds to the inclusions is, of course, not known. Indeed, the reality of a flaw corresponding to the calculated value of $\underline{a}$ is not proven. Nevertheless, the close agreement between microscopic evidence of the present study and the computed flaw size(41) is strongly suggestive of a correlation.

Though the modulus, E, does not decrease (in fact increases slightly)(40,41) with an increase in amine content, the overall plastic deformation should increase due to the plasticizing character of the amine. Hence, S increases (E itself may increase due to enhanced continuity of the network). At the same time the flaw size increases, but not as fast as S so that tensile strength actually increases a little. But with an epoxy excess, the decreased flaw size (corresponding to smaller aggregates) more than balances out the lower value of S so that the strength again increases. However, the toughness otherwise seen at high amine contents is vastly reduced by the high loading rate in impact, while with epoxy excess, the smaller flaw size is able to delay fracture.

In the case where the M_c is varied by varying the molecular weight of the epoxy resin, at equal stoichiometry (Series E), the ultimate tensile strength is independent of M_c but the impact strength decrease with M_c (see Chapter III). When the molecular weight of the epoxy is increased a different behavior occurs. The inherent S of the epoxy components is low compared to that of amine and hence the tensile strength does not increase and impact strength decreases.

The glass transition temperature

Samples having a bimodal distribution of molecular weight (Series F) showed the same T_g as their counterparts having a broad distribution, in the high (> 700) and the low (< 400) ranges

of M_c. At intermediate M_c's the T_g was found lower in samples having bimodal distribution (see Chapter III). Though the morphology of the bimodal and broad distribution was the same, the properties of the former will be determined by the dominant component in the final network. If this is a high-molecular-weight resin (which is more reactive) this network will dominate, and T_g will be low, perhaps because the initial fast reaction results in greater incoherence . At intermediate compositions a judicious balancing may occur, and result in a more coherent network, and thus properties may be governed by the low-molecular-weight component.

Although this discussion is clearly speculative, it does explain some of the behavior noted, and suggests ideas capable of testing in the laboratory.

The fact that small-angle X-ray scattering and stained or unstained microtomed thin sections fail to indicate a two-phase stucture(36, also see Chapter V) also supports the present model, which explains that heterogeniety in networks is primarily due to incoherence.

D. CONCLUSIONS

From the present study and the studies of other investigators (discussed earlier) it is clear that crosslinked networks in many epoxy resins and in some alkyd resins are heterogeneous in nature.

According to the proposed model small primary microgels ranging from 10-nm to 100-nm are formed much before the inset of

physical gelation. These primary microgels agglomerate together through weak connections to produce secondary microgels ranging from 0.5-μm to 50-μm. The secondary microgels coalesce together and the experimental gel point is observed. The final crosslinked network is produced after complete reaction of the unreacted prepolymers left in the interstices of the coalesced secondary microgels. As compared to primary microgels, these secondary microgels are generally connected to each other through weaker links. In networks prepared through non-stoichiometric compositions the secondary microgels are embedded in a matrix of lower crosslink density but still connected to each other through chemical bonds.

The coherence of the final network (macrogel) depends on the strength of the connections between the secondary microgels which in turn governs its tensile properties.

In the case when the prepolymers have a bimodal distribution of molecular weight the properties of the network are governed by the component that is more dominant in the microgels.

Though sufficient experimental evidence is not presently available, the optimization of curing conditions should also play an important role in achieving maximum coherence in the network.

REFERENCES

1. J.H. deBoer, Trans. Faraday Soc., 36, 10(1936).

2. F.Lohse, R.Schmid, H.Batzer, and W.Fisch, Br.Poly.J.,1, 110(1969).

3. R.Houwink, J.Soc.Chem.Ind. (London), 55, 247 T(1936); Trans Faraday Soc., 32, 122(1936).

4. R.E.Cuthrell, J.Appl.Polym.Sci.,11, 949(1967).

5. E.H.Andrews,"Fracture in Polymers", American Elsevier, (1968).

6. D.H.Solomon and J.J.Hopwood, J.Appl.Polym.Sci.,10,1898(1966).

7. R.E.Cuthrell, J.Appl.Polym.Sci., 12, 1263(1968).

8. D.H.Kaelble, in "Epoxy Resins, Chemistry & Technology", ed. by C.A.May and Y.Tanaka, Marcel Decker, N.Y., 1973, Chapt.5.

9. R.Blockland and W.Prins, J.Polym.Sci., A-2,7, 1595(1969).

10. L.Gallacher and F.A.Bettelheim, J.Polym.Sci.,58, 697(1962).

11. H.H.M.Balyuzi and R.E.Burge, Nature, 227, 489(1970).

12. A.S.Kenyon and L.E.Nielsen,J.Macromol.Sci.-Chem.,A-3,2, 275(1969).

13. J.L.Kardos, Trans. N.Y.Acad.Sci., 11,35(2), 136(1973).

14. S.S.Labana, S.Newman, and A.J.Chompff, in "Polymer Networks", eds. A.J.Chompff and S.Newman, Plenum Press,N.Y., 1971,p 453.

15. E.H.Erath and R.A.Spurr J.Polym.Sci., 35, 391(1959).

16. E.H.Erath and M.Robinson, J.Polym.Sci., C-3, 65(1960).

17. R.A.Spurr et al., Ind.Eng.Chem.,49,1839(1957).

18. T.Miyamoto and K.Shibayama, Kobunshi Kagaku(Eng.Ed.) 2, 203(1973).

19. A.I.Loskutov, M.P.Zagrebennikova, and L.A.Arsen'eva, Vysokomol. Soedin, B, 16, 334(1974).

20. H.P.Wohnsiedler, J.Polym.Sci., C-3, 77(1963).

21. T.G.Rochow, Anal.Chem., 33, 1810(1961).

22. T.G.Rochow and F.G.Rowe, Anal.Chem., 21,461(1949).

23. R.M.Kessenikh, L.A.Korshunova, and A.V.Petrove, Polym.Sci. USSR, 14, 466(1972).

24. V.Y.Basin, L.M.Korunskii,O.Y.Shokal'skaya, and N.V.Aleksandrov, Poly.Sci. USSR, 14, 2339(1972).

25. T.S.Carswell, "Phenoplasts;Their structure, properties and chemical technology", Interscience,N.Y., 1947, Chapt. 5.

26. A.N.Neverov et al., Vysokomol. Soedini, A-10,463(1968).

27. E.G.Bobalek, E.R.Moore, S.S.Levy, and C.C.Lee, J.Appl.Polym. Sci., 11,1593(1967).

28. D.H.Solomon, B.C.Loft, and J.D.Swift, J.Appl.Polym.Sci., 11, 1593(1967).

29. R.J.Morgan and J.E.O'Neal, Polym.Plast.Tech. Eng.,5,173(1975).

30. J.L.Racich and J.A.Koutsky, J.Appl.Polym.Sci.,20,2111(1976).

31. J.L.Racich and J.A.Koutsky, "Chemistry and properties of crosslinked polymers", ed. S.S.Labana, Acad.Press Inc.,N.Y.(1977) p. 303.

32. R.J.Morgan and J.E.O'Neal, "Chem. and properties of crosslinked poly." ed. S.S.Labana, Acad.Press Inc.,N.Y.(1977), p.289.

33. H.Batzer, F.Lohse, and R.Schmid, Agnew Makromol.Chem.,29/30, 349(1973).

34. W.Funke, J.Polym.Sci., C, 16,1497(1967).

35. U.T.Kreibick and R.Schmid, J.Polym.Sci.,Symp.No.53, 177(1975).

36. K.Selby and L.E.Miller, J.Material Sci., 10, 12(1975).

37. J.P.Bell, J.Polym.Sci., A-2, 8, 417(1970).

38. J.P.Bell, J.Appl.Polym.Sci., 14, 1301(1970).

39. M.A.Acitelli, R.B.Prime, and E.Sacher, Polym., 12,335(1971).

40. J.P.Bell, J.Appl.Polym.Sci., 14, 1901(1970).

41. S.L.Kim, M.Skibo, J.A.Manson, R.W.Hertzberg, and J.Janiszewski, presented at the A.C.S. Meeting, Chicago, August 1977.

42. D.H.Solomon, J.Macromol.Sci.,(Rev.),C-1(1), 179(1967).

CHAPTER V

EMULSION CURING

A. INTRODUCTION

In recent years latex-based protective coatings have become increasingly important for many applications. This trend reflects a combination of lower costs, lower consumption of petroleum-based solvents, and decreased pollution by hydrocarbons; thus continued research to improve and extend applications is of both technical and socioeconomical interest. In many cases, e.g.,styrene and acrylic resins, polymerization in emulsion leads directly to the desired latex, and development is therefore relatively straightforward. On the other hand, many polymers of interest such as epoxies and polyurethanes cannot be prepared by emulsion polymerization; instead, as described by Warson(1) and Blackley(2), different techniques such as direct emulsification must be used. Once the latexes of the epoxy resin and the curing agent are prepared they can be mixed together and cured to give a crosslinked network. The overall process of curing must of course be complex -- involving evaporation of the medium, physical coalescence of the particles, diffusion of the reactants, and the curing step itself. However, for convenience, the process will be referred to simply as " emulsion curing ".

During a program to develop an aqueous primer/topcoat system for aluminum alloys(3), it was shown that coherent films could be prepared by the use of directly emulsified components.

Even though the process of film formation involves an intricate balance between the evaporation of water, the physical coalescence of particals, interdiffusion of the reactive components, and the curing step itself, it was possible to obtain films showing promising physical and mechanical properties(4,5).

In any case, to have a good understanding of emulsion curing it is important to study both the film formation and the curing mechanisms. In this preliminary work, epoxy/polyamide emulsions were studied. Specifically, dynamic mechanical spectroscopy (DMS), transmision electron microscopy (TEM), swelling and extraction tests, and differential scanning calorimetry (DSC) were used to evaluate the behavior of the films in comparision with the behavior of a solution cured film having a similar composition.

B. FILM FORMATION IN CHEMICALLY REACTIVE EPOXY EMULSIONS

Before considering the experimental details of the study, it is pertinent to briefly review the principal aspects of film formation from emulsion.

It is well known that when an array of particles (metallic, ceramic, or polymer) is placed in contact, coalescence at temperatures below the melting point often occurs. While the mechanism of coalescence (or sintering) varies depending on the type of material in question, and while a variety of mathematical formulations have been proposed(6-10), it is clear that the origin of the driving force for sintering (i.e., coalescence after particle contact is established) is based on the development of surf-

ace forces which will tend to minimize overall surface energy(6). When the particles are suspended in the form of an emulsion, additional forces are contributed due to the particle-water and water-air interfacial forces. Generally, film formation from emulsion is considered to occur in several different stages, as follows:

Stage I : First the evaporation of water causes a progressive restriction on the Brownian motion of the particles until they are forced together to the point that the double-layer repulsion hinders their further mutual approach. On further evaporation, the water-air interfacial area increases, causing in turn an increase in the surface pressure (P_{wa}). At some point the double-layer repulsion (F_e) is overcome by the water-air interfacial pressure (P_{wa}), and the spheres are forced together to form a polymer-polymer contact. For monodispersed spheres packed in a rhombohedral array polymer-polymer contact is expected to occur at a 74%-solids concentration. Throughout this process, the rate of drying is essentially constant.

Stage II : Following the establishment of particle-particle contact in a close-packed array, further coalescence of the polymer particle takes place due to some or all of the following forces(7) : the force (F_s) produced due to the negative curvature of the polymer particle, capillary forces (F_c) produced by the negative curvature of the water present in the interstitial capillaries, forces (F_{pw}) produced by the polymer-water interfacial

tension, and van der Waal's forces (F_v) between the spheres. For coalescence to occur, these forces should be greater than the resistive forces (F_g) caused by the particle rigidity at that particular time, and the coulombic repulsion forces (F_e) of the charged spheres:

$$F_{wa} + F_s + F_c + F_{pw} + F_v > F_g + F_e \qquad (1\text{-}a)$$

While the precise magnitudes of the individual forces are not yet established(7-9) the role of the modulus (implicit in F_e) is established for both polymer sintering(6) and emulsion coalescence(7). In borderline cases slow rates of film formation or high temperatures permit the modulus of the polymer to reduce (7) facilitating coalescence.

During this stage of film formation a decrease in the overall rate of water evaporation takes place(11). In addition, internal stresses tend to be developed, depending on several factors such as : the rate of drying(12), the film thickness(13,15), the structure of the polymer(13,15), and the particle morphology (14).

Exudation of any incompatible emulsifier also begins to occur during this stage, while a compatible emulsifier diffuses into the polymer particles(16). In any case stage II is essentially complete when the concentration of 90% solids is reached(17).

Stage III : Now the particles diffuse into each other presumably by segmental motions - a process called "autohesion" (18). Such further gradual coalescence improves the properties of

the polymeric film and occurs at the rate depending on polymer molecular weight and structure(19). However, it does not depend on the type of the substrate and occurs at the same rate throughout the cross-section of the film(20). The internal stresses produced in stage II relax and achieve equilibrium values. The process of diffusion/exudation of the emulsifier is completed by this stage. The rate of film formation decreases considerably at 91-93% solids concentration(17) and the residual water evaporates by diffusion through capillary channels or the polymer itself. In most cases, the particles lose their identities by the end of stage III and give a smooth film.

a. Results and Discussion

Cold stage electron microscopy indicated that all Epon 1001 emulsions contained discrete particles ranging in size from 40-nm to 250-nm. The Epon 1001- bisphenol-A emulsion had similar but larger particles ranging in size from 40-nm to 500-nm. On the other hand, all Versamid 115 emulsions had discrete particles of 20-nm to 40-nm size, connected to each other with thin strands possibly formed by coalesced particles of even smaller size (see Figure 1).

1. Film Formation at Stage I : All thin films became transparent within four hours of casting. In all cases, there was a several-fold increase in particle dimensions -- a phenomenon not seen in regular emulsions. The increase in size was found to depend on the rate of reaction and the aging time. Figure 2 indicates

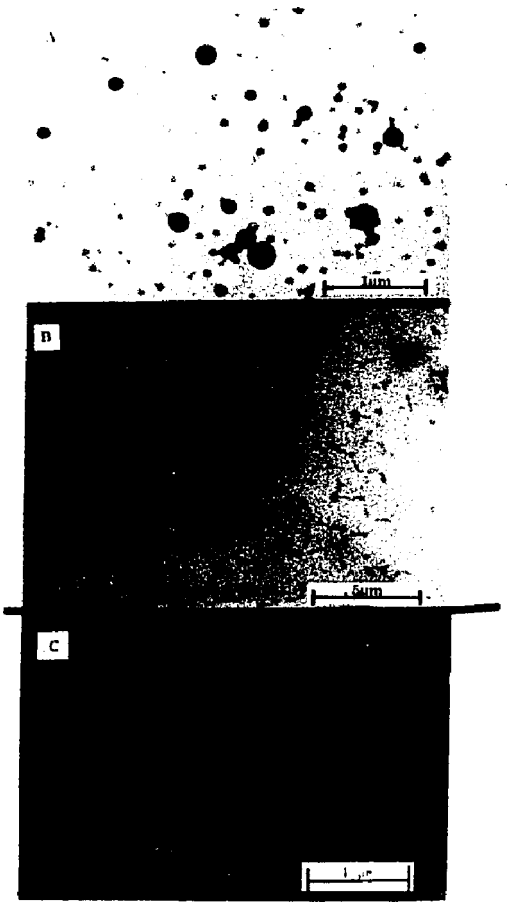

Figure 1. Cold stage transmission electron micrographs of diluted dispersions.
A) Epon 1001, B) Versamid 115,
C) Epon 1001-bisphenol A, 96:4 ratio.

that agglomerates of the curing agent and the epoxy particles are formed; the most common way being the agglomeration of the small epoxy particles on the entire surface of a larger epoxy particle alongwith the curing agent particles forming the interface. Such an agglomerate would appear in the electron microscope as one big particle. This phenomenon is attributed to the polydispersity of the emulsion mixtures and the reactive forces between the epoxy and the Versamid particles. Depending on the rate of reaction, the particles would react after a certain time of contact. This reaction would result in permanent agglomerates and the formation of a crosslinked structure on the interface of the particles. Thus the rate of agglomeration or the rate of increase in particle size would depend on the rate of reaction. This is confirmed by Figure 2, which indicates that at a fixed time the more reactive system IV had agglomerates twice the size of those in the less reactive system I. As expected, it was also found that the agglomerate size increased with time.

As discussed earlier, it is well known that the rate of coalescence decreases with an increase in particle size or an increase in the modulus/viscosity of the particles and at some limiting value there would be no coalescence. Therefore, if the film formation time in stage I is too long (for the chemically reactive emulsion mixture) the agglomerate size or modulus or both would reach the limiting value at which no coalescence would take place. Such cases where the particles did not coalesce are shown in Fig-

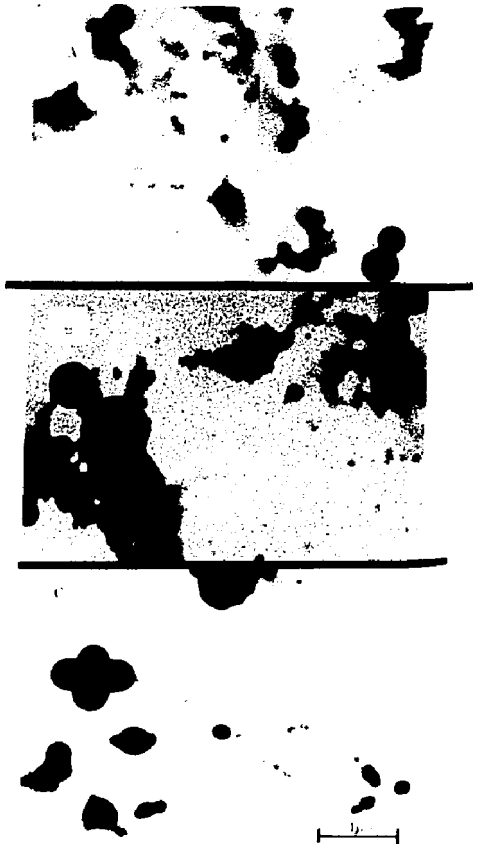

Figure 2. Cold stage electron micrographs of diluted aqueous dispersions of stoichiometric mixtures of different samples aged for 30 min.
A) System I, B) System II, C) System IV.

ures 3 and 4. In both cases thick films were prepared which took 22 to 24 hours to complete stage I of film formation (determined by the time taken to become transparent). During this time systems III and IV, which had a higher rate of reaction, formed some agglomerates having either modulus or size that had crossed the limiting value for film formation, thus inhibiting coalescence. However, these systems did not show uncoalesced particles for thin films, which had taken only 4 to 5 hours to complete stage I of film formation. This small time was not enough for the agglomeration to reach the limiting value of modulus or size that would hinder film formation. On the other hand, due to the lower rate of reaction systems I and II had not crossed the limiting value and therefore did not show any uncoalesced particles. Figure 5 nicely indicates the effect of time taken to complete stage I. In this case a mixture of system I was stored in a closed container for 7 days prior to the casting of the film. The agglomeration and premature curing of the outer surface of the particles had increased the modulus to such an extent that the initial coalescence producing a transparent film could occur but further gradual coalescence could not take place.

From the above discussion it is clear that the time for stage I should be as short as possible so that the size and modulus of the agglomerates do not reach a value that would prohibit film formation during stages II and III. This time can be reduced by increasing the rate of evaporation. However, it has been shown

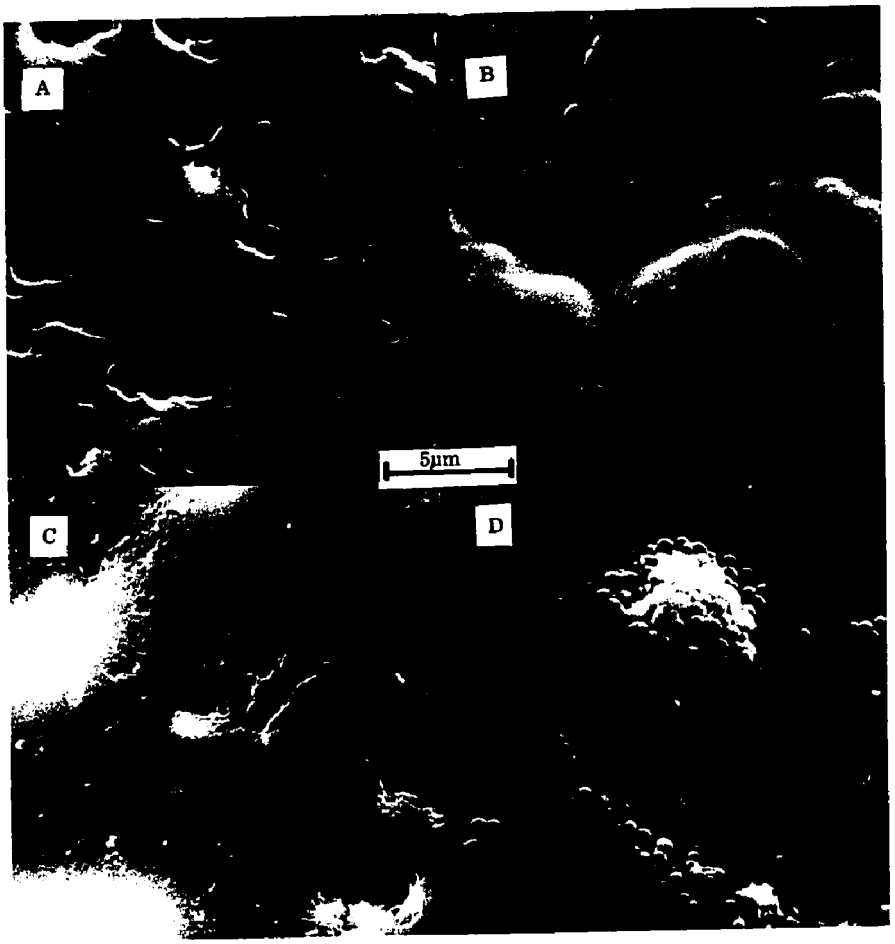

Figure 3. Scanning electron micrographs of surfaces of different emulsion-cured samples. A) System I, B) System II, C) System III, D) System IV.

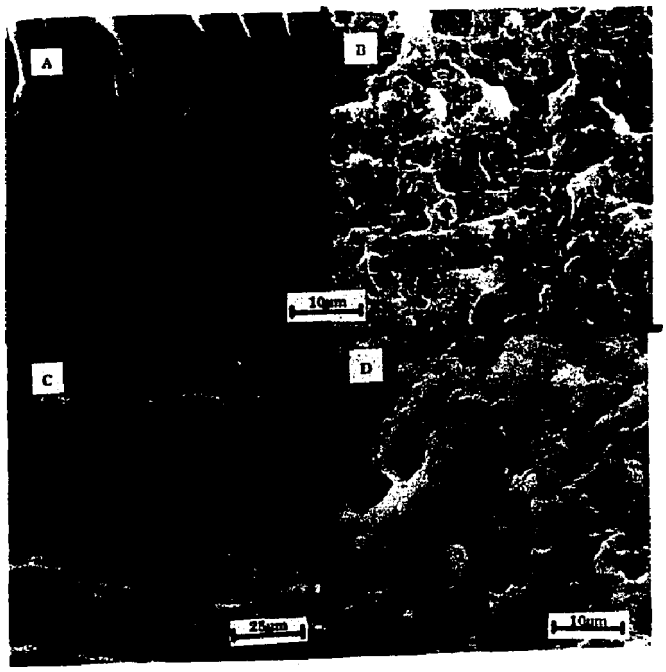

Figure 4. Scanning electron micrographs of fractured surfaces of System III.
A) Extracted film fractured at liquid N_2 temperature,
B) Unextracted film fractured at liquid N_2 temperature,
C) Unextracted film fractured at room temperature.
D) Extraction done after fracture at liquid N_2 temperature.

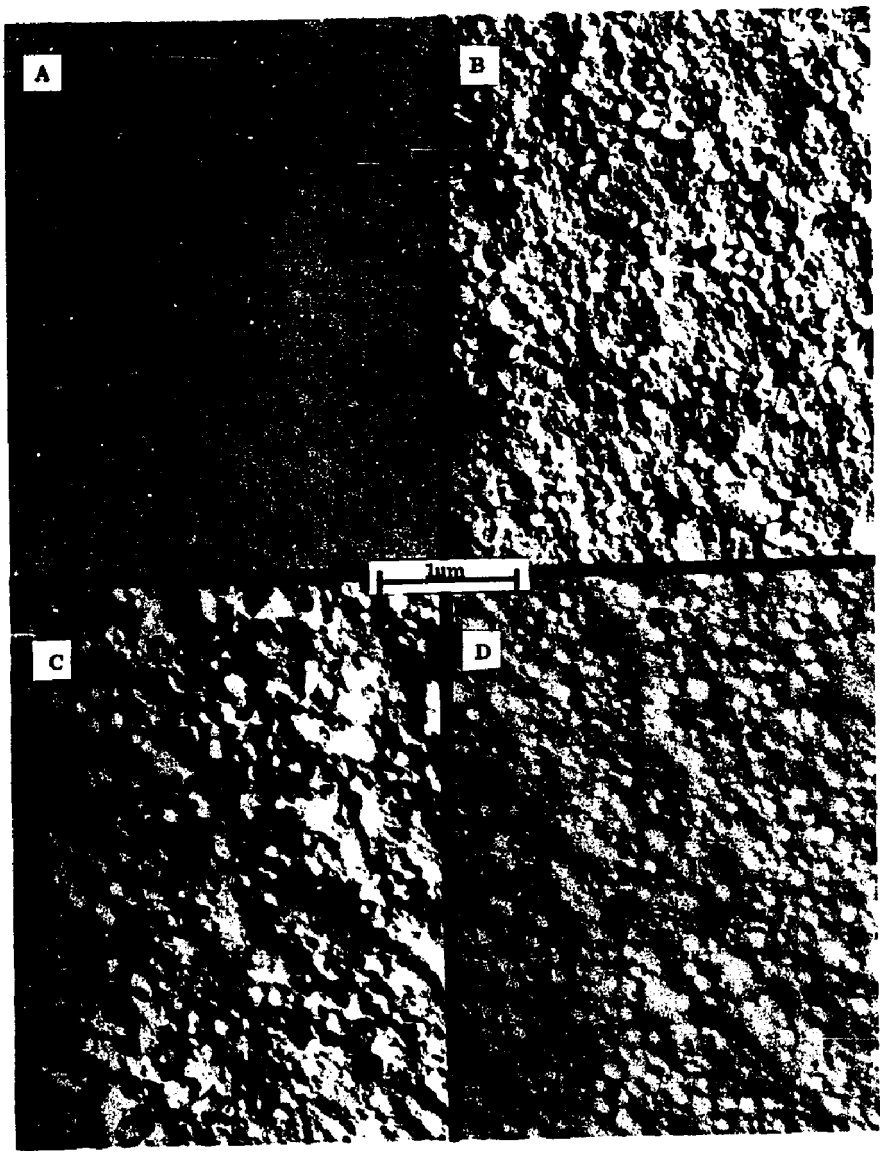

Figure 5. Transmission electron micrographs of two-stage surface replicas of System I having emulsifier combination B, kept in a closed container for 7 days before casting. The film was aged at room temperature for: A) 7 hr, B) 7 days, C) 15 days, D) 34 days.

earlier(13), and was also found in the present study that high rates of evaporation produce higher internal stresses that result in cracks in the final film. Therefore, a certain limit which cannot be exceeded exists for the rate of evaporation. Thus for highly reactive emulsion systems, it would be necessary to reduce the total time of stage I by using higher solids content, by applying thinner films, along with the optimum rate of evaporation.

Film Formation at Stages II and III : The electron micrographs of the replicas at different aging times, after stage I, were surprisingly different than those typical of the more common emulsions, such as styrene- butadiene. In the present case, the time for the disappearance of the particle contours was much shorter (6-15 hr.). This is mainly attributed to the small particle sizes (10-200 nm.) of the present emulsions. It was observed that the rate of reaction, the emulsion particle size, and the compatability of the emulsifier with the final film plays an important role in the film formation at stages II and III. These variables are discussed below .

Effect of rate of reaction : The particle contours of system I (Figure 6) had disappeared after aging times as short as 7 hours, whereas in system II (Figure 7) the particle contours disappeared only after 15 hours (not shown in the figure, system II is essentially system I preheated at 55°C for 15 minutes and then cooled to room temperature before casting). During the preheating period due to enhanced rate of reaction, agglomeration

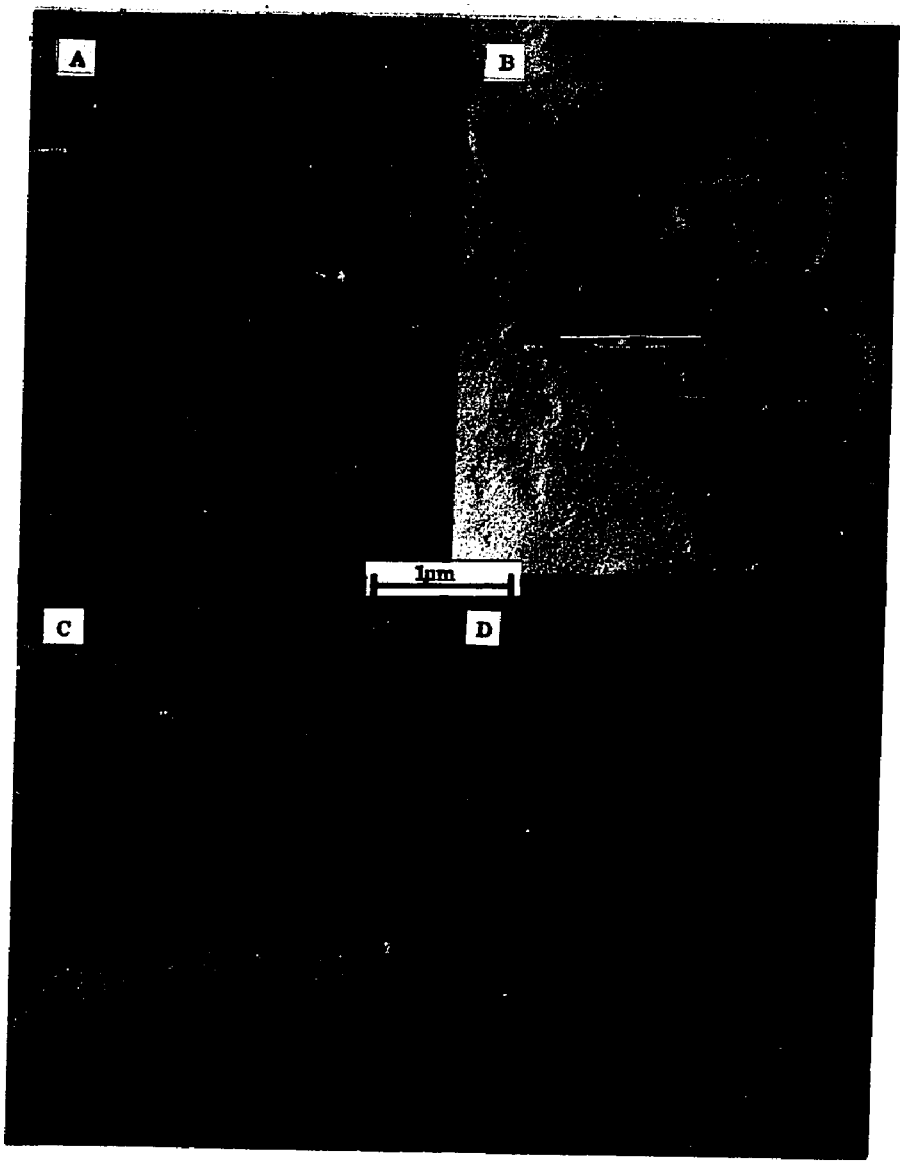

Figure 6. Transmission electron micrographs of two-stage surface replicas of System I, aged at room temperature for: A) 7 hr, B) 1.5 days, C) 11.5 days, D) 45 days.

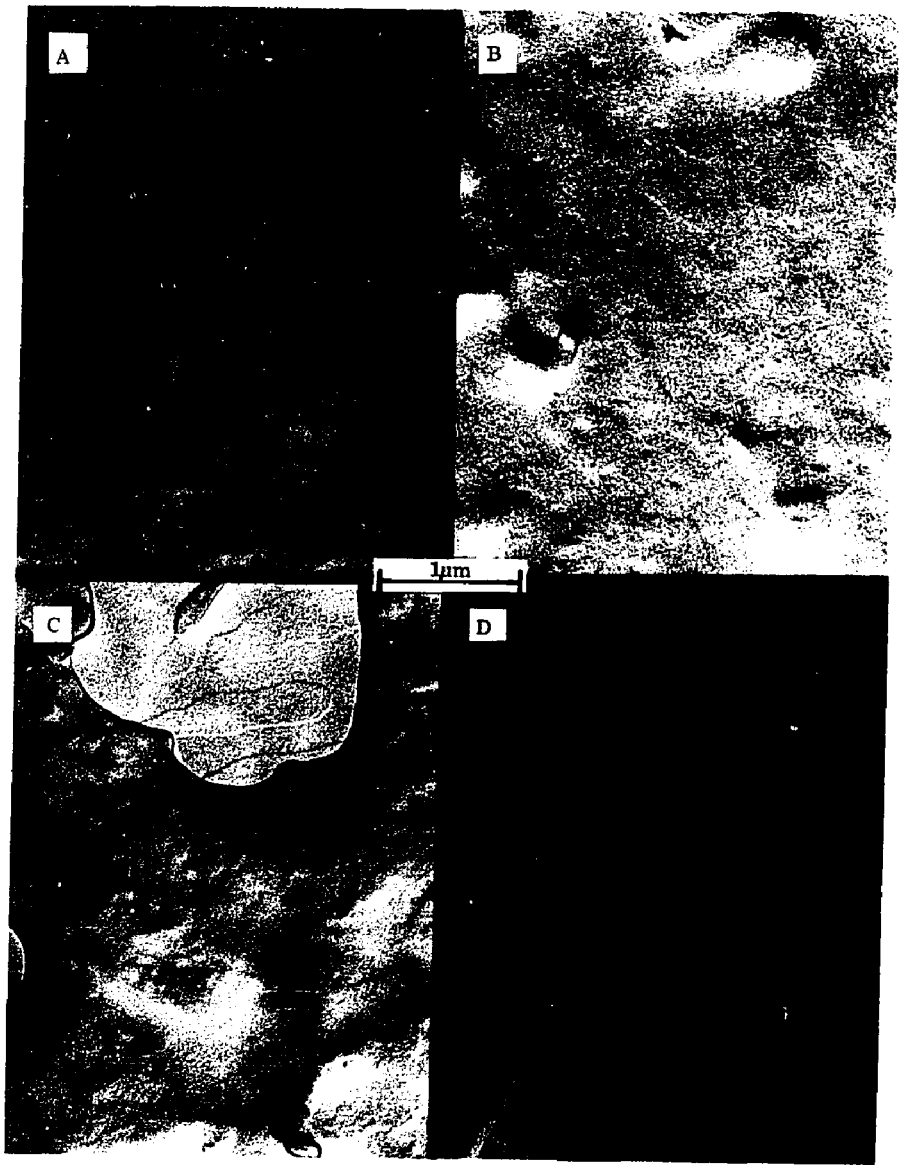

Figure 7. Transmission electron micrographs of two-stage surface replicas of System II, aged at room temperature for: A) 7 hr, B) 1.5 days, C) 11.5 days, D) 45 days.

takes place at a higher rate as shown earlier (Figure 2b). The larger size of the agglomerates formed in stage I results in a slightly slower rate of coalescence. System IV, which has the same particle size distribution but a higher rate of reaction than system I, showed a slower rate of coalescence than both systems I and II. The particle contours in this case disappeared in 1.5 days (Figure 8). The higher rate of reaction of this system results in an early increase of moduli of the interface. This in turn, slows the rate of coalescence. Similarly, in system III, which had particles of the largest size (Figure 1c) alongwith a faster rate of reaction, the contours vanished very slowly (see Figure 9), and were visible even after 45 days. The combined effect of large particle size and higher reactivity was responsible for the low rate of coalescence.

Effect of Emulsifier Compatibility : Incompatible emulsifier is exuded to the film surface(8,9) during stages II and III whereas compatible emulsifier diffuses into the particles and becomes distributed throughout the film. To study the effect of emulsifier compatibility, emulsions of Epon 1001 and Versamid 115 were prepared using two different emulsifier combinations. Combination A consisted of Hexadecyltrimethylammoniumbromide (HDTMAB) with cetyl alcohol whereas combination B consisted of HDTMAB with n-decane. It was observed that combination A was quite incompatible with the final film and hence was exuded to the surface (Figures 6 and 7). This was confirmed by the replicas of methanol-

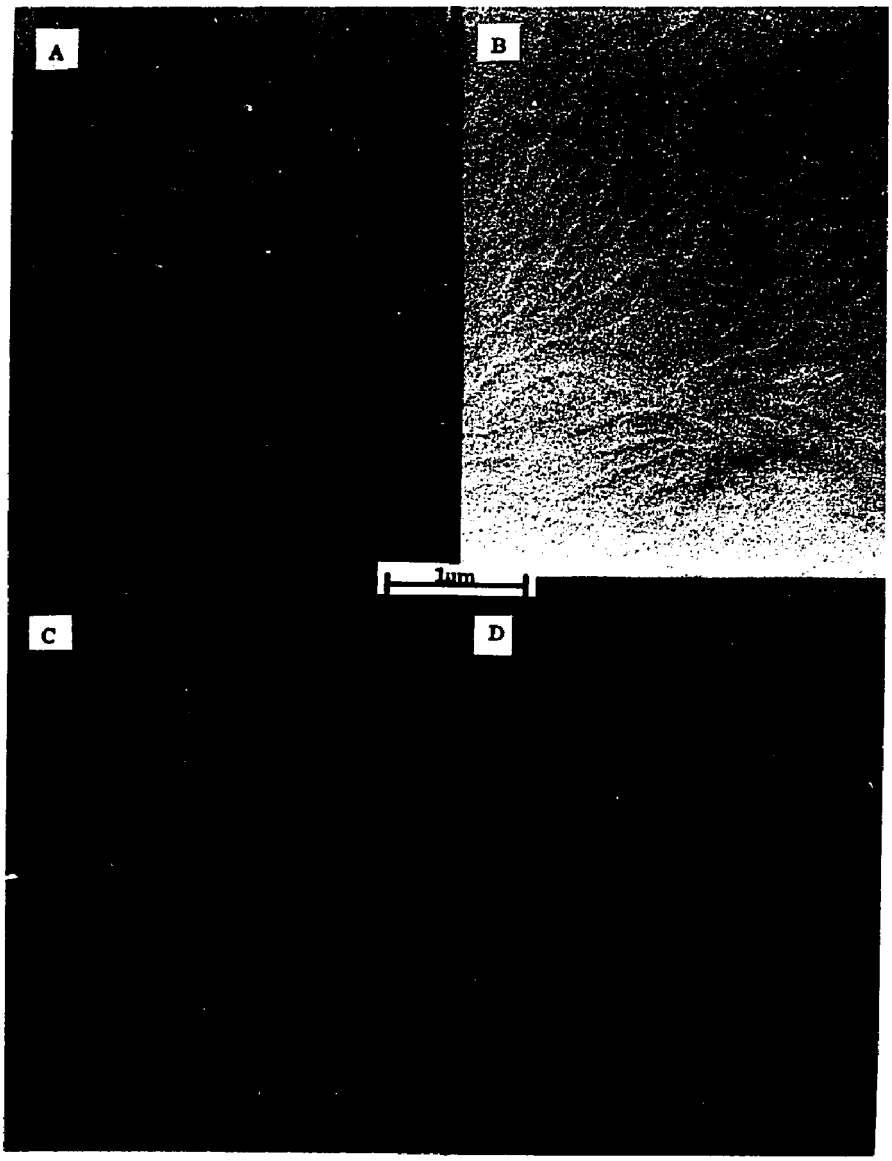

Figure 8. Transmission electron micrographs of two-stage surface replicas of System IV, aged at room temperature for: A) 7 hr, B) 1.5 days, C) 11.5 days, D) 45 days.

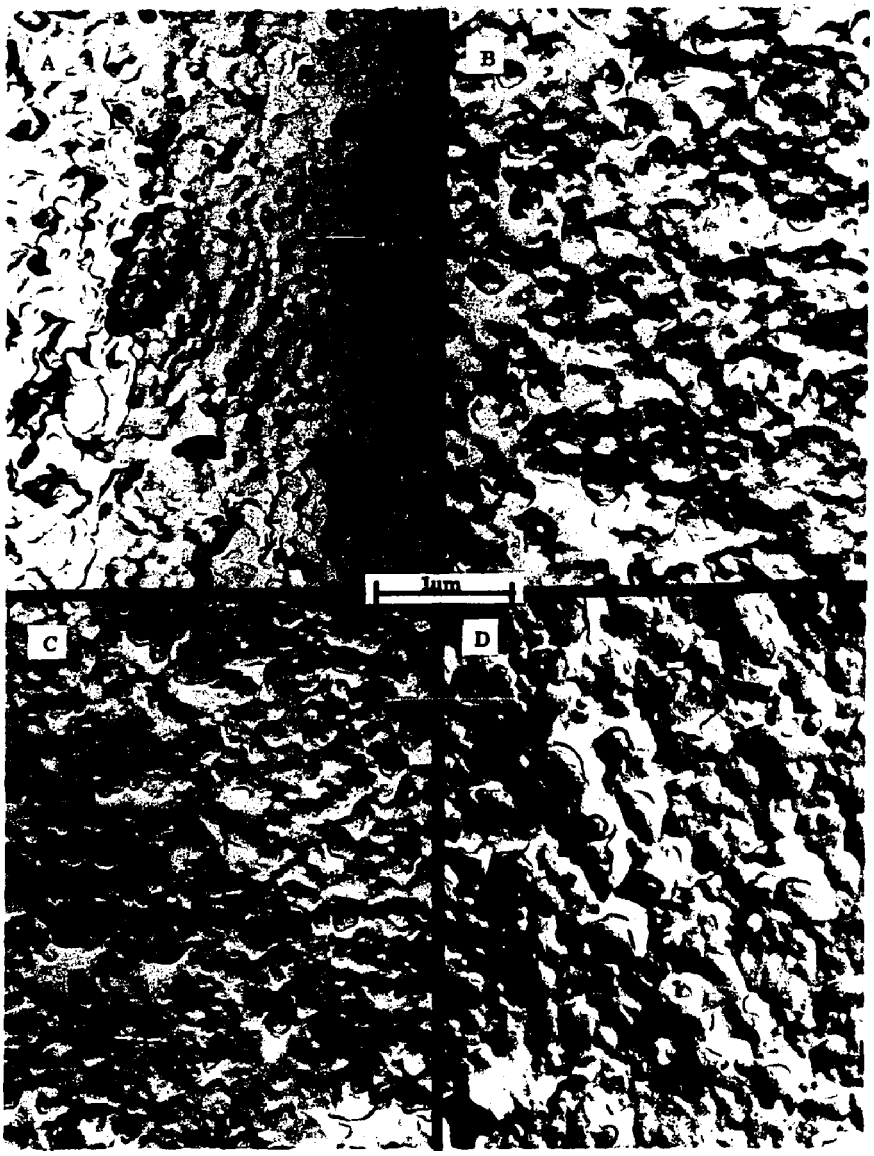

Figure 9. Transmission electron micrographs of two-stage surface replicas of System III, aged at room temperature for: A) 7 hr, B) 1.5 days, C) 11.5 days, D) 45 days.

etched samples. The electron micrographs shown in Figure 10 indicate that etching removed the emulsifier layer. They also indicate that the general film morphology was the same as predicted by the unetched films. On the other hand, the replicas of the etched and unetched films of sample prepared with emulsifier combination B looked alike indicating that combination B was compatible with the final film. It was observed that the rate of coalescence in films having combination B was slower than those having combination A (the particle contours disappeared gradually in 15 days for the former case as compared to 7 hours for the latter case, see Figures 11 and 6).

Thus it is clear that the emulsifier layer on the particles acts as a barrier to further gradual coalescence. The incompatible emulsifier, unlike the compatible emulsifier, exudes to the surface offering lower resistance to further gradual coalescence.

b. Proposed Mechanism

The present results indicate that the mechanism of film formation in chemically reactive emulsions is quite different than in regular one-component emulsions. A three-stage mechanism is proposed below:

Stage I: After mixing, the latex particles freely undergo Brownian motion. The polydispersity in size results in the flocculation of the small particles with the larger particles. Then a continuous agglomeration takes place due to the attractive forces between the reactive particles, the rate of agglomeration depend-

Figure 10. Transmission electron micrographs of two-stage surface replicas of System I, etched in methanol after aging at room temperature for:
A) 1.5 days, B) 4.5 days, C) 11.5 days, D) 16.5 days.

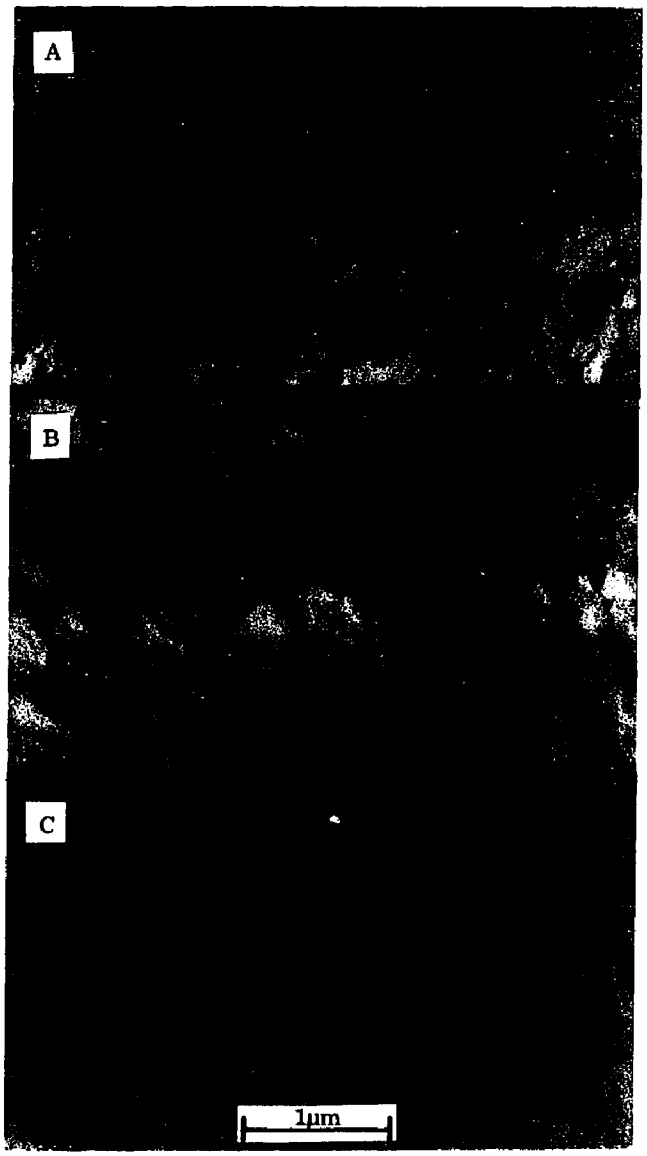

Figure 11. Transmission electron micrographs of two-stage surface replicas of System I with emulsifier combination B, aged at room temperature for:
A) 15 days, B) 7.5 days, C) 16 days.

ing on the reactivity of the particles. Chemical reaction begins at the interface of the reactive particles in the agglomerates. When a critical solids concentration (74% for monodisperse spheres) is reached, the particles pack in a rhombohedral arrangement and Brownian motion stops. At this point stage I is considered to end.

If the rate of evaporation is very low or the total time (t_1) taken during stage I of film formation is quite long then the size and modulus of the agglomerates could become sufficiently large to prevent the film formation process of stage II or stage-III.

Stage II: This stage of film formation should resemble stage II for non-reactive emulsions. On further evaporation of water, the particles and the agglomerates coalesce due to several forces(1-5) operative during the process. The formation of a continuous film will be expected provided that the forces developed are larger than the modulus of the unreacted particles and the agglomerates. However, the particles and the agglomerates may still essentially retain their identity.

Stage III: Further gradual coalescence takes place by the diffusion of the polymer molecules into each other by the mechanism of sintering or autohesion(6). The rate of further gradual coalescence will depend on the size and modulus of the agglomerates and on the rate of reaction of the reactive particles. If the rate of reaction is quite large, the crosslinked network at the interface will retard the diffusion of the molecules, thus slowing the rate

of further gradual coalescence. The rate of further gradual coalescence will be expected to decrease continuously because of the increase in the resistance to diffusion caused by the continuous increase in crosslink density at the interface. Also, resistance to further gradual coalescence may occur in the case of compatible emulsifiers which do not exude to the surface.

Therefore, the time (t_3) taken to give a smooth film should be considerably longer than for the non-reactive latexes, and must depend on the rate of reaction of the reactive particles. The mechanism of film formation in chemically-reactive emulsions is shown diagramatically in Figure 12.

c. Theoretical Model

Several theories and models for the film formation in latexes have been developed by now, but most of these studies had been conducted on non-reactive polymeric emulsions composed of one component only. The proposed model deals with the coalescence of chemically reactive viscoelastic particles. As discussed earlier, the chemical reaction results in a crosslinked network which has quite different properties than the starting material. Stewart and Johnson(21) derived a model -- based on the contact problem of the linear theory of viscoelasticity -- which describes the time depedence of the contact radius of two similar polymeric spheres. Based on the same principle, the time dependence of the contact radius of two different and chemically reactive particles has been derived here. This relationship should help in determining the time

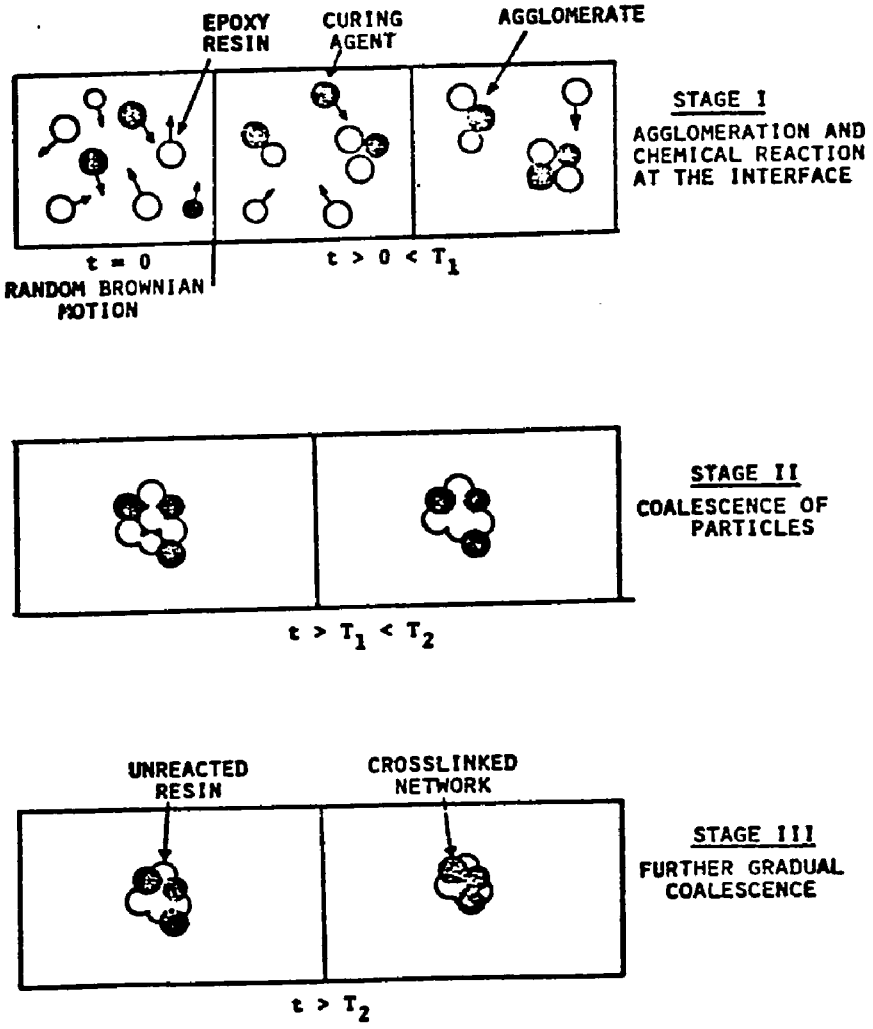

Figure 12. Proposed model for film formation in chemically reactive emulsions.

required for film formation in stage II.

Theory: For the case where the contact region is comparatively much smaller than the dimensions of the sphere, it can be assumed, with appropriate boundary and initial conditions, that the displacement field set up in each sphere is the same as that set up in the half space. Using this assumption, Graham(22) derived an expression given below that related the total thrust P(t) acting over a circular contact region of radius a(t) to the initial radius (R) of the spheres.

$$P(t) = [4/3R][1/2\ \{k_1(t) + k_2(t)\}^{-1} * d\{a^3(t)\}\ ] \qquad (1)$$

which can be inverted to give

$$a^3(t) = 3R/4[2\ \{k_1(t) + k_2(t)\} * d\{P(t)\}] \qquad (2)$$

where $k_1(t)$ and $k_2(t)$ are the auxiliary response functions of the two spheres. For incompressible viscoelastic spheres, the auxiliary response functions can be simplified(21) to the following form:

$$k_1(t) = [4G_1(t)]^{-1} \quad \text{and} \quad k_2(t) = [4G_2(t)]^{-1} \qquad (3)$$

where $G_1(t)$ and $G_2(t)$ are the shear relaxation moduli of the two particles, respectively.

Over a limited range of values of time, the creep compliance J(t) can be represented by a simplified form(23) given below:

$$J(t) = A\ t^m \qquad (4)$$

where A and m are constants.

Equation 4 can also be represented as

$$G(t) = E[t/\tau_o]^{-m} \qquad (5)$$

where E is the modulus at t=0 , τ_o is unit time, and m is a constant depending on the polymer (actually m is the slope of the relaxation time spectrum and is generally of the order of 0.5). It should be noted that equation 5 is valid for $t \geq \tau_o$. The shear relaxation modulus G(t) is related to the creep compliance by the following relation(24):

$$G(t) = \sin m\pi / m\pi \; J(t) \tag{6}$$

Using Equations 5 and 6 in Equation 3, the auxiliary response can be calculated to be:

$$\begin{aligned} k_1(t) &= \sin m\pi / 4m\pi E_1 [\, t/\tau_o]^m \\ k_2(t) &= \sin m\pi / 4m\pi E_2 [\, t/\tau_o]^m \end{aligned} \tag{7}$$

Vanderhoff and coworkers(9) showed that in stage II of film formation the pressure forcing the spheres together almost has the form of a step function. Based on their arguments, the total thrust can be expressed as

$$P(t) = a^2(t)\, P_o\, H(t) \tag{8}$$

where P_o is the pressure developed during film formation and is constant, $\pi a^2(t)$ is the contact area at time t, and H(t) is the Heavyside function.

Substituting Equations 7 and 8 in Equation 2, we get

$$a^3(t) = \left[\frac{3RP_o}{8}\right]\left[\frac{\sin m\pi}{m\,\tau_o^{\,m}}\right]\left[\frac{1}{E_2} + \frac{1}{E_1}\right]\left[t^m * \left\{a^2(t)\, H(t)\right\}\right] \tag{9}$$

Using Stieltjes convolution

$$\left[t^m * \left\{a^2(t)\, H(t)\right\}\right] = \int_{\tau=-\infty}^{\tau=t} (t-\tau)^m \, d[\, a^2(\tau)\, H(\tau)]\, d\tau \tag{10}$$

Equation 10 can further be simplified to

$$\left[t^m * \left\{a^2(t)\ H(t)\right\}\right] = \int_{\tau=0}^{\tau=t} \left\{m\ (t-\tau)^{m-1}\right\}\left\{a^2(\tau)\right\}\ d\tau \qquad (11)$$

Substituting Equation 11 in Equation 9, one can obtain

$$a^3(t) = Z_1 \int_{\tau=u}^{\tau=t} a^2(\tau)\ (t-\tau)^{m-1} d\tau \qquad (12)$$

where $Z_1 = \left[\frac{3RP_o \sin m\pi}{8\ \tau_o^m}\right]\left[\frac{1}{E_1} + \frac{1}{E_2}\right]$

In the case of chemically reactive particles, the modulus of the contact area should increase with crosslinking. Studies of Lewis(25) and Gillham(26) have shown that the modulus (E_o) is almost unchanged till the gelation time (t_{gel}), after which the modulus increases in a step manner and reaches its glassy value (E_g). This behavior of the modulus can be approximated by the following relationship:

$$E(t) = E_o\ H(t) + (E_g - E_o)\ H(t-t_{gel}) \qquad (13)$$

where H(t) is the Heavyside function, and $H(t-t_{gel})$ is the Heavyside function shifted to $t=t_{gel}$.

It is clear from the above discussion that the time-dependence of the area of contact of the two particles would be different for $t \leq t_{gel}$ and $t \geq t_{gel}$.

Case 1: When $t \leq t_{gel}$

In this range of time, the moduli of the two particles would be the same as that of the initial value, i.e., E_1 and E_2, respectively, and Equation 12 would be applicable.

By inspection, the solution of the integral-Equation 12

appears to be of the form

$$a(t) = C\, t^{m} \qquad (14)$$

where C is a constant (to be determined).

After substituting this in Equation 12, taking the Laplace transform and solving for C, one finds

$$C = Z_1 \left[\frac{\Gamma(2m+1)\,\Gamma(m)}{\Gamma(2m+1)} \right] \qquad (15\ a)$$

where $\Gamma(m)$ denotes the gamma function.

In turn,
$$a(t) = Z_1 \left[\frac{\Gamma(2m+1)\ \Gamma(m)}{\Gamma(3m+1)} \right] t^{m} \qquad (15)$$

For the case when $E_1 = E_2 = E$, Equation 15 can be simplified to get the same relation obtained by Stewart and Johnson(21).

Case 2: In this case the modulus of both the particles is the same as that of the crosslinked network i.e., E_g.

The auxiliary constant would be

$$k(t) = \frac{\sin p\pi}{4\ p\pi\ E_g} \left[\frac{t}{\tau_o} \right]^{p} \qquad (16)$$

where p is a constant (the slope of the relaxation time spectrum of the crosslinked network; values of p and m could be different from one another).

The total thrust P(t) would be the same as in case 1 because the total pressure developed (P_o) would be the same.

Substituting Equations 8, 11, and 16 in Equation 3 and simplifying, one can obtain

$$a^{3}(t) = Z_2 \int_{\tau=0}^{\tau=t} (t-\tau)^{p-1}\ a^{2}(\tau)\ d\tau \qquad (17\ a)$$

where $Z_2 = (3R\,P_o \sin p\pi)/(16\tau_o^{\,p} E_g)$

Following the same method as in case 1, Equation 17-a can be solved to give

$$a(t) = Z_2\left[\frac{\Gamma(2p+1)\ \Gamma(p)}{\Gamma(3p+1)}\right] t^p \qquad (17)$$

General case: For the general case where film formation is not complete before gelation, the time dependence of the contact area can be expressed by combining the results of case 1 and case 2 with the time shift method, as shown below.

$$a(t) = Z_1\left[\frac{\Gamma(2m+1)\ \Gamma(m)}{\Gamma(3m+1)}\right]\left[t^m H(t) + \left\{t_{gel}^{\,m} - t^m\right\}\left\{H(t-t_g)\right\}\right] + Z_2\left[\frac{\Gamma(2p+1)\ \Gamma(p)}{\Gamma(3p+1)}\right] t^p H(t-t_g) \qquad (18)$$

where

$$Z_1 = \frac{3\,R\,P_o \sin m\pi}{8}\left[\frac{1}{E_1} + \frac{1}{E_2}\right]$$

and

$$Z_2 = \frac{3\,R\,P_o \sin p\pi}{16}\left[\frac{1}{E_g}\right]$$

(Here $\tau_o^{\,m}$ and $\tau_o^{\,p}$ have been deleted because they are equal to unity).

Equation 18 reduces to Equation 15 for $t \leq t_{gel}$ whereas it simplifies to the following form for $t \geq t_{gel}$.

$$a(t) = Z_1\left[\frac{\Gamma(2m+1)\ \Gamma(m)}{\Gamma(3m+1)}\right] t_{gel}^{\,m} + Z_2\left[\frac{\Gamma(2p+1)\ \Gamma(p)}{\Gamma(3p+1)}\right] t^p \qquad (18\text{-a})$$

Calculation of the gelation time (t_{gel}): For an nth-order reaction we have:

$$- dc_1/dt = k\, c_1^{\,n} \qquad (19\text{-a})$$

where c_1 is the concentration of component 1, k is the reaction rate constant, and n is the order of reaction.

Equation 19-a may be integrated to get the gelation time;

$$t_{gel} = [1/k(n-1)][c_{gel}^{\,1-n} - c_o^{\,1-n}] \qquad \text{for } n \neq 1 \qquad (19)$$

and $$t_{gel} = (1/k)[\ \ln\ (c_o/c_{gel})] \qquad \text{for } n = 1 \qquad (20)$$

Calculation of the film formation time: Brown(12) hypothesized that stage II film formation is complete when a(t)=0.308R, where R is the particle radius. Using this hypothesis, one can calculate the film formation time for the following two cases using Equation 18.

Case 1: When film formation time, $t_{ff} \leq t_{gel}$,

$$(t_{ff_1})^m = \frac{0.821}{P_o \sin m\pi}\left[\frac{1}{1/E_1 + 1/E_2}\right]\left[\frac{\Gamma(3m+1)}{\Gamma(2m+1)\ \Gamma(m)}\right] \qquad (21)$$

Case 2: When $t_{ff} > t_{gel}$,

$$(t_{ff_2})^p = (1.642\ E_g)\left[1 - (t_{gel}/t_{ff_1})^m\right]\left[\frac{\Gamma(3p+1)}{\Gamma(2p+1)\ \Gamma(p)}\right] \qquad (22)$$

Equation 22 indicates that the smaller the value of t_{gel} (which is inversely proportional to the reaction rate constant, (Equations 19, 20), the larger will be the film formation time. The effect of initial particle radius, R, is not explicit in Equations 23 and 24, but is implicit in the term P_o (P_o is inversely proportional to the particle radius R). Thus, these equations, as has been observed experimentally by several investigators, predict that film form-

mation time in stage II would be longer for larger particles. These equations also indicate that chemically-reactive emulsions would take longer times for film formation as compared to non-reactive emulsions, and the time would also increase with the reaction rate constant. These predictions are in agreement with the observations made for epoxy emulsions of the present study. At present there are no data in the literature which would give the numerical values of film formation times for a reactive system which could be compared with the values predicted by these equations. Nevertheless, they show good qualitative agreement with the experimental observations made for epoxy emulsions.

d. Conclusions

For chemically-reactive emulsion mixtures it is concluded that;

1. An uncommon continuous agglomeration of particles takes place even in stage I of film formation.

2. Chemical reaction at the interface of the particles of the agglomerates begins in the emulsion state itself.

3. The rate of agglomeration increases with an increase in the reactivity of the particles.

4. The extent of coalescence depends on the dimensions and modulus of the agglomerates of stage I.

5. The rate of further gradual coalescence is reduced by the presence of compatible emulsifier and also by the higher reactivity of the latex particles.

C. CHARACTERIZATION AND PROPERTIES OF EMULSION-CURED FILMS

The mechanism of emulsion curing was studied by characterizing the emulsion cured films through different techniques such as electron microscopy, DSC, DMS, and swelling and solubility in a solvent.

a. Results and discussion

Morphology: The Versamid 115 molecules have unsaturated double bonds which are not involved in the curing reaction; a completely cured sample will still have unsaturated double bonds that can be stained by osmium tetroxide. Under the transmission electron microscope, the Versamid 115-rich regions in the stained samples appear dark while the epoxy-rich regions appear light. A completely cured region will have a color intermediate between that of the Versamid- and epoxy-rich regions.

The electron micrographs of the stained sections of the different samples are shown in Figures 13 to 16. It was observed (see Figures 13 and 14) that all the room-temperature emulsion-cured samples had a multiphase structure. The dispersed phase consisted of unreacted prepolymers while the continuous phase was made up by the crosslinked network. The micrographs also show a distribution of diameters of the unreacted epoxy core, ranging from 28-nm to 140-nm. The initial particle size in the epoxy emulsions ranged from 20-nm to 200-nm, and from 10-nm to 20-nm for the Versamid 115 emulsion. The epoxy particles having the smallest

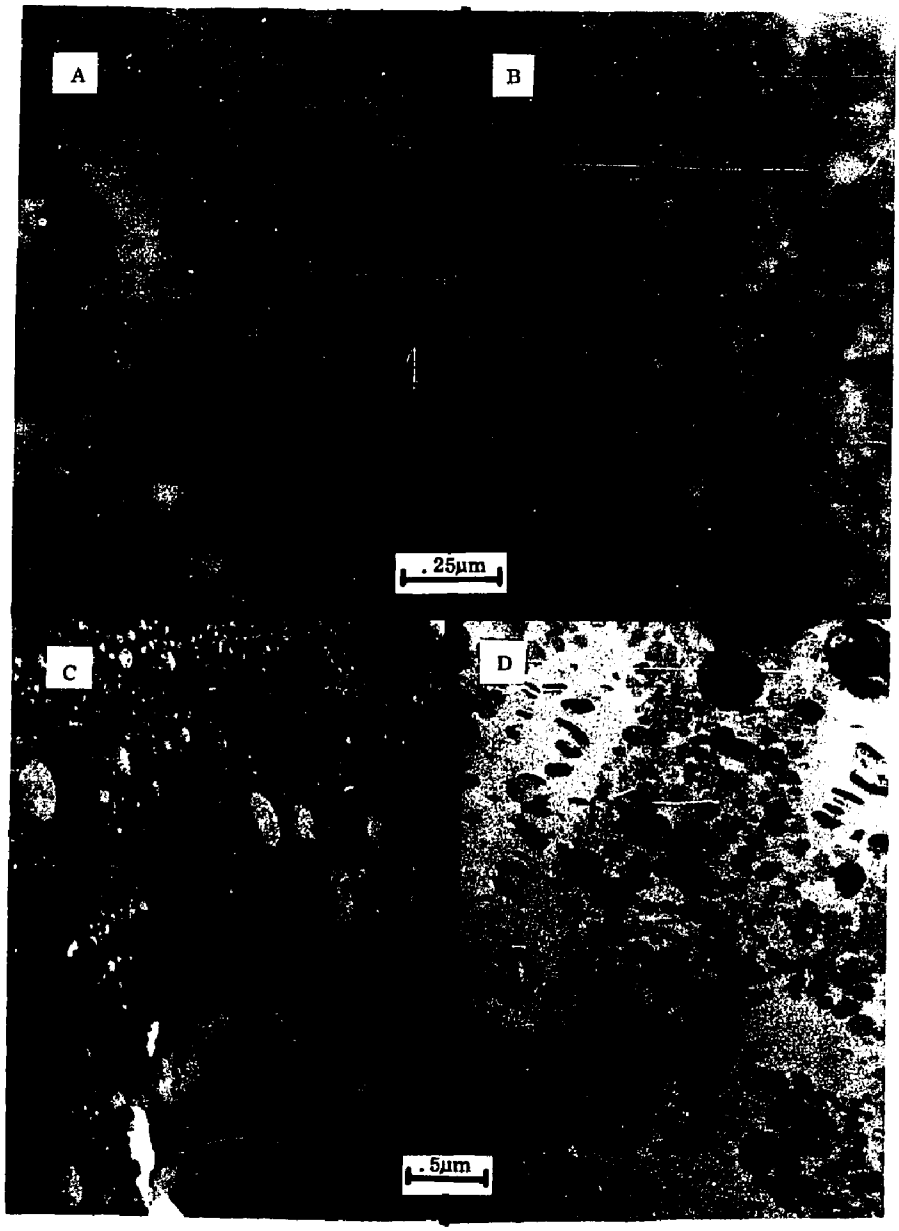

Figure 13. Transmission electron micrographs of stained microtomed sections of emulsion films. A) B-1, B) B-2, C) B-3, D) B-4.

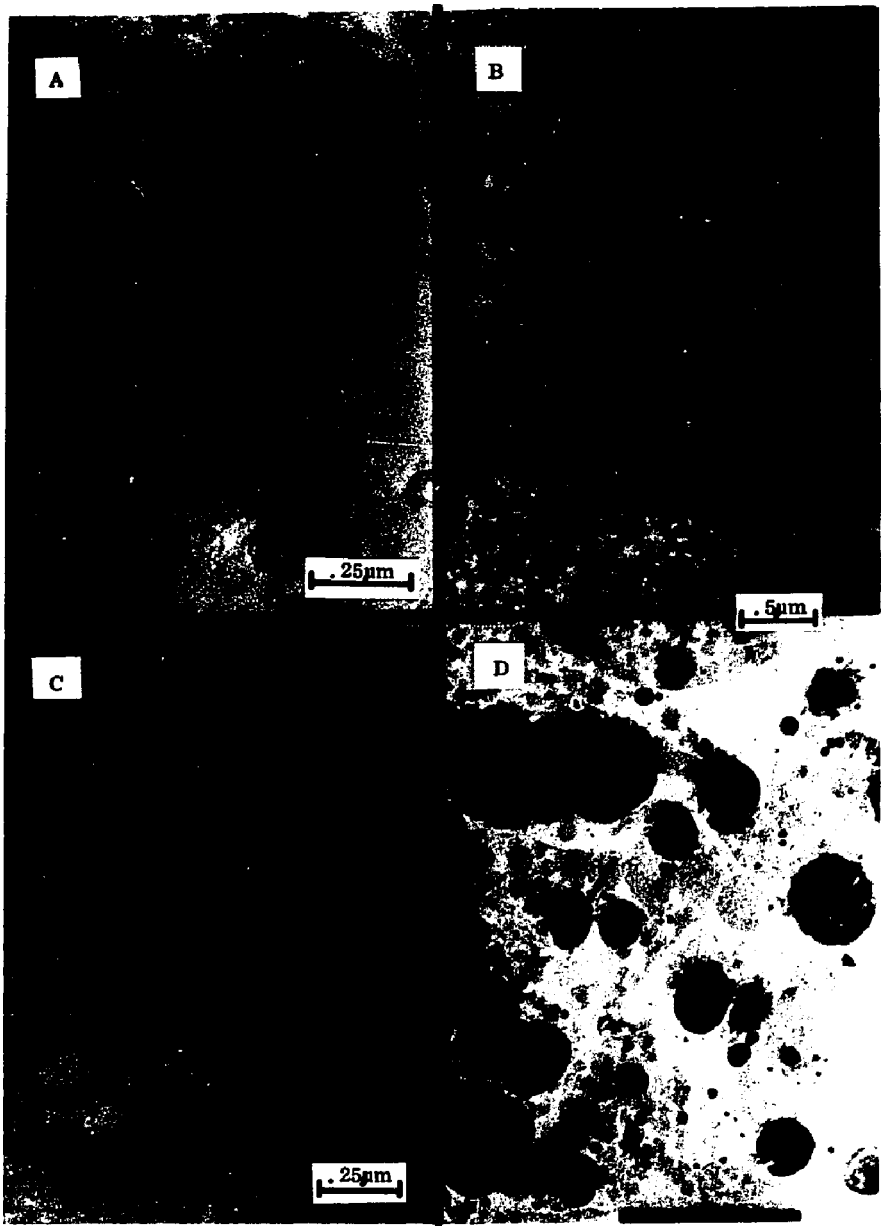

Figure 14. Transmission electron micrographs of stained microtomed sections of emulsion films - extracted in toluene at -20°C for 15 days.
A) B-1, B) B-3, C) B-2, D) B-4.

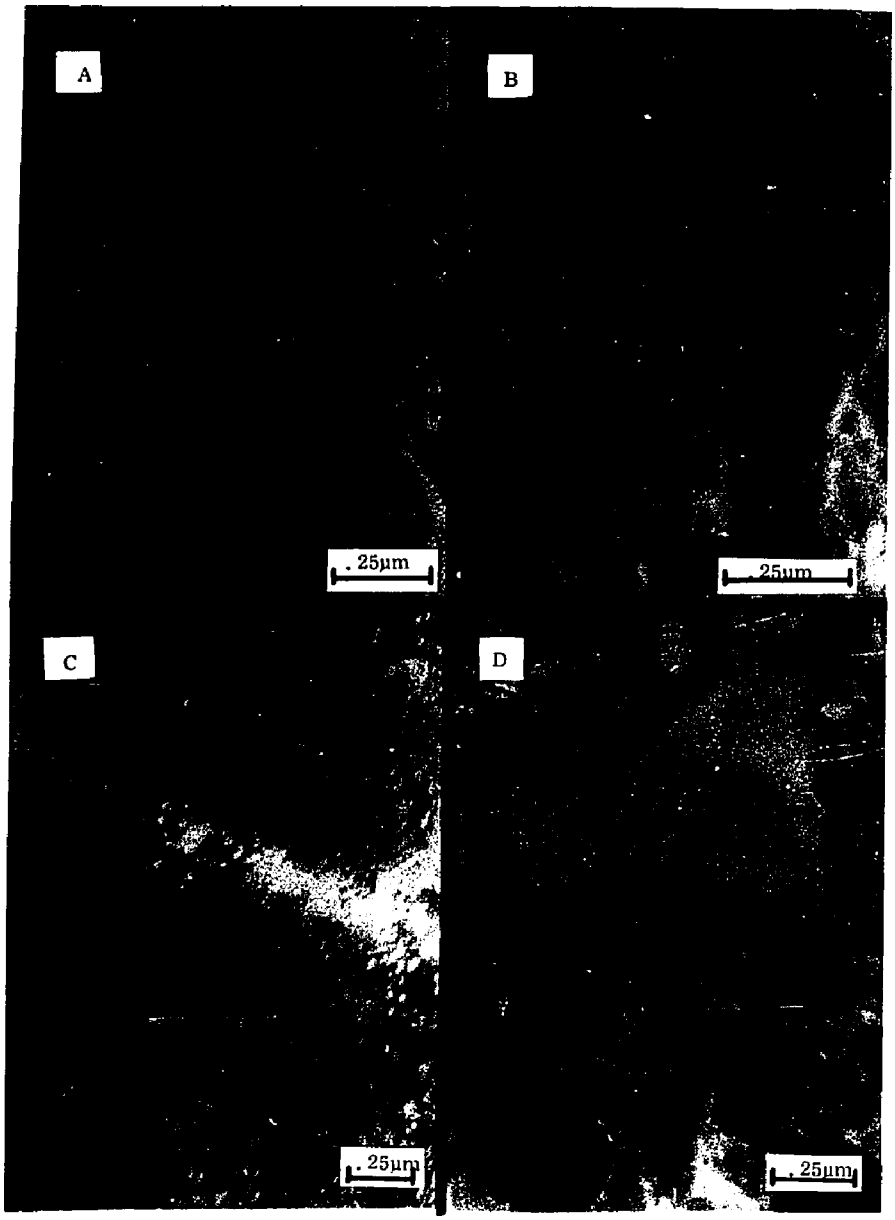

Figure 15. Transmission electron micrographs of stained microtomed sections of emulsion films post-cured at higher temeratures.
A) C-1, B) C-2, C) C-3, D) C-4.

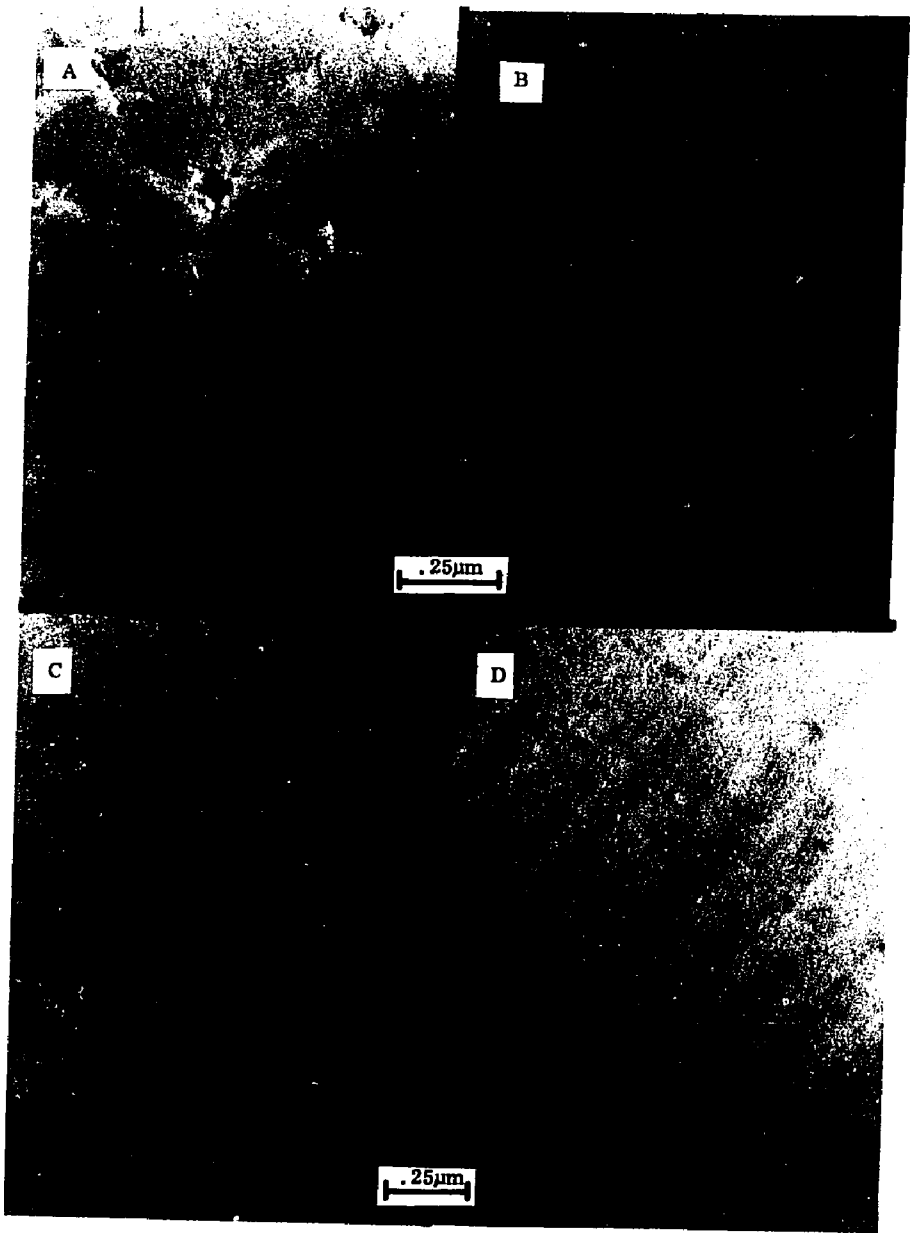

Figure 16. Transmission electron micrographs of stained microtomed sections of different samples. A) D-1, B) D-4, C) B-5, D) C-5.

initial diameters (20-nm) appear to have completely reacted. In fact, the micrographs also indicate that particles having diameters up to 60-nm would completely react (200-140=60 nm.).

Samples B-2, B-1, and B-3 had very similar morphology but had increasing amounts of unreacted prepolymers. Dark streaks of Versamid 115 particles were observed in room-temperature emulsion-cured samples (Figure 13). However, these streaks could be extracted by solvent or consumed on post-curing the samples B-1, B-2, and B-3. Cold stage electron microscopy had shown (Figure 1) that Versamid particles were connected to each other by small strands made of still smaller particles. Some of these unreacted particles appear as dark streaks which get extracted or diffuse into the epoxy particle core to react on post-curing.

On the other hand, large spherical Versamid-rich regions were observed in sample B-4 (which had Dion molecules to accelerate the rate of reaction). These Versamid-rich regions, unlike other samples, did not disappear on solvent extraction or on post-curing indicating that the Versamid particles, though in excess, are attached to the network. This can be explained as follows. In samples B-1 and B-2 the rate of reaction is quite slow, and therefore, the Versamid particles form transient rather than permanent agglomerates whereas the higher rate of reaction induced by the Dion molecules in sample B-4 results in permanent agglomerates. Sample B-3 which has a curing mechanism similar to that of B-4, and in which the bisphenol-A molecules initiate the reac-

tion, does not form permanent agglomerates of the Versamid-rich regions probably because the diffusion of the bisphenol-A molecules is slower and also because their concentration in the epoxy particle is only 4% as compared to the 33% concentration of the Dion molecules in the Versamid particles.

Furthermore, Figure 15 also indicates that further curing (post-curing) reduces the number density of the unreacted epoxy core. Similarly Figure 16 indicates that emulsion-curing at 50°C gave a more homogeneous network structure and also that the number density of the unreacted core of the epoxy particles is much smaller than the equivalent samples B-1 or C-1 of series B and C, respectively. In contrast to the emulsion-cured films a one phase structure (ie., the absence of unreacted prepolymer molecules was observed in the solvent-cured films (see Figures 16-c and 16-d).

Dynamic mechanical spectroscopy: The loss modulus (E") and storage modulus (E') curves of the different series are shown in Figures 17 to 20. Results are summarized in Tables I and II.

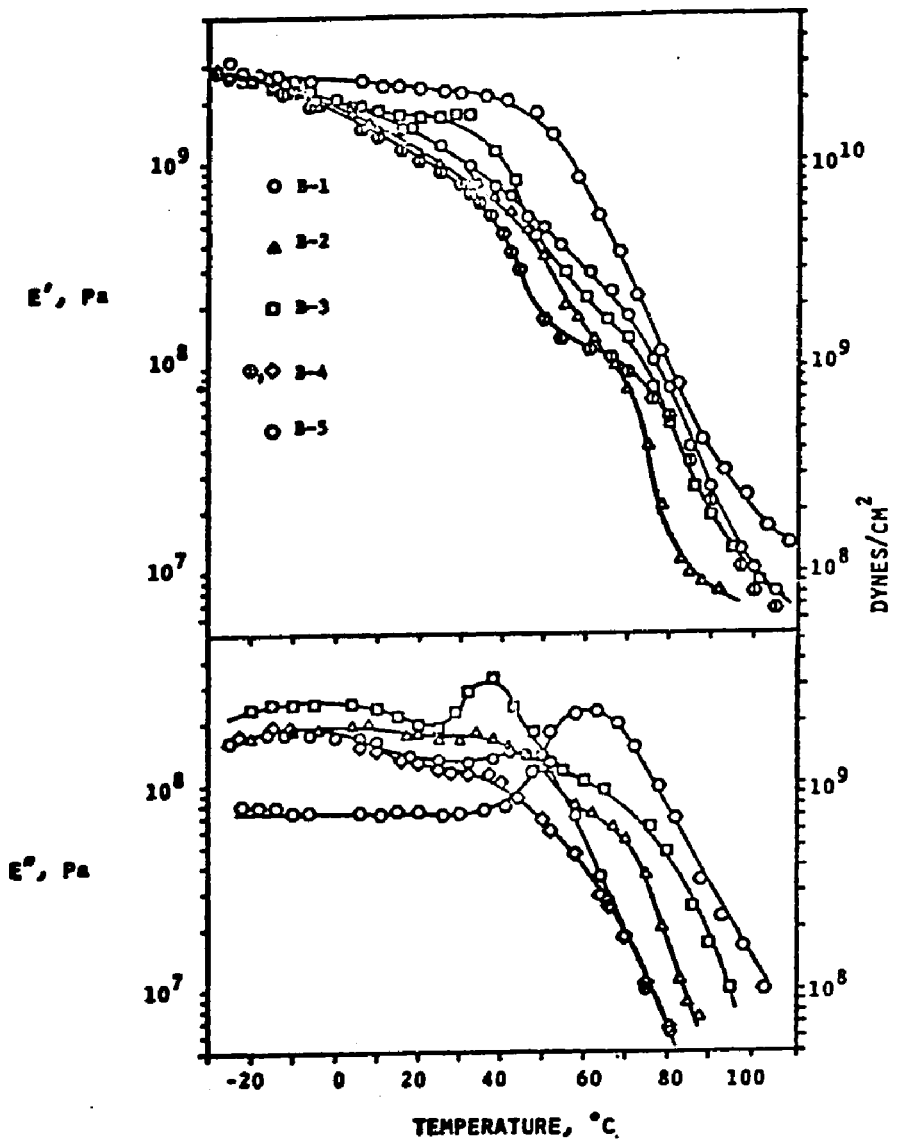

Figure 17. Dynamic mechanical spectra for room temperature cured films of epoxy/polyamide system, (1st run).

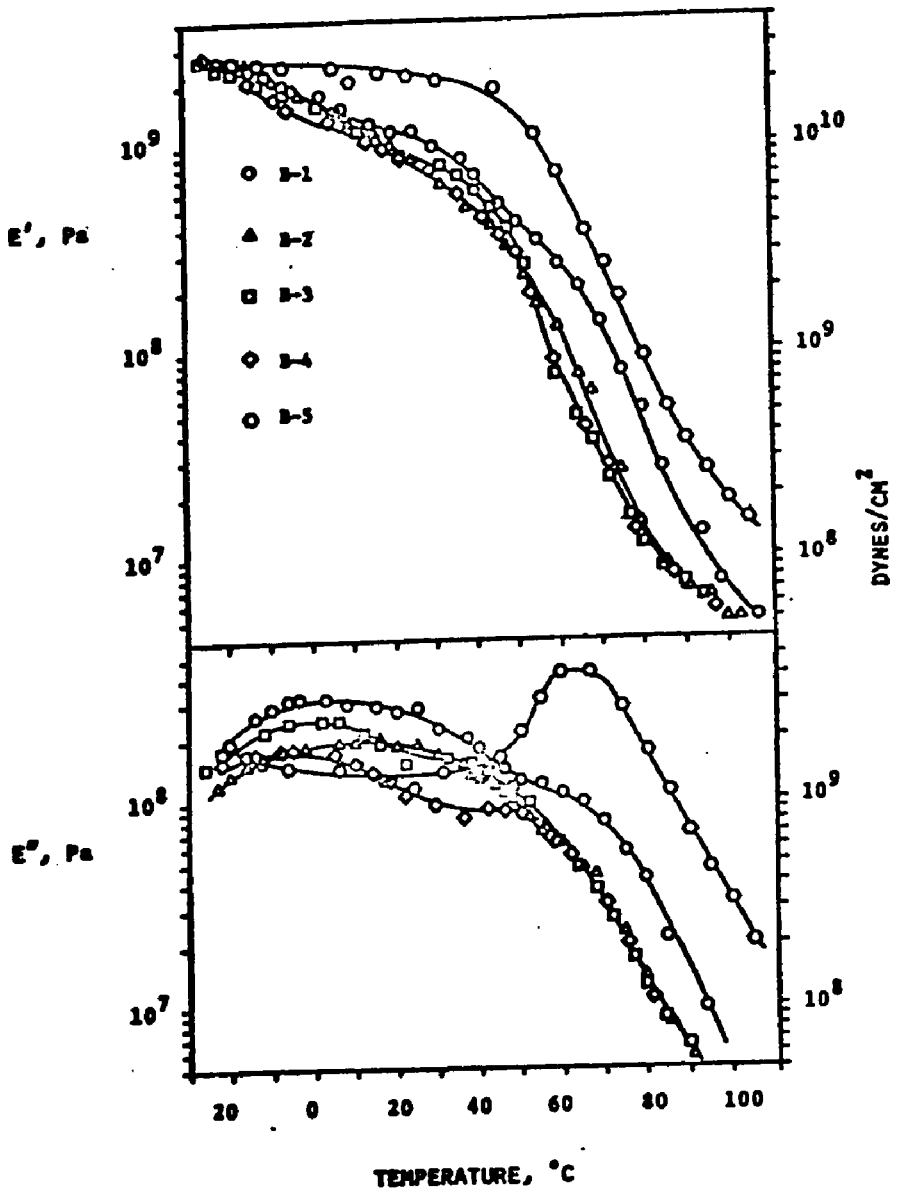

Figure 18. Dynamic mechanical spectra for room temperature cured films of epoxy/polyamide system, (2nd run).

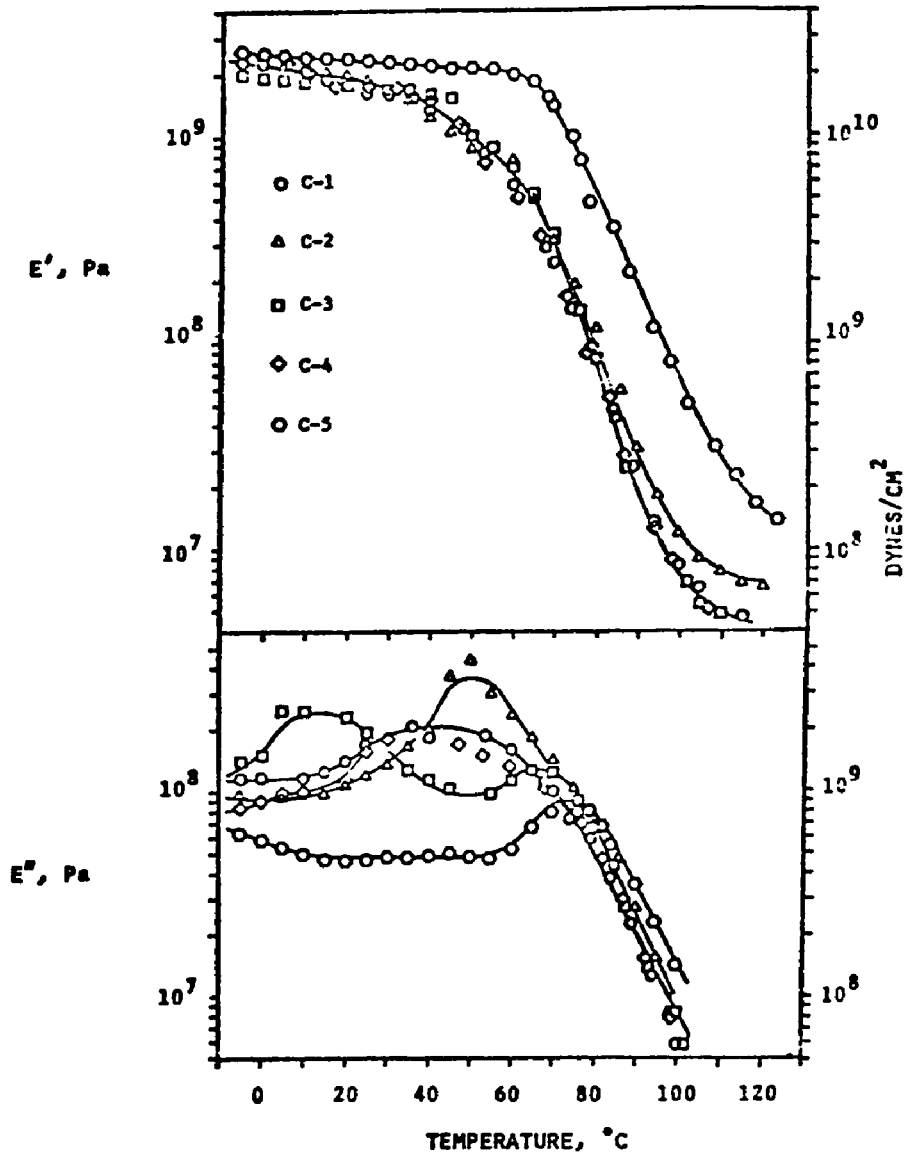

Figure 19. Dynamic mechanical spectra of epoxy/polyamide films subjected to high temperature post curing.

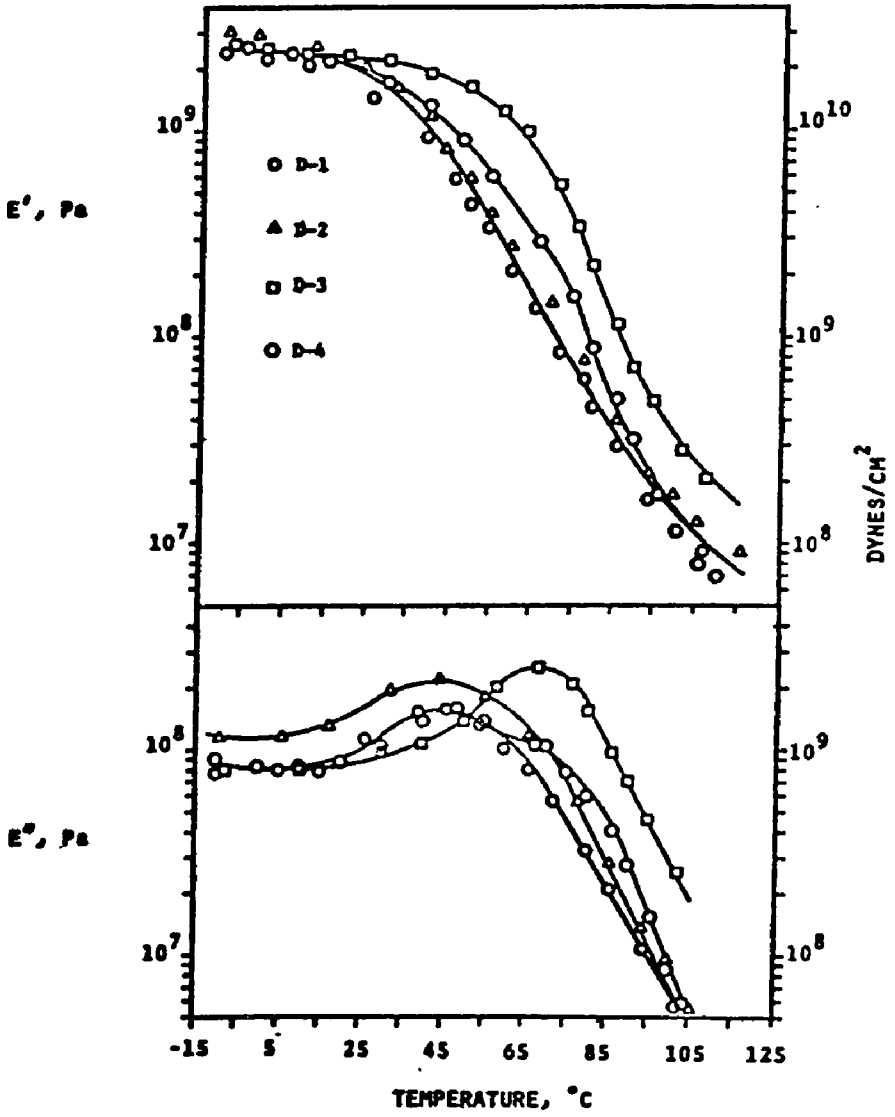

Figure 20. Dynamic mechanical spectra of epoxy/polyamide films cured at 50°C (D-4 post cured as well).

TABLE I. DYNAMIC MECHANICAL DATA FOR SERIES B.

Sample No.	E_r (MPa)		T of peaks in E"[a] (°C)		tan δ_{max} near T_g			
	Run I	Run II	Run I	Run II	Run I Value	Run I T(°C)	Run II Value	Run II T(°C)
B-1	4.2	4.2	-5,45	10,65	0.9	86	0.85	88
B-2	4.2	4.2	0,40,65	15,60	0.95	80	0.90	85
B-3	4.2	4.2	-5,40,65	-5,50	1.1	75	1.0	86
B-4	4.2	4.2	-10,40	-5,50	1.1	75	1.0	86
B-5[b]	10.1	10.1	65	67	0.85	80	0.80	85

TABLE II. DYNAMIC MECHANICAL DATA FOR SERIES C AND SERIES D.

Sample No.	E_r (MPa)	T of peaks in E" (°C)	tan δ_{max} near T_g	
			Value	T(°C)
C-1	4.0	53	0.95	95
C-2	7.0	60	0.90	90
C-3	4.0	22,75[c]	1.1	90
C-4	4.0	50	1.2	90
C-5[b]	10.1	83	0.80	105
D-1	6.5	44	0.70	90
D-2	8.0	44	0.72	90
D-3[b]	10.5	68	1.0	90
D-4	6.5	48,70[c]	0.9	96

[a] The highest value corresponds to T_g (or T_α). This T_α could be an artifact of the tests (a result of further curing during the tests).

[b] Control sample (solvent-cured).

[c] With sample C-3 the lower temperature corresponds to the T_g of the unreacted prepolymer. With sample D-4, the lower temperature corresponds to the T_g for the initially-cured prepolymer. In each case the higher temperature corresponds to the T_g of the final film.

Swelling and Extraction: The swelling and extraction results are given in Table III.

TABLE III. SWELLING AND EXTRACTION AND DENSITY OF SAMPLES OF DIFFERENT SERIES.

Sample No.	Density gm/ml	Swell ratio[a]	% Extraction[b]
B-1	1.1135	1.755± 0.020	13.29 ± 0.5
B-2	1.1225	1.730± 0.016	10.9 ± 0.5
B-3	1.1262	1.759± 0.021	14.6 ± 0.3
B-4	1.1525	1.735± 0.010	23.9 ± 0.6
B-5[c]	1.1430	1.396± 0.014	6.8 ± 0.2
C-1	1.1437	1.439± 0.016	7.1 ± 0.4
C-2	1.1330	1.369± 0.014	6.0 ± 0.6
C-3	1.1475	1.385± 0.014	7.1 ± 0.5
C-4	1.1525	1.367± 0.008	7.9 ± 0.6
C-5[c]	1.1437	1.343± 0.007	4.5 ± 0.1
D-1	1.2240	1.518± 0.007	9.7 ± 0.4
D-3[c]	1.4380	1.308± 0.008	3.0 ± 0.5
D-4	1.2250	1.389± 0.007	7.3 ± 0.5

[a]Swell ratio = $\frac{\text{volume of the swollen network}}{\text{volume of the dry, extracted network}}$

[b]The amount of extracted includes a fraction of emulsifier. Although the amount of emulsifier actually extracted is unknown, the maximum percentage possible is 9 -- the percentage originally present.

[c]Control samples (solvent-cured).

Differential Scanning Calorimetry: Fava(27) has shown that the residual heat of reaction of a partially cured sample is a good indication of the degree of cure; the smaller the value of the exotherm, the greater is the degree of cure. In this study the residual heats of reaction could be detected by the DSC only in the emulsion-cured samples of series B (cured at room temperature). These exothermic peaks did not appear in the second scan, indicating that the curing reaction was completed in the first scan or that at least there was no further curing during the second scan. The samples were tested on the DSC after 11 and 50 days of film formation; results are given in Table IV.

TABLE IV. RESIDUAL HEAT OF REACTION OF SAMPLES OF SERIES B.

Sample No.	Heat of Reaction, J/kg x 10^3 After 11 days	After 50 days	% increase/day of aging
B-1	28.42	53.00	2.25
B-2	13.79	15.72	0.36
B-3	14.30	22.95	1.15
B-4	3.51	3.97	0.34
B-5[a]	0.0	0.0	0.0

[a]Control Sample (solvent-cast).

Crosslink Density or M_c: The theoretical value of M_c was determined by considering the epoxy and Versamid molecules as bifunctional and trifunctional, respectively, and by assuming that both the molecules are parts of the network chains. If M_e and M_v are the respective molecular weights of the epoxy and Versamid molecules, then at equal stoichiometric compositions:

$$M_c \text{ (theoretical)} = (3 M_e + 2 M_v)/3 \qquad (23)$$

Taking molecular weights of Epon 1001 and Versamid 115 as 1000 and 705, respectively, the theoretical value of M_c at stoichiometric compositions was 1470. The M_c values determined through different methods are given in Table V.

TABLE V. M_c VALUES DETERMINED THROUGH DIFFERENT METHODS.

Sample	M_{cs}	M_{cr}
B-1	---	2613
B-2	---	2634
B-3	---	2643
B-4	---	2706
B-5[b]	1687	1143
C-1	5528	2820
C-2	1047	1560
C-3	1370	2757
C-4	1038	2769
C-5[b]	751	1146
D-1	---	1701
D-2	---	1401
D-3[b]	530	1308
D-4	1439	1701

[b]Control Samples (solvent-cured)

These results indicate that the mechanical properties of the emulsion-cured films depend on the curing conditions and the rate of reaction.

Room Temperature Curing: The dynamic mechanical and transmission electron microscopy results of the room-temperature-cured samples of Series B indicate a two phase structure for all the emulsion-cured samples (see Figures 13,17,and 18). The first peak corresponds to the unreacted prepolymers while the second peak corresponds to the T_g of the cured network. The second run in the Rheovibron gave the same value of rubbery modulus but a higher T_g for all the samples. This indicates that further curing of the unreacted prepolymers took place during the first run and also that T_g, as compared to the rubbery modulus, is more sensitive to the plasticizing effect of the unreacted prepolymers in the network.

Samples B-3 and B-4 had a lower T_g than samples B-1 and B-2. This indicates that samples B-3 and B-4 contained greater proportions of unreacted prepolymers -- a conclusion confirmed by transmission electron microscopy (Figure 13) and by swelling and extraction experiments (Table III).

The DSC results of Table IV indicate that sample B-4 had the highest degree of cure (smallest residual exotherm) which is contrary to the DMS, TEM, and swelling and extraction results

discussed earlier, where it was shown that sample B-4 actually had the lowest degree of cure. Another interesting point is that the films aged for 50 days showed higher exotherms than those aged for 11 days. Usually the exotherms are reduced on aging as a result of further curing of the unreacted prepolymers.

This apparent anomaly is attributed to the diffusion-controlled kinetics of curing in epoxy emulsions. During film formation, the epoxy resin particles coalesce with the curing agent particles and the curing reaction begins at the interface. The formation of the three dimensional network hinders further diffusion of the reactive molecules. In the systems that have faster reactions (e.g., samples B-3 and B-4), the network forms at the interface of the reacting particles at an earlier stage. In the less reactive system, on the other hand, the reactants diffuse to a greater distance before the formation of the network, thus resulting in a higher T_g and a higher extent of cure.

In sample B-4, the smaller, less numerous Dion DPM-3-800-LC molecules diffuse rapidly to the interface between the epoxy resin and the curing agent particles and initiate the curing reaction, which quickly forms a tightly crosslinked network of polymer throughout the interfaces between the coalesced particles. This tightly crosslinked layer hinders the diffusion of the larger, more numerous Versamid 115 molecules to such an extent that a significant proportion of the Epon 1001 resin of the particle core remains uncured. This explanation is consistent not only with the exother-

mic heats of reaction, but also with the solvent extraction, dynamic mechanical and transmission electron microscopy results.

The foregoing explanation can also be applied to other films. Sample B-1, which had Epon 1001-Versamid 115 combination, showed the greatest residual exothermic heat of reaction (and hence the smallest degree of cure) of all the emulsion-cured samples. Sample B-2, which is same as B-1 but pre-cured in emulsion state before casting, showed a smaller residual heat of reaction. On the other hand, sample B-3 had a residual heat of reaction which was greater than that of sample B-1. This system is similar to that of sample B-4 except that it is the bisphenol-A that diffuses to the interface and increases the rate of the crosslinking reaction which in turn slows down the diffusion of the reactive molecules. Because sample B-3 displayed a smaller proportion of uncrosslinked polymer as compared to B-4, it appears that bisphenol-A is not as effective as Dion.

When the film is subjected to the DSC or the Rheovibron scan, the temperature increase,in both cases, results in a sudden exothermic reaction and an increased rate of diffusion. However, the curing reaction soon becomes diffusion-controlled and, for all practical purposes, ceases so that the second scan on the DSC shows no exothermic peaks even though the curing reaction may still be incomplete. The diffusion-controlled kinetics of the curing reaction is also confirmed by the greater reaction exotherms of the

50-day-old films. These greater values are attributed to the increased availability of curing agent molecules resulting from the diffusion during the 50 days of aging relative to those available in 11 days of aging. If the curing reaction were not diffusion-controlled and the reaction exotherms represented its completion during the DSC scan then the reaction exotherms of the 50-day-old samples should have been smaller than those of the 11-day-old samples because some curing should have occured during the 39-day interval. That the opposite was observed indicates that the curing observed during the DSC scan involves only those curing agent molecules that have diffused to the epoxy resin molecules, leaving the curing reaction still incomplete.

The percent increase in the exothermic heat of reaction per day of aging time, as observed in all the emulsion-cured samples, would therefore depend on the following two factors:

1. Overall diffusion coefficient of the molecules. If the rate of reaction is larger, the formation of the network at the interface would take place earlier thus reducing the diffusivity. Besides, diffusivity would also depend on the size of the reactive molecules.

2. Concentration gradient of the unreacted molecules. If the reactive molecules are present in small concentration, the net flux of the reactive molecules at the reaction site would be small which would result in a smaller increase in exotherm per day of aging time. These observations indicate that the residual heat of reac-

tion cannot exclusively be used as a measure for the extent of cure in systems with diffusion-controlled curing kinetics.

The solvent-cured sample B-5 had T_g higher by 25°C and 2.4 times higher rubbery modulus than the emulsion-cured counterparts. It only had 7% extractables in comparision to 10-24% extractables in emulsion-cured samples. The loss modulus curve (Figures 17 and 18) for B-5 had only one peak indicating a one phase structure (i.e., the absence of any unreacted prepolymer molecules in the network), which was also confirmed through electron microscopy (see Figures 16c and 16d). No exothermic peaks could be detected by the DSC. This system comprises a molecular mixture of the epoxy resin and the curing agent molecules. Therefore, the reaction mechanism, in this case, is not basically diffusion-controlled.

Elevated-Temperature Curing: The Rheovibron could not detect two phases in sample D-1, which was cured at 50°C, indicating that the unreacted prepolymers were present in very low quantities. This was further confirmed by transmission electron microscopy (Figure 16a), DSC (no exothermic peaks could be observed), and extraction experiments. The percentage soluble content in this sample was 3.5% lower than that for the room-temperature-counterpart, sample B-1. The swell ratio was also smaller than that of sample B-1. In good agreement with other observations, the rubbery modulus of this sample was 1.4 times higher than that of samples B-1 and C-1.

It appears that the elevated temperature increased the

diffusivity of the molecules more than the rate of reaction, thus resulting in a greater extent of cure. Sample D-2 was cured at 50°C for twice the time as sample D-1 but no differences in properties were observed (i.e., it showed the same T_g and rubbery modulus). This indicates that the unreacted prepolymer molecules could not diffuse through the crosslinked interface (during the extra time of cure employed for sample D-2) to give further curing. Again this confirms that emulsion curing follows diffusion-controlled kinetics.

The glass transition temperature, rubbery modulus, and swell ratio in the 50°C-cured, solvent-based sample D-3 were similar to those of the room-temperature-solvent-based sample B-5. This indicates that almost complete curing had taken place in the solvent-based sample, at room temperature.

Effect of Post-Curing: The loss modulus curve of the post-cured samples of Series C showed one peak except for samples C-3 and C-4. This indicates that the unreacted prepolymers in samples C-1 and C-2 were in such small quantities that they could not be detected by the loss modulus curve. Electron microscopy (Figure-14) and extraction experiments (Table III) also show that the amount of unreacted prepolymer is reduced on post-curing. The glass transition temperatures of the emulsion-cured samples of Series C are as high or higher than those of Series B, but are still lower by 20-25°C from that of the solvent-cured sample, C-5.

The rubbery modulus of the samples of Series C is similar to their counterparts in Series B but the swell ratios are slightly

smaller. This anomally could be because samples of series C have lower soluble fraction and also because the present experiments, due to experimental difficulty, could not be extended to the rubbery plateau region.

The solvent-cured system shows a higher T_g and 2.5% lower extraction on post curing. Its T_g and rubbery modulus is still higher by 23°C and 1.4 times that of the emulsion-cured samples of series C, respectively.

Post curing of the emulsion sample, cured at 50°C (having only one peak in the loss spectrum) resulted in two peaks; one corresponding to the initial temperature of cure and the other corresponding to a higher temperature. Post curing results in the counter current diffusion of the reactive molecules through the network which react within the network and result in an apparent increase in crosslink density at that point. This apparent high crosslink density shows up as a second peak, corresponding to a higher T_g, in the loss tangent spectrum.

Average molecular weight between crosslinks (M_c): The swelling data did not give reasonable values of M_c for the emulsion-cured samples B-1 to B-4, and D-1. The present method of swelling includes the amount of solvent that stays in the voids created by the extraction of the unreacted prepolymer along with that which is present in the network itself. In some cases the M_c determined from the swelling data is in reasonable agreement with those calculated from the rubbery modulus. In other cases the agreement

is poorer. Based on much experience, the values of M_c derived from rubbery moduli are believed to be more reliable(28).

The M_c values calculated from the theory of rubber elasticity, for samples B-1 to B-4, C-1, C-3, and C-4 are twice those of the solvent-cured sample B-5, which is approximately the same as the theoretical value. This is not unexpected because the above mentioned emulsion-cured samples have a lower degree of cure -- a fact confirmed through DSC and electron microscopy. The M_c values for sample of Series D are approximately equal to the theoretical value, thus indicating that almost complete conversion had taken place. The microscopy results supplement this observation.

b. Conclusions

The DMS, DSC, electron microscopy, swelling, and extraction results lead to the conclusion that emulsion curing is a diffusion-controlled phenomenon and is quite different from solvent curing. Generally, the unreacted prepolymer is dispersed in a completely reacted network. An emulsion system having a lower rate of reaction gives a more homogeneous network and a smaller-sized dispersed phase. Although optimization of the conditions of film-formation was not sought in this study, the crosslink density, solubility, and modulus temperature curves for at least several formulations closely resembled those of solution-cured controls. Finally, with a judicious balancing of reactivity and diffusivity of the epoxy and polyamide co-reactants, both useful degrees of physical coalescence and curing can be obtained in these systems.

D. MECHANISM OF EMULSION CURING

The film formation, mechanical properties, and the morphological studies clearly indicate that curing in emulsion state involves the evaporation of water, coalescence of the particles, diffusion of the reactants and the chemical reaction between them (see earlier discussion in this Chapter and also Chapter VI). Though all the steps are important, the steps involving the diffusion and the chemical reaction of the reactants result in the crosslinked network.

A three-stage diffusion-controlled mechanism is proposed for emulsion curing.

Stage A: This stage involves the evaporation of water and the coalescence of the reactive particles. The formation of a smooth film marks the end of this stage. The homogeneity of this film depends on the rate of evaporation of water (high rates give rise to high internal stresses which relax by creating cracks in the film), the particle size (larger particles besides having lower rates of coalescence also have a larger volume of the unreacted core), and the rate of reaction between the coalesced particles (higher rates result in curing of the particle surface in the emulsion state which hinders particle coalescence).

Stage B: This stage involves the diffusion of the reactive molecules through the unreacted interface of the coalesced particles till the onset of gelation. Further diffusion of the molecules becomes negligible after gelation due to the high resi-

stance to diffusion offered by the gelled phase. Thus further crosslinking of the unreacted particle-core practically stops after gelation takes place at the particle interface.

The size of the unreacted core depends on the gelation time and the particle size -- high reactivity gives a small gel-time and thus a larger size of the unreacted core. In other words, there is a maximum particle size for every combination of reaction rate constant and effective diffusivity (which of course depends on the temperature of cure) that would give a homogeneous network composed of completely reacted particles.

Stage C: This stage involves the diffusion of the reactive molecules through the crosslinked interface of the particles. Appreciable amounts of molecules diffuse through the network only when the temperature is raised above that of the initial cure (diffusivity increases with temperature). Obviously, the diffusion of the same molecule would be larger through a lower crosslink density network. Equimolar counter diffusion in stage C would take place when both the reactants have a similar molecular size whereas diffusion of only one component would take place when the molecules of that component are much smaller than the other component. In the case of equimolar counter diffusion the curing reaction between the diffused molecules takes place somewhere in the crosslinked interface which results in an apparent increase in the crosslink density at the reaction site. When a large number of molecules react in this manner a network having two T_g's results -- the lower

T_g corresponding to the initial crosslink density (generally close to the temperature of cure) while the higher T_g corresponding to the apparent high crosslink density portion of the network. Further curing at still higher temperatures should not show any changes in network structure because this apparent highly crosslinked zone would practically stop the diffusion of the molecules through it, even at higher temperatures.

On the other hand, when only one phase diffuses through the crosslinked network into the other phase then there would be no apparent increase in crosslink density of any part of the interface and further reaction would take place in a manner similar to stage-B. In this case only one T_g would be observed.

The amount of further curing in stage C would be much lower than that in stage B because the diffusion of the molecules through the gelled surface would be much smaller than that through the ungelled surface. The T_g of the network after stage C would be higher than that after stage B. The difference in T_g's of the two stages would depend on the amount of the unreacted molecules consumed in stage C.

The three stages are shown schematically in Figure 21.

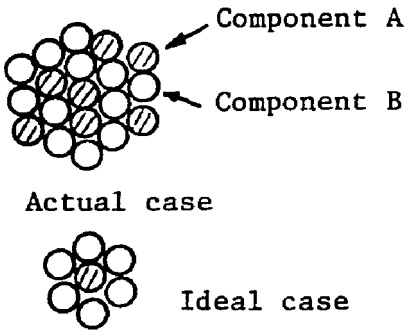

(A) EMULSION CURING AT STAGE-A

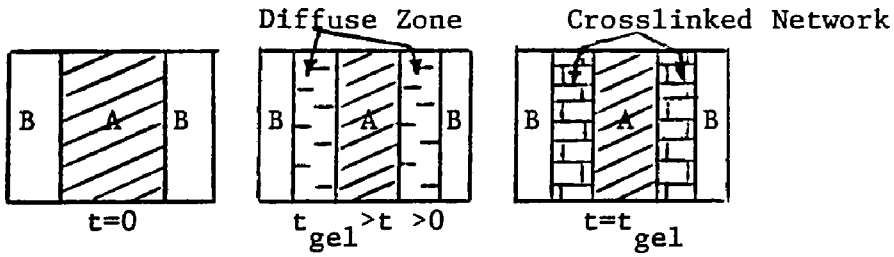

(B) EMULSION CURING AT STAGE-B

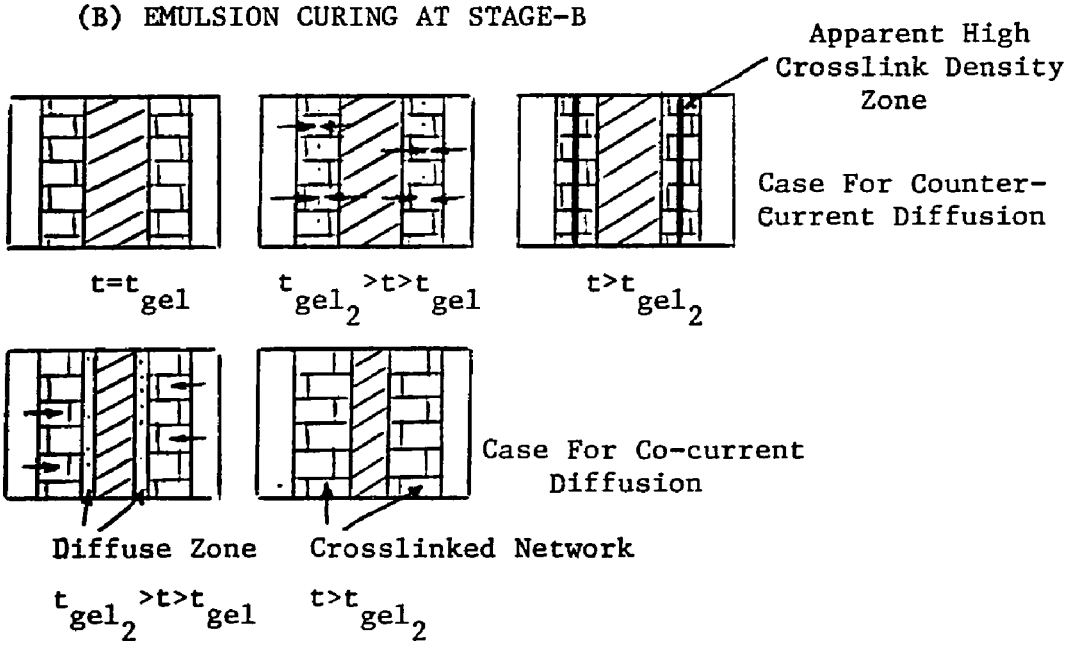

(C) EMULSION CURING AT STAGE-C

Figure 21. Proposed model for emulsion curing.

REFERENCES

1. H.Warson, "The Application of Synthetic Resin Emulsions", Benn., London (1972).

2. D.C.Blackley, "High Polymer Latices", Vol. 1. Maclaren, London (1966).

3. J.W.Vanderhoff, Final Report, AFML Project "Exploratory Development of Improved Water Based Coatings", Contract F33615-73-C5179, (1975).

4. M.S.El-Aasser, J.W.Vanderhoff, S.C.Misra, and J.A.Manson, J.of Coatings Technology, 49(635),71(1977).

5. S.C.Misra, J.A.Manson, and J.W.Vanderhoff, Presented at the ACS meeting, March 1978.

6. R.E.Dillon, L.A.Matheson, and E.B.Bradford, J.Coll.Sci., 6, 108(1951).

7. G.L.Brown, J. Polym. Sci., 22, 423(1956).

8. D.P.Sheetz, J.Appl.Polym.Sci., 9, 3559(1965).

9. J.W.Vanderhoff, H.L.Tarkowski, M.C.Jenkins, and E.B.Bradford, J. Macromol. Chem. 1(2), 361(1966).

10. S.L.Bertha and R.M.Ikeda, J.Appl.Polym.Sci., 15, 105(1971).

11. J.W.Vanderhoff, E.B.Bradford, and W.K.Carrington, J.Polym.Sci.-Symp. No. 41, 155(1973).

12. R.R.Myers and R.K.Schultz, J.Appl.Polym.Sci., 8, 755(1964).

13. L.A.Sukhareva, V.A.Voronkov, P.I.Zubov, and D.A.Milein, Soviet Rubber Tech., 29, 19(1970).

14. L.A.Sukhareva, M.R.Kiselev, and P.I.Zubov, Kolloid Zhurnal, 36(1), 176(1974).

15. P.I.Zubov and L.A.Lepilkina, Kolloid Zhurnal, 23(4), 418(1961).

16. E.B.Bradford and J.W.Vanderhoff, J.Macromol.Chem., 1(2), 355(1966).

17. V.I.Yeliseyeva, "Polymerization Film Forming Materials", Khimiya Press, Moscow, 1971.

18. S.S.Voyutskii, J.Polym.Sci., 32, 528(1958).

19. V.I.Yeliseyeva, I.S.Avetisyan, S.S.Drezels, and P.I.Zubov, Polym.Sci. U.S.S.R., 8(1), 103(1966).

20. E.B.Bradford and J.W.Vanderhoff, J. Macromol. Sci.-Phys., B6(4), 671(1972).

21. C.W.Stewart and P.R.Johnson, Macromolecules, 3(6), 755(1970).

22. G.A.C.Graham, Int. J. Eng. Sci., 3, 27(1965).

23. W.N.Findley, J.S.Lai, and K.Onaran, "Creep and Relaxation of Nonlinear Viscoelastic Materials", North-Holland Publishing Co., Amsterdam (1976), p. 86.

24. E.Baer, ed., "Engineering Design of Plastics", Reinhold Publishing Corp., N.Y. (1964), p. 164.

25. A.F.Lewis and J.K.Gillham, J.Appl.Polym.Sci. , 6(22), 422(1962).

26. J.K.Gillham, J.A.Benci, and A.Noshay, J.Appl.Polym.Sci., 18, 951(1974).

27. R.A.Fava, Polymer, 9, 137(1968).

28. J.A.Manson and L.H.Sperling, final report AFML Contract No. F33615-75-C-5167, 1977 (to be published).

CHAPTER VI

EFFECT OF PREPOLYMER STATE -- BULK, SOLUTION, AND EMULSION -- ON THE ENGINEERING BEHAVIOR OF NETWORKS

A. INTRODUCTION

Though curing is done in bulk, solution, and sometimes in emulsion, very little is known about how these different methods affect the properties of the final network.

Since the present research was concerned with network structure, and its effect on engineering properties it seemed important to elucidate the effects of prepolymer state -- bulk, solution, and emulsion -- on the engineering behavior of bisphenol-A type epoxies. The effect of prepolymer state was studied at three different levels of crosslink density. This was done by useing a common curing agent for three epoxy prepolymers of the same homologous series.

B. RESULTS AND DISCUSSION

a. Film formation

i) Solution curing: Use of a high temperature cure cycle in the presence of large amounts of solvent caused excessive bubbling. However, bubble-free films could be obtained after most of the solvent was allowed to evaporate at room temperature for 24 hours, and provided that the thickness of the final films was less than 0.15-mm.

ii) Emulsion curing: Although homogeneous films could not be obtained from emulsions having particles larger than 5-μm, good

films were generally obtained when the particle size was smaller than 0.6 μm.

b. Dynamic mechanical properties

The plots of the tanδ, and dynamic loss and storage moduli, as a function of temperature, are shown in Figures 1,2,3, and 4. The glass transition temperature (T_g), rubbery modulus (E_r), tanδ peak value, and residual solvent content of the networks are given in Table I.

TABLE I. DYNAMIC MECHANICAL PROPERTIES OF SAMPLES PREPARED FROM PREPOLYMERS IN DIFFERENT STATES.

Prepolymer State	Residual Solvent wt.%	T_g (°C)	Rubbery Modulus (MPa x 10^{-1}) at T_g+40°C	at T_g^a+40°C	$\tan\delta_{max}$ value	$\tan\delta_{max}$ temp.,°C
Epon 828						
bulk	0.0	191	3.0	3.0	0.75	202
emulsion	0.0	155	1.9	-	1.0	168
solution	2.12	137	2.5	2.0	0.37	185
solution	1.32	185	2.0	2.0	0.87	198
solution	1.10	189	2.5	2.5	0.80	199
Epon 1001						
bulk	0.0	145	0.90	0.90	1.25	158
emulsion	0.0	128	0.80	-	1.40	144
solution	2.82	94	0.95	0.90	1.25	153
solution	1.51	140	0.90	0.90	1.25	154
solution	1.38	142	0.90	0.90	1.25	158
Epon 1002						
bulk	0.0	135	0.85	0.85	1.40	147
emulsion	0.0	114	0.33	-	1.60	132
solution	1.12	133	0.84	0.84	1.40	145

[a] T_g of the bulk-cured sample.

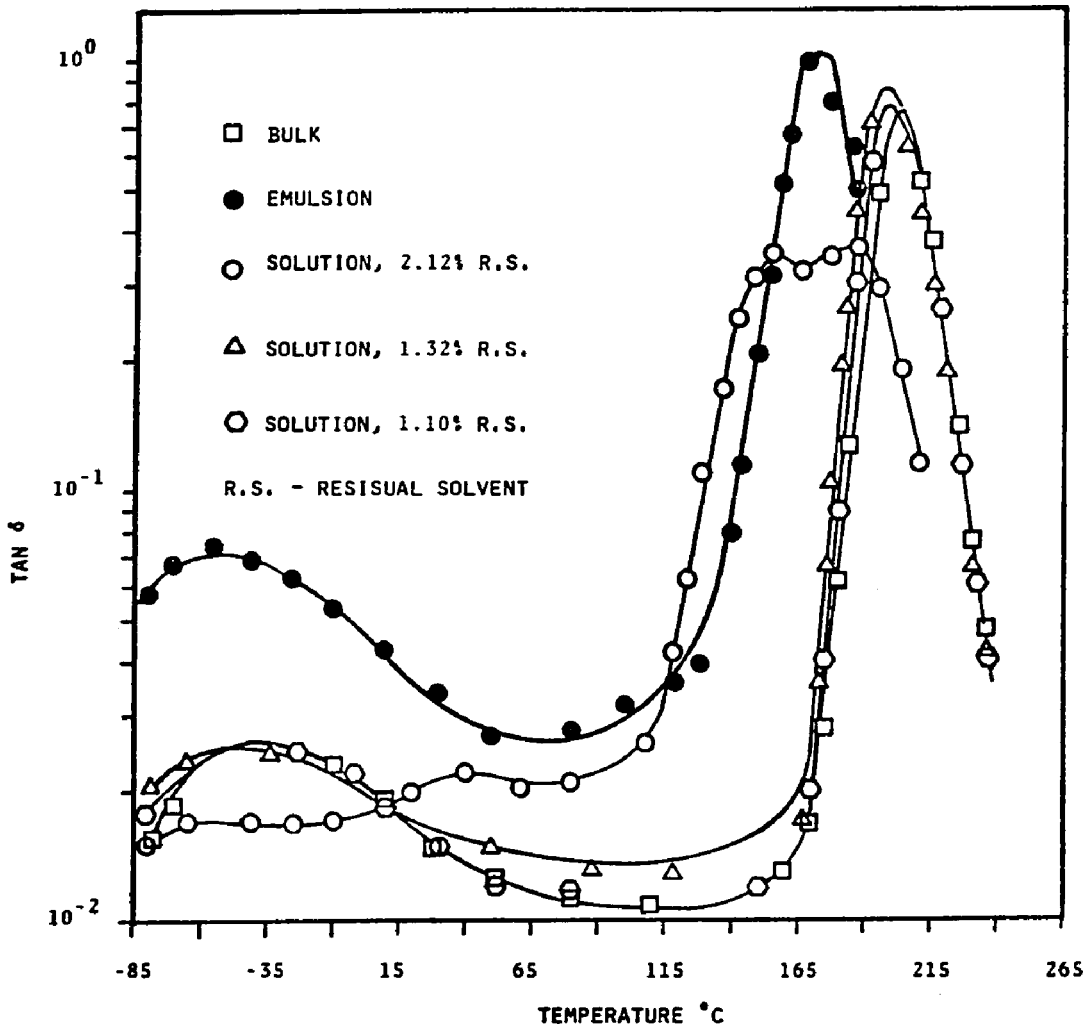

Figure 1. Loss-tangent spectra for networks prepared through prepolymers in different states, using Epon 828-MDA combination.

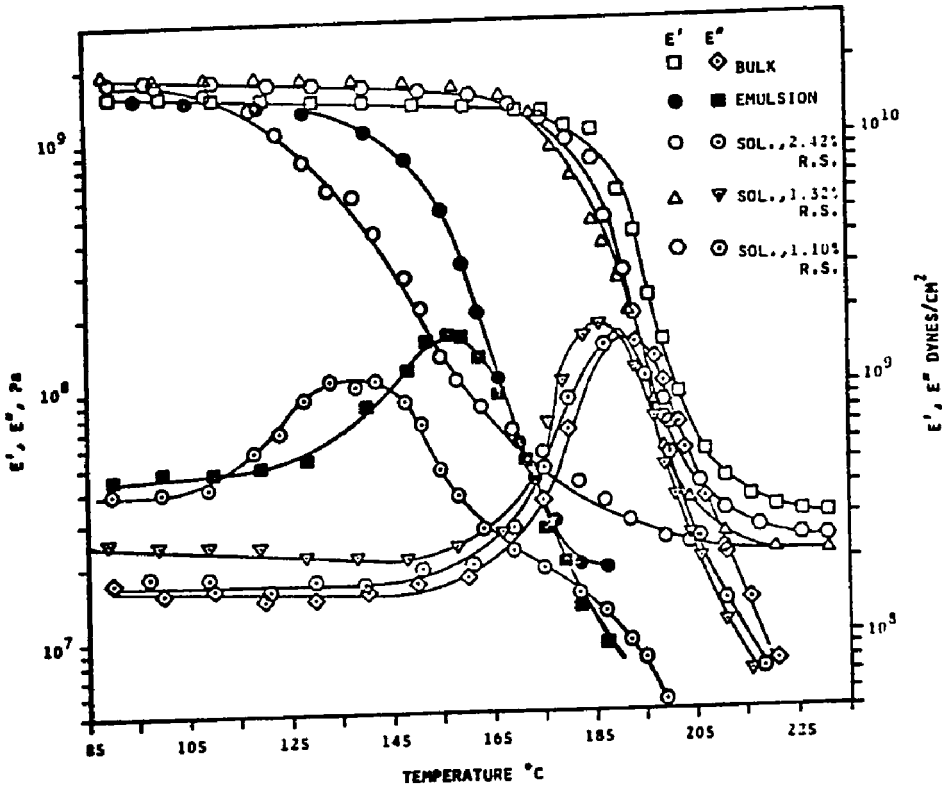

Figure 2. Dynamic mechanical spectra for networks prepared through prepolymers in different states, using Epon 828-MDA combination.

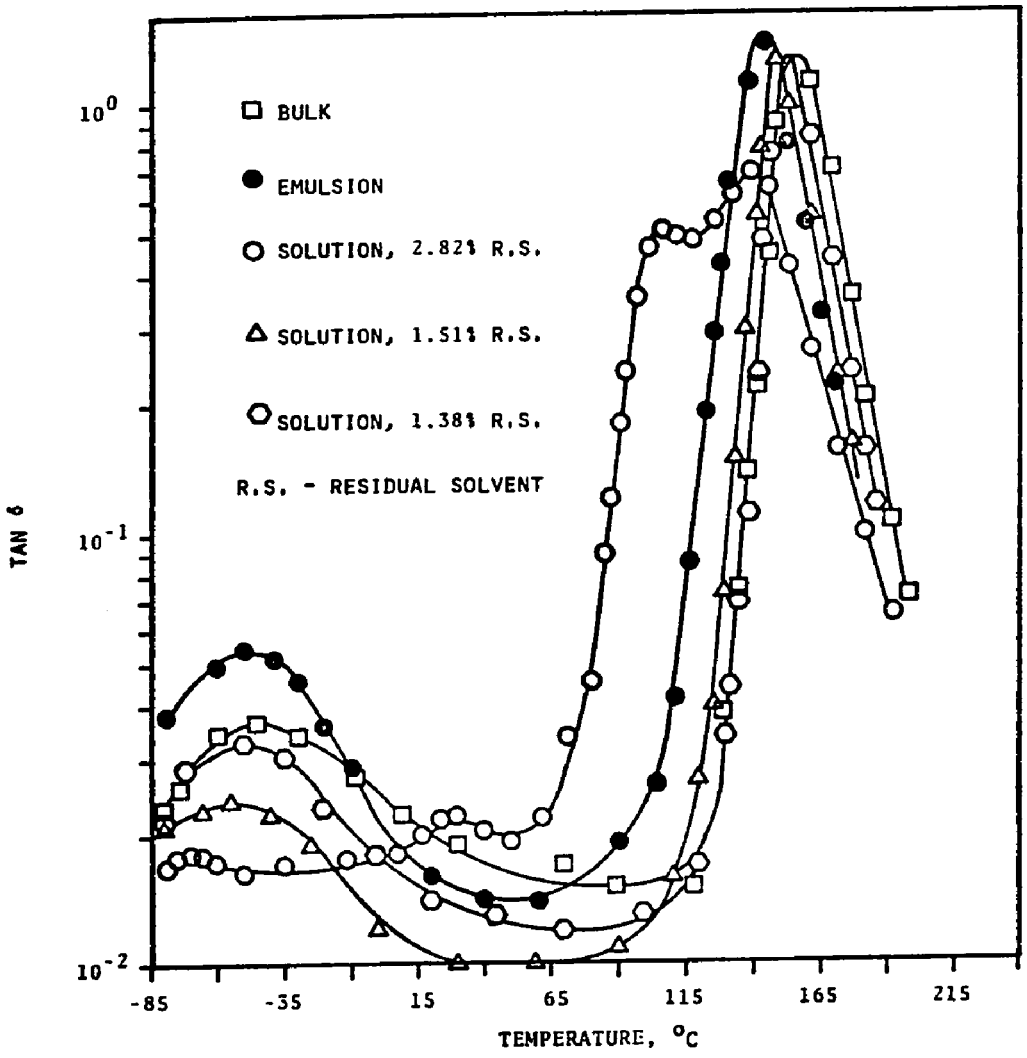

Figure3. Loss-tangent spectra of networks prepared through prepolymers in different states, using Epon 1001-MDA combination.

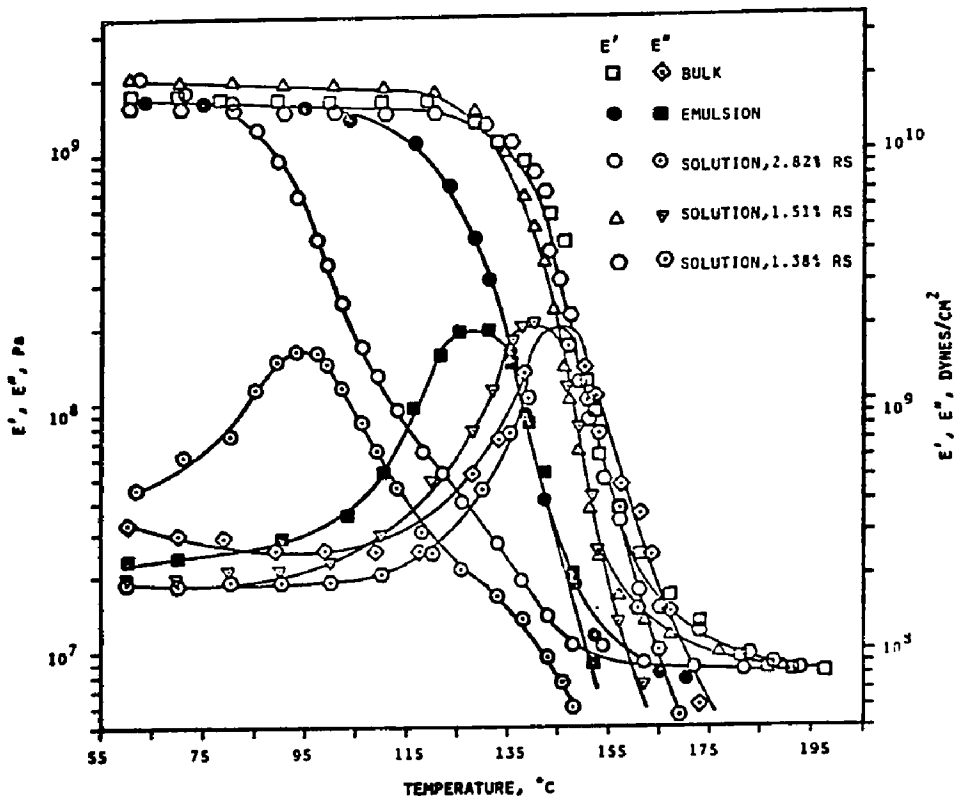

Figure 4. Dynamic mechanical spectra for networks prepared through prepolymers in different states using Epon 1001-MDA combination.

The amount of residual solvent, as expected, increased with an increase in thickness or crosslink density of the network. The unevacuated samples had 2.0 to 2.5% residual solvent.

Solution curing: Table I indicates that for all the epoxy prepolymers an increase in the percentage residual solvent increases the tanδ peak height and reduces the peak temperature. Above a 2% residual concentration the peak, as expected, is observed at a lower temperature but is considerably broader and reduced in height. The broadening of the peak at higher concentration of residual solvent is attributed to the evaporation of the solvent during the dynamic mechanical test. Repeated experiments, confirming the above hypothesis, showed higher T_g and tanδ peak values. The dynamic mechanical behavior of the unevacuated networks is similar to that reported by Kenyon and Neilsen(1). The dynamic mechanical spectroscopy further indicates that the solvent, when present in amounts less than 1.6 weight percent, does not evaporate during the experiment and acts as an external plasticizer. This could be due to the strong interaction of the polar groups of acetone with the epoxy network(2).

The glass transition temperature as a function of residual solvent for the different epoxies is shown in Figure 5. This figure indicates that T_g of the bulk and solution cured networks would be the same at 0% residual solvent. This implies that the structure of these epoxy networks, in contrast to lightly crosslinked networks, was the same whether cured in bulk or solution

For lightly crosslinked networks several investigators(1,3-6) have shown that solution curing results in large number of dangling chains and closed loops. For a similar epoxy system, Bell(7) showed that negligible crosslinking took place in the presence of acetone, at room temperature. Therefore, in the present case most of the curing would have taken place during the high temperature cure. Since this cycle was employed after the evaporation of most of the acetone, it appears that the presence of small amounts of solvent did not affect the final network structure. The relationship between T_g and weight percent residual solvent in the network appears to be complex. Though more data are required to draw a definite conclusion, it appears that T_g is independent of residual solvent content (for all values of M_c) atleast up to an inflection point (see Figure 5). The latter seems to shift to higher percent residual solvent with an increase in M_c (though data exist for only two values of M_c).

An increase in the amount of solvent (acetone), acting like a typical antiplasticizer(8), reduced the β-transition peak height and shifted it to a lower temperature. It is known that the β-transition peak height depends on the number of free hydroxyl groups(9, also see discussion in Chapter III). Being highly polar the acetone molecules can interact with the hydroxyl groups and hinder their motion. Therefore an increase in the concentration of acetone in the network reduces the β-transition peak height.

Emulsion curing: The tanδ peak for emulsion-cured films

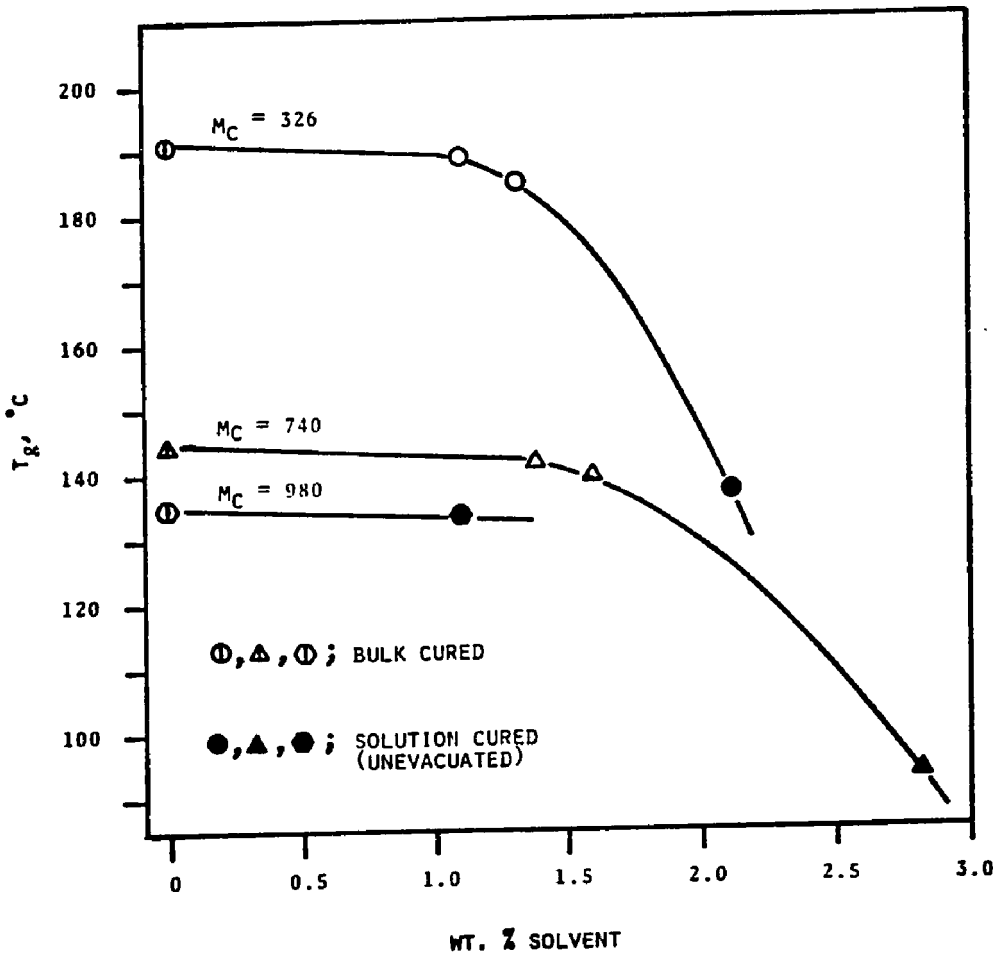

Figure 5. T_g as a function of residual solvent in the network.

were higher than the bulk or solution-cured networks (see Table I), probably because of the presence of some unreacted prepolymers. The similarity in the shape of the tanδ curves of the bulk and emulsion-cured networks indicates that further reaction did not take place during the dynamic mechanical test. This is because the unreacted molecules could not diffuse through the crosslinked network during the experiment. Similar behavior was observed for an epoxy/polyamide system (see Chapter V, post-cured samples of Series C) in which electron microscopy indicated the presence of unreacted prepolymers in the network but dynamic mechanical study did not indicate further reaction. The emulsion-cured samples have a lower glass transition temperature and rubbery modulus than their bulk-cured counterparts. Figure 6 shows that the difference in the glass transition temperatures (ΔT_g) of the bulk and emulsion-cured samples decreases initially with decreasing crosslink density but increases again with a further decrease in crosslink density. Thus ΔT_g is minimum for an optimum crosslink density. This can be explained as follows: The diffusion of the reactants into one another takes place till the gel point is reached (also see discussion in Chapter V). An increase in the temperature allows further reaction by enabling the reactants to diffuse through the network. At low values of M_c the resistance to further diffusion caused by the network is large. This results in a smaller degree of cure and therefore a larger value of ΔT_g. On the other hand, for high molecular weight prepolymers early

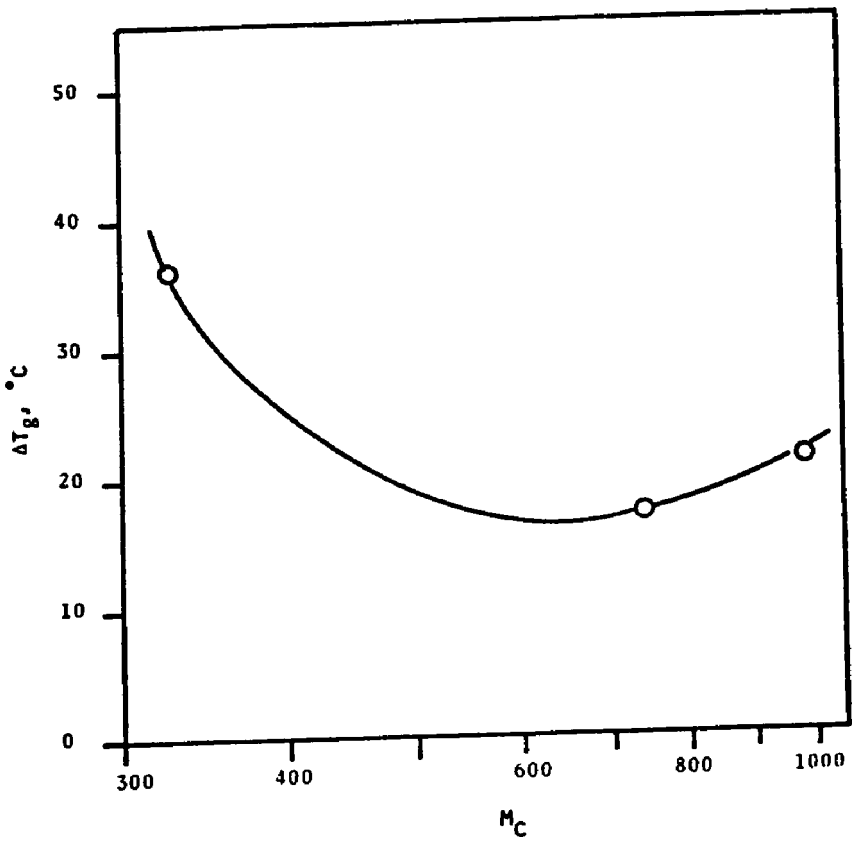

Figure 6. ΔT_g as a function of M_c.

gelation takes place due to high reactivity. Though the high value of M_c causes a lower resistance to diffusion of the prepolymers, but the high reactivity more than compensates for it. This again results in a lower degree of cure. Therefore, at an optimum value of M_c the rate of diffusion would be larger than the rate of reaction of the prepolymers, as observed experimentally.

The β-transition temperature of the emulsion-cured samples was the same as their bulk-cured counterparts. Although the peak height, because of the presence of unreacted prepolymers, is expected to be lower than for the bulk-cured counterpart, observed values were actually higher. This inversion of order is due to the fact that the tanδ values determined in the glassy region are very sensitive to the cross-sectional area of the specimens; smaller cross-sectional areas give higher tanδ values (see discussion in Chapter II). For emulsion-cured films, unfortunately, smaller cross-sectional areas were used, and therefore higher tanδ values were obtained.

c. Tensile properties

It was observed that thin samples showed lower percent elongation and ultimate tensile strength (σ_u) as compared to thick samples. Since only thin samples (0.3 mm) could be made from emulsion-curing, both thin (0.3 mm) and thick (1.2 mm) films were made from solution curing. This provided an internal calibration to compare the data with 1.2-mm thick bulk-cured samples. Thin films gave smaller values, probably because they were more

sensitive to very small flaws produced during the preparation of tensile specimens. The results are given in Table II.

TABLE II. EFFECT OF PREPOLYMER STATE ON TENSILE PROPERTIES.

Prepolymer State	Residual Solvent (wt%)	% elongation	σ_u^a MPa x 10^{-1}	σ_y^b MPa x 10^{-1}	E^c GPa
Epon 828					
bulk[d]	0.0	12.7 ± 1.4	7.5 ± 0.3	-	1.2 ± 0.1
emulsion	0.0	4.3 ± 1.2	4.2 ± 1.0	-	1.3 ± 0.2
solution	1.45	7.9 ± 0.6	6.8 ± 0.4	-	1.2 ± 0.1
solution	1.38	6.8 ± 0.7	6.8 ± 0.6	-	1.3 ± 0.1
solution[d]	1.38	11.3 ± 1.1	7.6 ± 0.3	-	1.3 ± 0.1
solution	1.36	7.5 ± 1.4	6.0 ± 1.1	-	1.1 ± 0.2
Epon 1001					
bulk[d]	0.0	10.5 ± 0.7	6.8 ± 0.4	7.5±0.2	1.5 ± 0.1
emulsion	0.0	6.0 ± 0.8	4.7 ± 0.1	-	1.0 ± 0.2
solution[d]	1.45	11.0 ± 1.1	6.6 ± 0.5	-	1.0 ± 0.1
solution	1.45	6.1 ± 0.8	6.0 ± 0.3	-	1.3 ± 0.1
solution	1.14	8.1 ± 1.6	6.5 ± 1.5	-	1.4 ± 0.3

[a] Ultimate tensile strength.

[b] Yield strength.

[c] Young's modulus.

[d] Samples having 1.2-mm thickness, others were 0.3-mm thick.

Except for yielding, bulk and solution-cured samples showed the same tensile properties. Epon 1001 resin, showed yielding when cured in bulk but did not show any yielding when cured in solution even though it had the same percent elongation, initial modulus, and modulus-to-break. This implies that the residual

acetone acts as an antiplasticizer. An actual antiplasticizer generally increases the Young's modulus. In the present samples, the amount of acetone was quite small; the slight changes could have been overshadowed by the experimental scatter. For a different antiplasticizer Litt and Tobolsky(10) had also observed a significant reduction in yielding without any changes in modulus.

The emulsion-cured samples had 30 to 40% lower σ_u and percent elongation to break than their bulk or solution-cured counterparts. Emulsion-cured Epon 1001, unlike its bulk-cured counterpart, did not show any yielding. The low tensile strength and elongation to break alongwith the absence of yielding observed in emulsion-cured samples can be explained on the basis of their composite morphology having the low molecular weight prepolymer dispersed in a crosslinked matrix. This morphology was observed in Epon 1001/Versamid 115 networks prepared through emulsion curing (see Figures 13 to 16, in Chapter V). The low molecular weight dispersed phase constituted by the prepolymers does not share the load applied to the network. This results in the observed lower tensile properties in the emulsion-cured films as compared to their bulk or solution-cured counterparts.

d. Swelling and Extraction

The swelling and extraction experiments were conducted at room temperature using acetone as the solvent. Equilibrium swelling was achieved within 15 days. The results are given in Table III.

TABLE III. SWELLING, EXTRACTION, AND DENSITY MEASUREMENTS.

Prepolymer State	Residual Solvent wt%	ρ^a (kg/m^3 x10^3)	Swell ratio[b]	% extraction
Epon 828				
bulk	0.0	1.1972	1.381 ± 0.01	1.3 ± 0.1
emulsion[c]	0.0	1.1933	1.440 ± 0.02	8.1 ± 0.5
solution	2.12	1.1970	1.380 ± 0.01	3.1 ± 0.1
solution	1.10	1.1970	1.381 ± 0.01	1.3 ± 0.1
Epon 1001				
bulk	0.0	1.1925	1.638 ± 0.02	2.5 ± 0.5
emulsion[c]	0.0	1.1755	1.628 ± 0.03	8.2 ± 1.1
solution	2.82	1.1930	1.638 ± 0.02	6.2 ± 0.1
solution	1.38	1.1930	1.607 ± 0.02	2.4 ± 0.4

[a] density of extracted samples, 1 gm/ml = 10^{-3} kg/m^3.

[b] Swell ratio = $\frac{\text{swollen vol. of network}}{\text{dry, extracted vol. of network}}$

[c] Sample contained 9% emulsifier by weight.

The swell ratios of bulk, solution, and emulsion-cured samples were the same indicating that all had the same degree of cross-linking. The percent extraction in the emulsion-cured samples was higher probably because of the presence of 9% emulsifier by weight. On assuming that none of the unreacted prepolymers are extracted the results can account for only 6% extractable emulsifier. This indicates that some emulsifier does not get extracted.

e. Molecular weight between crosslinks, M_c

The molecular weight between crosslinks M_{cr} and M_{cs} were determined from the rubbery modulus (obtained through DMS, using the theory of rubber elasticity(11a) and swelling data (using the Flory-Rehner Equation(11b)), respectively. The results are given in Table IV.

TABLE IV. M_c VALUES DETERMINED THROUGH DIFFERENT METHODS.

Prepolymer State	Theoretical M_c	M_{cs}	M_{cr}
Epon 828			
bulk-cured	326	104	525
emulsion-cured	326	125	730
solution-cured	326	104	650
Epon 1001			
bulk-cured	740	265	1530
emulsion-cured	740	256	1660
solution-cured	740	265	1475

These results indicate that the M_c values calculated from swelling data are half, whereas those from rubbery modulus are twice, the theoretical values. Similar results were observed with other networks too (see Chapter III) indicating that the M_c values calculated from rubbery modulus are more reliable (for reasons see discussion in Chapter III).

f. Morphology

The scanning electron micrographs of the bulk, emulsion, and solution-cured networks are shown in Figure 7. The surface of the networks was examined after etching in a 1-M aqueous solution

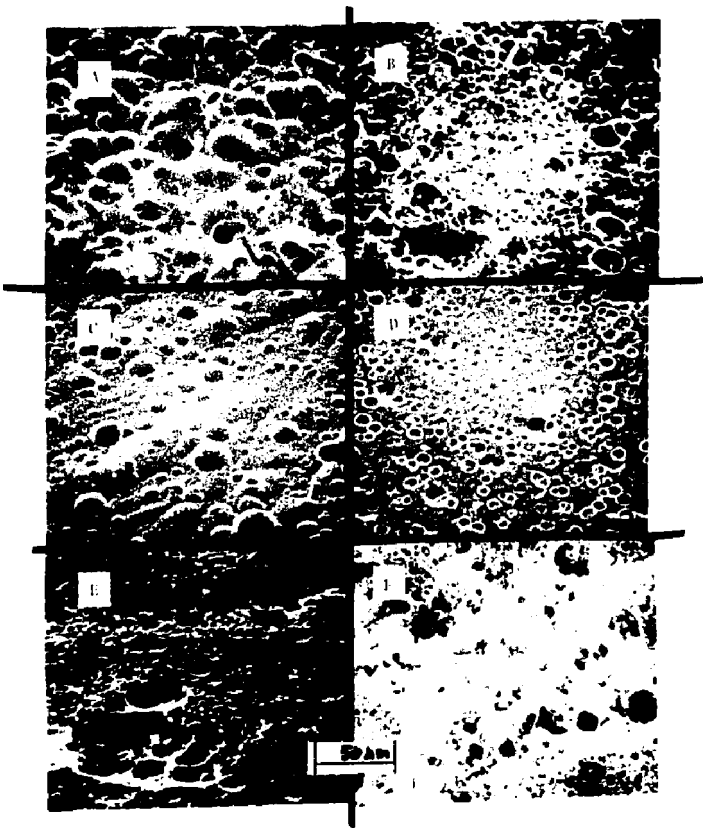

Figure 7. Scanning electron micrographs of networks prepared from prepolymers at different states, after etching for 7 hr in 1-M aq Cr_2O_3.
A),C), and E) : Epon 828-MDA networks prepared from bulk, solution, and emulsion-curing, respectively.
B),D), and F) : Epon 1001-MDA networks prepared from bulk, solution, and emulsion-curing, respectively.

of Cr_2O_3 at 80°C for seven hours. This figure indicates a two-phase structure in all the samples (due to the etching out of the primary and secondary microgels -- see discussion in Chapter IV). The bulk and solution-cured networks have similar morphologies but the emulsion-cured networks have a rougher surface. With the help of osmium tetroxide-stained-microtomed-sections of Versamid 115-cured samples it was shown (see Chapter V) that emulsion-cured networks have some unreacted prepolymers as the dispersed phase. Thus in emulsion-cured networks the etching out of the unreacted prepolymers alongwith the primary and secondary microgels results in a rougher surface as compared to their bulk or solution-cured counterparts.

C. CONCLUSIONS

The present study indicates that the presence of small amounts of solvent (acetone) during curing does not affect the structure of the final network. Acetone acts as an antiplasticizer for the epoxy networks. Emulsion-cured films on the other hand have somewhat lower T_g as compared to the bulk-cured counterparts. This difference in T_g (ie., ΔT_g) is smallest for an optimum M_c where an increase in temperature increases the rate of diffusion more than the rate of reaction. The tensile properties also are 30 to 40% lower than their bulk-cured counterparts because of the presence of unreacted prepolymers as the dispersed phase in the former networks.

It is concluded that epoxy coatings prepared by

solution curing would have properties similar to their bulk-cured counterparts if almost all the residual solvent is removed. For thin coatings, as generally is the case, the residual solvent would of course be very small. However, different solvents may have slightly different effects (such as acetone, in the present case, acted as an antiplasticizer). Due to the problem of solvent bubbling solution-curing is not feasible in applications, such as in structures or composites, where high temperature cure cycles are used.

Since emulsion-cured samples had reasonable, though slightly inferior, properties compared to their bulk or solution-cured counterparts (also see results in Chapter V), they can be used as a good substitute for solvent-based coatings. Further improvements such as development of stable latexes with still smaller particle size and emulsifier concentration alongwith the optimization of curing conditions would help in achieving better properties.

REFERENCES

1. A.S.Kenyon and L.E.Nielsen, J.Macromol.Sci.-Chem., A3(2), 275(1969).

2. S.S.Ivanova et.al., Koll.Zhurnal, 36, 4, 666(1974).

3. P.J.Flory,"Principles of Polymer Chemistry", Ithaca, Cornell Univ. Press, 1953, Chap. 9.

4. M.C.Shen and A.V.Tobolsky, J.Polym.Sci., A(3), 629(1965).

5. S.S.Labana, S.Newman, and A.J.Chompff, in "Polymer Networks", ed. A.J.Chompff and S.Newman, N.Y.,Plenum Press,(1971), p 469.

6. D.H.Solomon, B.C.Loft, and J.D.Swift, J.Appl.Polym.Sci., 11. 1593(1967).

7. J.P.Bell, J.Polym.Sci., A-2, 8, 417(1970).

8. N.Hata , R.Yamuchi, and J.U.Kumanotani, J.Appl.Polym.Sci., 17, 2173(1973).

9. J.C.Patterson-Jones and D.A.Smith, J.Appl.Polym.Sci., 12, 1601(1968).

10. M.H.Litt and A.V.Tobolsky, J.Macromol.Sci.-Phy., B 1(3), 433(1967).

11. P.J.Flory, "Principles of Polymer Chemistry", Cornell Univ. Press, Ithaca , N.Y., (1953), (a) p 464, (b) p. 579.

CHAPTER VII

SUMMARY AND CONCLUSIONS

A. SUMMARY

The effect of crosslink density and distribution of crosslink density on morphology and on thermal and mechanical behavior was studied for a homologous series of DGEBA-type epoxy resins cured with stoichiometric amounts of methylene dianiline. Specifically, dynamic mechanical spectroscopy, transmission electron microscopy, differential scanning calorimetry, creep study, impact and tensile tests, swelling, and extraction experiments were used.

An increase in crosslink density (i.e., decrease in M_c) increases T_g, T_β, the rubbery modulus, and the characteristic creep time -- but decreases the slope of the modulus-temperature curve at T_g, the height of the tanδ curve near T_g, and the degree of swelling and extractability. Tensile properties were nearly independent of M_c; apparent energies of activation for creep were also independent, both above and below T_g. In contrast, impact strengths were higher, the higher the crosslink density.

At a given M_c, most properties were not much affected by small differences in the distribution of M_c; creep response was a notable exception, being quite sensitive to changes in M_c distribution. However, big differences in distribution of M_c affect T_g (the component forming the more continuous network controls T_g) slope of the transition region (slope decreases with an increase in the broadness of distribution), height of the tanδ peak (peak

broadens and decreases in height with an increase in the broadness of the distribution). On the other hand, room temperature tensile properties and impact strength, β-transition temperature, bulk density, and soluble content is not affected by the distribution of M_c.

Curing and gelation in bulk takes place through the formation of the primary microgels which combine together (not very coherently) to give the secondary microgels. Later, these secondary microgels combine (less coherently than the primary microgels) to give the final network.

Emulsion-curing, a diffusion-controlled process, is complex -- involving evaporation of the water, physical coalescence of the particles, diffusion of the reactants, and the curing step itself. Though optimization of cure conditions or emulsifier combinations was not sought in this preliminary study, reasonably good properties comparable to those of bulk or solution-cured networks were obtained.

B. CONCLUSIONS

Interestingly, the highest crosslink density network, besides having the lowest swelling and slowest creep, also has the highest T_g, rubbery modulus, and impact strength. For a change, none of the engineering properties have to be sacrificed in this case.

From a design standpoint, the effect of distribution of crosslink density does not play any significant role unless there

is a wide distribution of crosslink density, that too in a range where the properties are very sensitive to the average crosslink density.

Generally crosslinked networks are not perfectly coherent and are formed through primary and secondary microgels. The engineering properties, to a certain extent, depend on the size and coherence of the secondary microgels.

With optimization of the cure conditions and the emulsifier combinations, epoxy emulsions can be used as a convinient substitute for solvent-based coatings; in addition to having similar properties, the water-based systems will be less expensive and lead to less atmospheric polution.

C. DIRECTIONS FOR FUTURE RESEARCH

Though the present study has given a good insight to the effects of the distribution and average value of crosslink density, further work on tensile properties in the rubbery state is needed. The literature study has indicated that the effect of the functionality of the crosslinks on the engineering behavior of networks is not very well understood A systematic study of this important aspect would be very useful from an engineering design standpoint. Furthermore, a detailed kinetic and morphological study during gelation would help to elucidate the mechanisms of network formation. Lastly, but not least, optimiztion of the cure conditions and emulsifiers is needed for epoxy emulsions to ensure good physical properties and surface adhesion. It is possible that excess

amounts of curing agent may give better properties, therefore the study of stoichiometry in epoxy emulsions would be very important.

These studies, though different in nature, would significantly contribute to the field of network science.

VITA

The author was born on January 1, 1949 in India, the second son of Mr.Justice T.S.Misra and Mrs. S.Misra.

He received his Bachelor of Science in Chemical Engineering from Harcourt Butler Technological Institute, Kanpur, India in 1970. That same year he entered Indian Institute of Technology, Kanpur, India and received his Master of Technology in Chemical Engineering in 1972. He had been a recipient of Merit Scholarship in India since High School.

In 1974, he came to the United States for his Doctoral studies at Lehigh University under a teaching assistantship from the department of Chemical Engineering.